SYNTHESIS, CHARACTERIZATION AND POLYMERIZATION OF OLEFINS USING SUPPORTED TRANSITION METAL CATALYSTS

A thesis submitted to the

UNIVERSITY OF PUNE

for the degree of

DOCTOR OF PHILOSOPHY

in

CHEMISTRY

by

SAPTARSHI RAY

Division of Polymer Chemistry

National Chemical Laboratory

PUNE - 411 008

INDIA

February, 2004

CONTENTS

CHAPTER-5

GLOSSARY

bd	Bulk density
[C*]	Active site concentration
CGC	Constrained geometry catalyst
Cp	Cyclopentadienyl
Cp*	Pentamethylcyclopentadienyl
d	Density
DEAC	Diethyaluminum chloride
EDTA	Ethylene diamine tetra acetate solution salt
eV	Electron volt
Flu	Flurenyl
FWHM	Full width at half maxima
ICP	Inductively coupled plasma spectroscopy
Ind	Indenyl
k_{tr}	Rate constant for transfer
k_p	Rate constant for propagation
$\overline{M_n}$	Number average molecular weight
$\overline{M_w}$	Weight average molecular weight
MAO	Methylaluminoxane
MI	Melt index
Mp_1	Peak molecular weight of lower molecular weight fraction
Mp_2	Peak molecular weight of higher molecular weight fraction
P	Pressure
PDI	Polydispersity index
PE	Poly(ethylene)
PET	Poly(ethyleneterephthalate)
R_P	Rate of polymerization

S.A.	Surface area
t	time
T	Temperature
TCB	1,2,4-trichlorobenzene
T_m	Crystalline melting point
TEAL	Triethylaluminum
TEM	Transmission electron microscopy
TIBAL	Triisobutylaluminum
TMA	Trimethylaluminum
WAXD	Wide angle X-ray diffraction
XPS	X-ray photoelectron spectroscopy

ABSTRACT

This thesis investigates the nature of reaction of different kinds of olefin polymerization catalysts with the surface functionalities of silica. One of the catalysts is *Cp_2ZrMe_2*, capable of reacting with the surface hydroxyl functionalities of silica and the other is *2,6- diacetylpyridine-bis-(2,6-diisopropylphenylanil) iron(II) dichloride*, which cannot react with the surface functionalities of silica.

It is known that the surface of silica contains various kinds of hydroxyl functionalities, the relative ratio of which can be controlled by calcining silica at different temperatures. The surface hydroxyls present at the surface of silica are either isolated or paired (geminal or vicinal). *Cp_2ZrMe_2* can react with both these types of hydroxyl groups generating different catalytic sites some of which can be inactive for ethylene polymerization. The stoichiometry of the reaction between the Cp_2ZrMe_2 and silica was examined. The nature of active sites was investigated using X-ray photoelectron spectroscopy. The effect of heterogenization Cp_2ZrMe_2 on the kinetics of ethylene polymerization as well as polymer properties was studied. A relationship between the nature of active sites and polymer properties was established.

In case of silica supported iron catalyst X-ray photoelectron spectroscopy showed no significant change in the electronic environment of the metal center when compared with the unsupported catalyst. This indicates that the catalyst has no significant interaction with the surface functionalities of silica. Unlike Cp_2ZrMe_2, no beneficial effect of heterogenization was observed in this case. The supported iron catalyst showed a rapid decay of polymerization activity with time.

In another separate study, two late transition metal catalysts were supported onto the surface of a modified clay. One was a nickel catalyst known for generating branched polyethylene and the other, an iron catalyst, known to produce a linear polyethylene. Ethylene polymerization was performed using these two supported catalysts. The nature of the resulting polymer-clay nanocomposites was studied using X-ray diffraction and transmission electron microscopy. It was observed that the extent of exfoliation/intercalation of the polymers into clay depends on the experimental conditions used for the synthesis of the polymer.

LIST OF TABLES

LIST OF FIGURES

LISTS OF SCHEMES

1. Ethylene polymerization using supported metallocene catalysts

1.1. Introduction

The polyolefin industry is witnessing a continuing growth around the world. With opening of new markets worldwide and with the rise in the demand for new materials there is a competition for producing value-added products, resulting in an upsurge in both fundamental and applied research. Companies are diverting a substantial quantity of their revenues in research and development projects. This is leading to greater innovation in products and processes.

The discovery of metallocenes-methylaluminoxanes as a highly active catalytic system for olefin polymerization has stimulated substantial new research in the area of olefin polymerization (1). These single-site catalyst systems are capable of producing tailor made polyolefins with a precise control over the microstructure of the polymers. This was largely achieved by the appropriate choice of ligand environment. Several new polymers were made using metallocenes which could not be made by conventional Ziegler-Natta catalysts. For example Brintzinger and co-workers in the '80s first reported *ansa* rac- bis(indenyl)zirconium complex (2,3) capable of producing isotactic polypropylene. In 1988 Razavi and co-workers followed this by synthesizing Cp-Flu complex which was capable of synthesizing syndiotactic polypropylene (4). Since then there are numerous examples of metallocenes reported both in published and patent literature (5-9). The single site character of these catalysts leads to relatively narrow distribution of molecular weights (PDI ~ 2). One more interesting feature of metallocene is the ability to copolymerize ethylene with higher α-olefins. The extent of comonomer incorporation can be modulated by the choice of the ligand environment. Also the comonomer distribution on the polymer is more uniform compared to heterogeneous Zieglar-Natta catalysts.

The arrival of the late transition metal catalysts as an alternative to metallocenes has opened a new chapter in olefin polymerization catalysis. The first late transition metal catalyst used was a neutral nickel (II) catalyst with a chelating P$^\frown$O ligand, used for oligomerization of ethylene (10,11). Unlike the metallocenes these catalysts are tolerant to the heteroatoms, so much so, that in case of Ni (II) catalysts the preferred solvent is 1, 4-butanediol. In 1980 Ostaja-Starzewski (12) and Klaubunde et al (13)

modified this catalyst system by replacing the strongly bound triphenylphosphine ligand with a weaker phosphine oxide or pyridine ligand and, thereby, eliminating the necessity for a phosphine scavenger. Using these catalysts linear polyethylenes with very high molecular weight with high catalyst activity could be achieved. These catalysts were also found to be active in polar solvents like acetone, DMF or alcohol. In 1995 Brookhart (14,15) reported a new class of Ni and Pd based catalysts capable of polymerizing ethylene and other ∝-olefins. The unique feature of these catalysts is the capability to produce highly branched and high molecular weight polyethylenes.
In 1998, Brookhart (16), Gibson (17) and Bennet (18), reported cationic Fe (II) and Co(II) catalysts (Structure IV, Fig. 1), capable of polymerizing ethylene into highly linear and high molecular weight polymers. The activities of these catalysts were found to be extremely high. At the same time Grubbs and co-workers (19) disclosed a neutral Ni (II) ligand based on salicylaldemine catalysts (structure V, Fig. 1) capable of producing branched polyethylenes. Phosphine scavengers (e.g. $Ni(COD)_2$) were used to abstract PPh_3 attached to the metal and thereby generate the active species. The literature on late transition metal catalysts have been summarized in several recent reviews (20).

1.1.1. Need for supported homogeneous catalysts

Homogeneous metallocene catalysts have significant advantages for the synthesis of polyolefins with relatively narrow molecular weight distribution, high catalyst activity, excellent copolymerization activity and uniform comonomer distribution. Yet they are beset with certain disadvantages. These are, poor morphology of the polymer, reactor fouling, wherein, the polymers produced are deposited on the wall of the reactors, leading to a poorer heat transfer, short catalyst lifetimes and the need to use large excess of MAO as cocatalyst to realize reasonable catalyst activity. It has been observed that supporting the homogeneous catalysts onto an inert matrix several of the above-mentioned problems can be mitigated. Rendering a homogeneous catalyst heterogeneous also has the beneficial effect of improving the molecular weight of the obtained polymers. Furthermore, supported metallocene catalysts have attracted attention in view of the fact that they can be “drop in” catalysts in gas phase and slurry phase reactors which today use supported Mg-Ti catalysts.

1.2 Silica supported early and late transition metal catalysts

For reasons mentioned above supported metallocene catalysts has been an area of significant research throughout the last decade (21-25). Various kinds of supports, like silica, alumina, $MgCl_2$, zeolites, polymers etc. have been used for this purpose. However the most widely used solid support is silica. The reason why silica enjoys such an important role as a support is discussed in the following section.

1.2.1. Properties of silica

Of all the other solid supports known (e.g. alumina, zirconia, titania etc.) silica is the support of choice because of the following reasons (26),

1. Low chloride residue in the polymer leading to less color and corrosiveness.
2. No needs of prepolymerization step as the polymerization rates are generally more uniform.
3. Low cost of catalyst manufacture.

Broadly silica can be defined as material of formula SiO_2 or $SiO_2[H_2O]_x$, which is essentially amorphous. It has high porosity and high specific surface area. The surface of silica contains variable amounts of free hydroxyls, which are Bronsted acid in nature. Silica can be either natural or synthetic. Synthetic silica can be made either by a vapour phase process or by a liquid phase process. In the vapour phase process pyrogenic or fumed silica (also known as aerosil) is obtained by decomposition of precursors like $SiCl_4$ at high temperature. The hydrolysis agent is generally water vapour. Examples of liquid phase processes are the hydrolysis and condensation of sodium silicate, tetraalkoxysilanes in acidic solution. The silicas thus obtained are often called xerogels or aerogels.

The first silica-based olefin polymerization catalyst successfully used was the thermally activated chromium catalyst (27), popularly known as the Philips catalyst. This catalyst resulted in an efficient slurry based catalyst for the making of HDPE. The catalysts were synthesized by reacting the surface hydroxyls of silica with silyl chromate (VI) by high temperature activation (400-900ºC), which, in turn, reacted with ethylene to form the active site (28). Extensive research in this field revealed that

proper porosity of the silica is essential to get the desirable activity (29). It was also found that the average pore size of the silica affects the polydispersity and the molecular weight of the polymer produced (23). The porosity of the silica allows the gaseous monomer to diffuse to the active site. As the polymer chain grows the silica particles fragment exposing the monomer to newer catalytic sites. The specific surface area of silica used in such catalyst is very high. For a comparison, 15 g of silica with $300 m^{-2} g^{-1}$ of specific surface area is equivalent to the area of a football field.

The next important property of silica is related to its surface functionalities (30). Silica contains free hydroxyl groups on the surface, which are acidic in nature and can react with a suitable functional group forming a covalent bond. Different kinds of silinols are found on surface of silica and are depicted in Fig. **1.1** (31). They are:

(a) Single or isolated silanols,
(b) geminal silanols,
(c) triple terminal silanols, the existence of which is not universally accepted,
(d) hydrogen bonded hydroxyls, which can either isolated or vicinal and
(e) internal silanols, located inside the pores and not on the surface and, thus, not accessible to bulkier molecules.

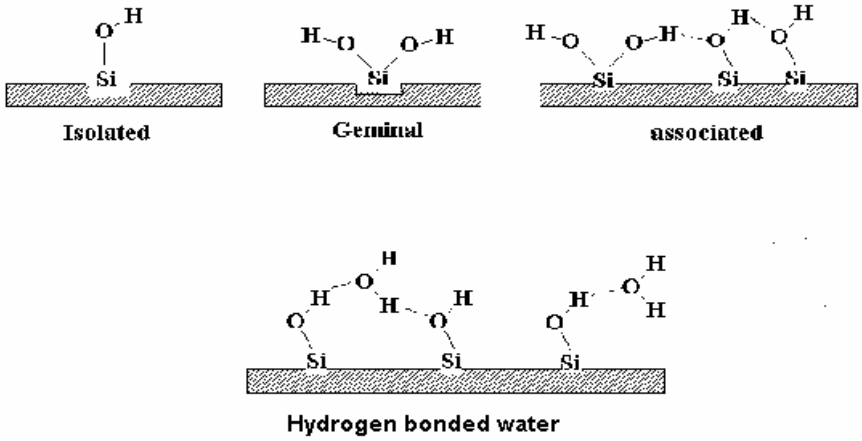

Figure 1.1: Various kinds of hydroxyl groups present on the surface of silica, sometimes associated with water molecules

The surface silanols exhibit diverse range of reactivities (Table **1.1**). The acidic property allows it to reacts with bases like ammonia, amines, amides or pyridines. The hydroxyl hydrogen can be substituted by reacting with thionyl chloride, HF and HCl gas, phosgene etc. It also reacts with organometallic reagents like methyl lithium, dimethyl zinc, methyl magnesium iodide and different organoaluminum compounds. It also reacts with various sesquestering agents like boron derivatives (diborane, boron trichloride), silanes (silicon tetrachloride, alkyl or alkoxysilanes, hexamethyldisilazane), Titanium compounds (titanium tetrachloride, alkoxytitanium), metallocenes, Cp_2Cr. Utilising this property of silica, the surface of silica can be modified for various applications.

Table 1.1: Reactions of silanol with various compounds

Compounds	Products
RNH_2	$Si—O^-RNH_3^+$
$SOCl_2$	$Si—Cl$
$MeLi$	$Si-OLi$
BCl_3	$Si-OBCl_2$
$(MeO)_3Si(CH_3)$	$Si-OSi(OMe)_2(Me)$
$Ti(O^iPr)_4$	$Si-OTi(O^iPr)_4$
Cp_2Cr	$Si—OCrCp$

Calcining silica at different temperatures changes the relative concentration of these surface OH groups of silica. Silica dehydrates in the following manner (30) during calcinations.

a) Heating at 200°C removes most of the adsorbed water.

b) Heating at 600°C, the hydrogen bonded hydroxyls get eliminated with the removal of a water molecule and the formation of siloxane bridge. All the hydrogen bonded hydroxyls are completely removed at 800°C under vacuum.

c) Above 600°C, the silica surface mainly contains isolated and paired hydroxyls. Isolated single hydroxyls predominate.

The amount of surface hydroxyls groups is independent of the surface area of the silica. Normally the distribution of OH on the surface is 5 to1.5 OH per 100 Å, which also depends on the calcination temperature. Other than the silanols there are siloxane bridges which form the network of the silica matrix. Also the surface of silica contains a large quantity of adsorbed water molecules which are loosely bound to the surface through hydrogen bonding with silanols.

Several studies are extant in the literature on the characterization of surface silanol groups, using IR and NMR techniques, both, qualitatively and quantitatively. Infrared spectroscopy of the silanols exhibits a strong absorption mainly in the region 3800-3200 cm^{-1}. The silanol peaks of silica consists mainly of two parts, first, a broad peak in the region 3530 cm^{-1} due to the hydrogen bonded hydroxyls and a sharp peak at a higher absorption region of 3747 cm^{-1} due to the isolated hydroxyls. Also there is a absorption at 3715 cm^{-1} which has been assigned to terminal silanols (Fig. **1.2**).

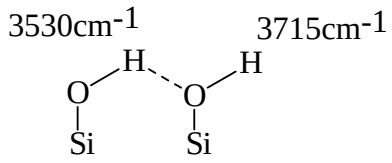

Fig. **1.2:** IR frequency of terminal and hydrogen bonded silanols in silica

Other then these, there is a peak in the region 3650-3670 cm^{-1}, attributed to the internal silanols. Burneau *et al* had compared the hydroxyl content of different kind of dehydrated silica after evacuation at 100°C (Fig.**1.3**) (32). For Aerosil (A), which is a kind of pyrogenic silica from Degussa with the free hydroxyl content of 4 OH nm^{-2}, absorption due to isolated silanol (3747 cm^{-1}) dominates over the other peaks. In comparison, the precipitated and gel silica (with free hydroxyl content of 12 and 14 OH nm^{-2} respectively) have a higher degree of hydrogen-bonded hydroxyls. The fourth kind of silica with a very high degree of free hydroxyls contains no peak due to the isolated hydroxyls. Thus a relation between the quantity and the kind of free hydroxyls could clearly be seen.

Morrow and Mcfarlan (33) showed the influence of steric factors inside the silica in chemical modification by H/D exchange of the surface silanols, using D_2O, ND_3 and deuterated methanol, isopropanol and *tert*-butyl alcohol. They found that, although the silanols in precipitated silica is more accessible for chemical modification than the pyrogenic silica by a factor of two, still with a particular reagent the same percentage of the total silanols react in the two silicas. It was also concluded that both kind of silicas contain nearly the same number of isolated silanols but the precipitated silica contains approx. 3.2 times the number of hydrogen bound silanols which are accessible to small molecules like water or ammonia.

The infrared study of thermally treated silica is very well documented in the literature. Gallas *et al* (34) showed that in case of Aerosil the intensity of the bands at 3715cm^{-1} and 3530 cm^{-1} simultaneously decrease even at 250°C, suggesting that the reaction of the type (1) and (2) taking place (Fig **1.4**) (Scheme **1.1**). In case of silica gel and precipitated silica, the absorption between other 3700 and 3730 cm^{-1} remain almost constant upto 250°C, but absorption at 3530 cm^{-1} decreases. Dehydroxylation of hydrogen bound hydroxyls is complete at 450°C. Above 600°C only isolated hydroxyls stay on the surface. Elimination of these hydroxyls is determined by the mobility of the protons on the surface.

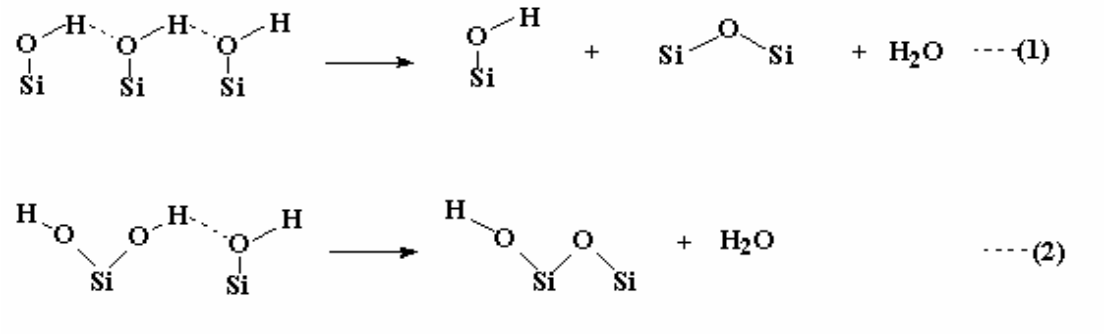

Scheme 1.1: Various kinds of dehydroxylation reactions that can take place in silica

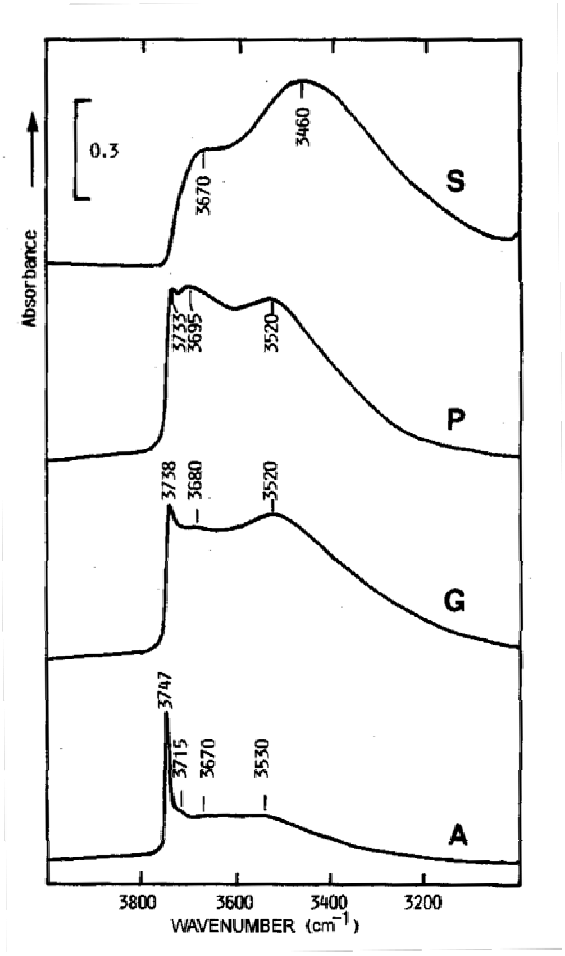

Fig. **1.3:** Infrared transmission spectra of silicas in vacuo at 20°C after pretreatment at 100°C, A: Aerosil; G: Gel; P: Precipitated; S: silica with very high hydroxyls content (700 OH nm^{-2}).

The surface hydroxyls of silica have also been studied using NMR techniques, mostly high-resolution ^{1}H and ^{29}Si NMR with different cross polarization (35). ^{29}Si NMR spectroscopy is the most useful technique for this purpose (Fig **1.5**). Mostly $^{1}H \rightarrow ^{29}Si$ cross polarization is used. Generally three signals are observed from such experiments; namely, one at -90 ppm/TMS due to the geminal silanols $=Si(OH)_2$, at -100 ppm/TMS due to the isolated silanols $\equiv Si(OH)$ and the third one at -100 ppm/TMS corresponding to the silanol bridge. Performing MAS NMR of the silicon nucleus and then coupling it with cross polarization with different contact time it is possible to estimate two important parameters, f_g, the fraction of geminal silanols over all the silanols, and f_s, the fraction of silanols over all silicon species. From such a study lot of information regarding the properties of silica can be understood. It is also possible to estimate the fraction of paired and isolated silanols over the total silanols using such techniques.

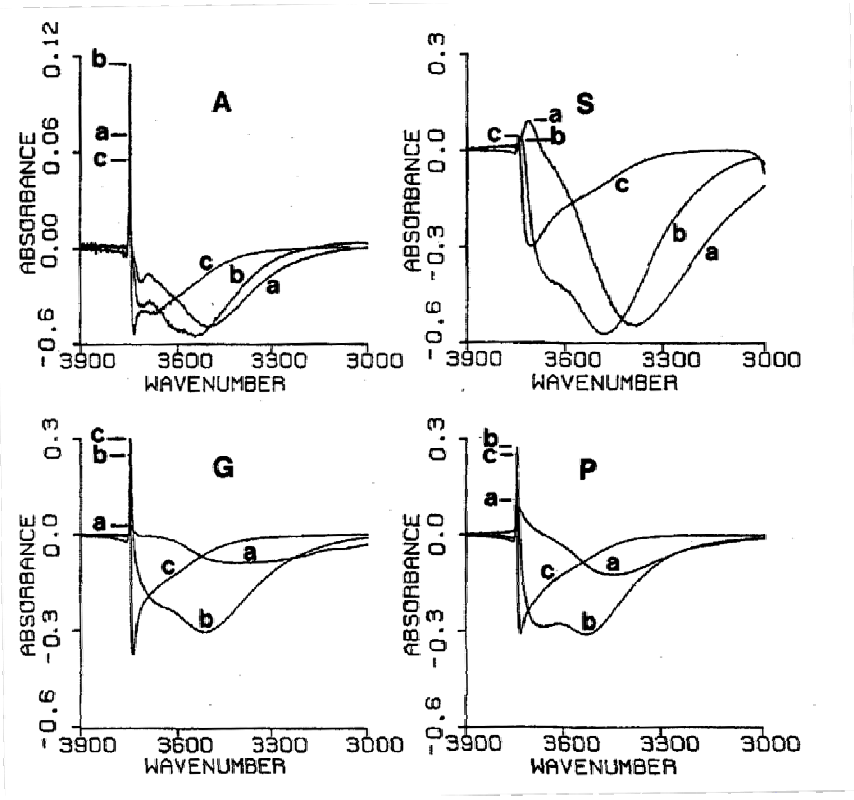

Fig 1.4: FTIR spectra of different kinds of silica heated at different temperatures; (a) 250-100°C; (b) 450-250°C; (c) 600-450°C. Meaning of A, P, G and S are the same as in Fig. **1.3**

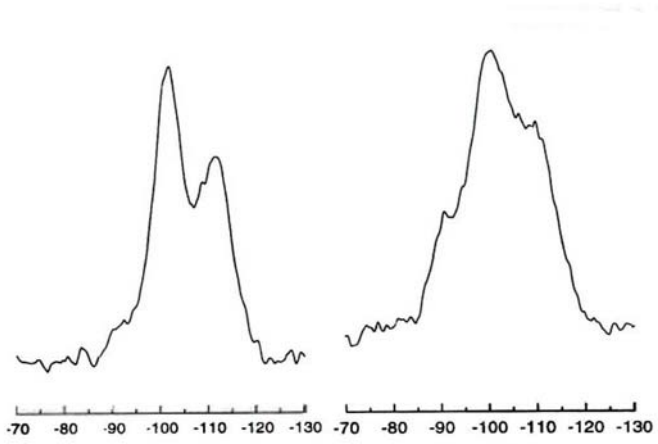

Fig 1.5: ^{29}Si CP/MAS NMR spectra of two silicas prepared by two different methods, (left) precipitated silica; (right) pyrogenic silica

1.2.2. Silica supported group IV metallocenes

Silica is the most extensively studied support in olefin polymerization catalysis. Homogeneous metallocene exhibit high activity for ethylene polymerization, $>10^{10}$ g PE mol Zr^{-1} h^{-1}. Heterogenizing the homogeneous catalysts results in a significant loss in the catalytic activity. One of the reasons for this loss in the activity is the generation of sites which are no longer polymerization active. On the other hand homogeneous catalysts suffer significant loss in activity during polymerization due to the loss of catalytic sites. It is generally seen that heterogeneous catalysts possess longer catalyst lifetimes. Besides, several other advantages like higher molecular weights and better morphology can be obtained using heterogeneous catalysts.

1.2.2.1. Methods of supporting metallocenes on silica

There are several methods reported for supporting metallocene catalysts onto the surface of silica. Of them the two most extensively used methods are

- Metallocene reacted directly with silica.
- Metallocene supported on silica pretreated with organoaluminum compounds.
- Generation of the single site catalysts on the surface of silica.

In the first method silica support is brought into direct contact with a solution of metallocene. The solid part is then recovered by filtration, washed with a hydrocarbon diluent, to ensure the removal of physically adsorbed catalysts and finally dried under reduced pressure. Metallocenes are directly supported on silica using either high or low temperature. Kaminaka and Soga (36) and Soga and Kaminaka (37) used mild conditions (room temperature, for 10 min). The silica used in this method was calcined at 400°C for 6 h. Kaminsky and Renner (38) reported direct reaction of the catalyst with silica at high temperature (70°C) and longer time (16 h). Some of the reports of directly supporting metallocenes onto silica is listed in Table **1.2.**

The second approach, which has been predominantly used for the preparation of the supported metallocene catalysts involves the treatment of silica with a small quantity of MAO in a slurry of hydrocarbon diluent at room temperature. The pretreated silica is then added to a solution of the metallocene. The supported metallocenes thus obtained were found to be activated by MAO or by common aluminum-alkyls. In some of the cases the pretreatment of the silica was done by use of other aluminum alkyls, $(C_2H_5)MgCl$, MeLi and Me_3SiCl (41).

In another approach Chang reported the direct synthesis of aluminoxane on the silica surface, by contacting trimethylaluminum with the surface (42). The surface anchored MAO, thus synthesized was then reacted with a solution of metallocene.

In another method, metallocene is first reacted with MAO in a solution of toluene and the resulting complex treated with silica. Thus, a mixture of $Me_2Si(2\text{-}Me\text{-}4\text{-}Ind)_2ZrCl_2$ and MAO in toluene was allowed to stand for 18 h and then added to silica (43). This catalyst showed improved activity in propylene polymerization.

Table 1.2: Direct reaction of silica with metallocenes

Metallocene	Calcination of silica	Method of preparation	Reference
$CpTiCl_3$	800°C,3 h	100°C, 3 h	39
$Et[IndH_4]_2ZrCl_2$	400°C, 6 h	rt, 10 min	36
i-Pr(Flu)(Cp)$ZrCl_2$ or Cp_2ZrCl_2	400, 8 h	rt, 10 min	37
$Et[Ind]_2ZrCl_2$	500°C, 3 h	70°C, 16 h	38
$Et[Ind]_2ZrCl_2$ or Cp_2ZrCl_2	650°C, 5 h	70°C, 16 h	40

Some of the more recently developed methods for supporting metallocenes on silica are as follows:

- Incipient wetness method (44,45): In this method the silica-supported catalyst was synthesized from a solution of metallocene in a liquid monomer. The monomer was allowed to polymerize yielding a catalyst containing poly(hexane-1), poly(styrene) and poly(octadecene-1). These catalysts were then used for the polymerization of ethylene. These catalysts were reported to be to be active even after exposure to air for 5 h due to a protective coating of polymers over them.
- In situ supported metallocene catalysts (46,47): In this method the metallocene was supported to silica in situ, i.e., during the polymerization reaction. Thus $Et[Ind]_2ZrCl_2$ was supported to silica during the polymerization of ethylene, the activity of which was enhanced by the addition of trimethylaluminum. The kinetics of polymerization was shown to be characteristic of supported catalyst, i.e., low decay in activity with time.

There are several reports of silica-supported metallocene catalysts activated by borate cocatalysts. However, in order to get an active catalyst, it is necessary to passivate the silica support with an alkyl aluminum, to prevent the cationic species generated (as a result of the reaction between the metallocene and the activator) from deactivation due to the surface hydroxyls of silica. For example, Soga and coworkers have shown that $CpTiCl_3$ supported to silica and does not show polymerization activity with TMA, but on addition of $[Ph_3C][B(C_6F_5)_4]$ or $B(C_6F_5)_3$, it polymerizes propylene (48). In another method the metallocene was first alkylated with an alkylaluminum and then reacted with Al^iBu_3 pretreated silica. The resulting supported catalyst can be activated by $B(C_6F_5)_3$ for the polymerization of ethylene (49). Triisobutylaluminum is the most chosen among the common alkyl aluminums since it is known to be non-interacting with metallocenes.

In a method reported in a recent patent (50) the authors pretreated the activator $[N(H)Me(C_{18}H_{37})_2][B(C_6F_5)_3(C_6H_4OH)]$ with triethylaluminum and then supported on silica, also pretreated with triethylaluminum. A constrained geometry titanium catalyst $(C_5Me_5SiMe_2N^tBu)Ti(\eta^4$-1,3-pentadiene) was then added to the support followed by further addition of triethylaluminum. The supported catalyst was used for gas-phase ethylene-hexene copolymerization and claimed to have an improved productivity.

1.2.2.2. Ethylene polymerization using silica supported metallocene

Kaminsky and Renner (38) were among the first to polymerize ethylene using supported metallocene catalysts. The poly(ethylene)s they obtained were of much higher molecular weight in comparison to those obtained from homogeneous catalyst under similar conditions. Dufrenne et al. reacted Cp_2MCl_2 directly onto silica (51) calcined at 600°C and treated with hexamethyldisilazane (HMDS). The order of reactivity was $Cp_2HfCl_2 > Cp_2ZrCl_2 > Cp_2TiCl_2$. Sacchi *et. al.* compared ethylene polymerization using Cp_2ZrCl_2 in homogeneous and on dehydroxylated silica at 50°C (cocatalyst MAO, Al/Zr = 300,500) (40). Some of the observations made during this study are as follows:

a. The activity of the homogeneous catalyst is about ten times more than the supported catalysts. However the supported catalysts shows good activity even at

very low Al/Zr ratio. The activity of the silica-supported catalyst is less than that of the SiO_2/MAO supported catalyst.

b. While homogeneous catalysts do not polymerize with traditional alkylaluminum, some of the supported catalysts show activity even in combination with triisobutylaluminum.

c. The polymers obtained from both homogeneous and SiO_2/MAO supported catalysts similar molecular weights and melting points. The molecular weight of the polymers obtained with silica-supported catalysts is higher than that of SiO_2/MAO supported and the homogeneous catalysts.

Several papers have been published describing the effect of different parameters in the ethylene polymerization using supported metallocene catalysts. The most important of them are porosity of the support, activation temperature of silica, grafting temperature of the catalysts, polymerization temperature, effect of hydrogen during polymerization etc. Parameters like effect of reactor type, stirring speed (52) and even effect of light (53) are also reported. Effects of calcination temperature of silica upon polymerization activity and the polymer properties have also been reported (54,55).

Dos Santos et al. (55) supported $(nBuCp)_2ZrCl_2$ onto silica activated at 373-723 K and showed that the metal loading reduces with the increase in the activation temperature of silica (due to the depletion of the free hydroxyls at the surface of silica). However, a substantial amount of free hydroxyls were left, which was attributed to the limitation of accessibility of the bulky catalysts to the silanol sites. Also the polymerization activity was shown to increase with increase in the activation temperature of silica.

The effect of grafting temperature, grafting time and solvent upon the metal content on silica and ethylene polymerization, have been reported (56). The reaction of metallocenes with the surface of silica was almost instantaneous. Also the polymerization activities were lower for the catalysts which were grafted for a longer period of time. Maximum activity was achieved only when the support was grafted within 1 to 6 h. This was attributed to the hydrolysis of chloride ligands with time, destroying potential alkylating sites necessary for polymerization. The molecular weights of the polymers were found to be higher with catalysts grafted for 30 min to 6 h time-range.

Increase in the grafting temperature shows an increase in the metal content of the support. However the catalyst activity did not always increase with the rise in metal content. The highest activity was obtained when the temperature was kept 80°C. The effect of solvent (used during supporting) on the metal loading and polymerization activity was also studied. It was observed that when THF was used (in comparison to toluene, dichloromethane and chlorobenzene) the metal loading as well as polymerization activity was enhanced. Overall, the authors suggested that a grafting temperature of 723 K and an intermediate grafting time with non-polar solvent gave the best activity and narrowest molecular weight distribution.

In yet another publication (57) the same authors studied the effect of Al:Zr mole ratio, reaction temperature, monomer pressure and the age and concentration of the catalyst in silica supported $(nBuCp)_2ZrCl_2$.

Quijada et al. (52) reported that in case of supported metallocene catalysts the most pronounced influence on the catalytic activity is related to the type of support and its porosity. Two metallocenes, namely, $Et(Ind)_2ZrCl_2$ and Ind_2ZrCl_2 were supported on Aerosil (nonporous), EP10 (av. Pore radius ~ 110Å, mesoporous) and ES70 (av. Pore radius ~ 8-100Å, microporous). It was seen that aerosil showed the highest activity, since most of the catalytic sites are on the surface of silica and thus are more accessible to the monomers in comparison to the other two types of silica.

In a recent publication Lin and Sheu (58) showed the effect of method of preparation of the supported catalyst upon the polymer morphology. Two different methods were examined method, $(nBuCp)_2ZrCl_2$ was premixed with MAO and then treated with silica and in the second the same metallocene was treated with MAO pretreated silica. It was seen that in case of the premixed catalyst the polymers have large granular size and very few fine particles compared with polymer derived from the catalyst prepared by adsorption method. The same paper also reported that the polymerization activity of the latter catalyst was higher then the former.

In some of the publications hydrogen was used to control molecular weights obtained from supported metallocene catalysts. Soares and coworkers (59) reported that effect of hydrogen concentration on the behavior of MAO modified silica supported $Et(Ind)_2ZrCl_2$ and Cp_2HfCl_2. It was observed that the molecular weight and the molecular weight distribution do not change very significantly with change in the

hydrogen concentration in case of the zirconium catalyst. However in the case of hafnium catalyst the molecular weight is inversely proportional to the concentration of hydrogen. The difference was attributed to the difference in the sensitivity of the two catalysts towards the presence of hydrogen during the polymerization. The combination of the two catalysts produced high-medium range bimodal molecular weight distribution in the absence of hydrogen and medium-low range broad unimodal molecular weight distribution in presence of hydrogen. Thus, the MW peak corresponding to the polymer derived from hafnium catalyst moved towards the peak corresponding to the polymer derived from zirconium catalyst.

It is also possible to control the polydispersity of the polymers produced from a supported bimetallic system by varying the temperature and pressure of polymerization (60). Using a combination of $Et(Ind)_2ZrCl_2$ and Cp_2HfCl_2 it was shown that with an increase in the temperature the molecular weight distribution changed from bimodal distribution to broad unimodal distribution. This was explained by assuming that the activation energy for $Et(Ind)_2ZrCl_2$ sites is higher or that Cp_2HfCl_2 sites deactivates faster at high polymerization temperature. It was also observed that in case of the polymer derived from Cp_2HfCl_2 the molecular weight increases slightly with the increase in the monomer pressure. However in presence of hydrogen, which acts as a chain transfer agent and reduces the molecular weight, there is distinct rise in the molecular weight of the polymers with the increase in the monomer pressure. In case of the $Et(Ind)_2ZrCl_2$ it was observed that with the increase in the monomer pressure polymer molecular weight decreases in the low monomer pressure range (<690 Kpa). At higher monomer pressure the peak molecular weight is not affected by the change in the monomer pressure. In presence of hydrogen the molecular weight decreases with increasing hydrogen concentration in the low-pressure range, indicating chain transfer to hydrogen is significant, but, again, at high pressure the molecular weight is independent of the concentration of hydrogen.

Roos et al. (61) studied the influence of temperature on the gas phase polymerization of ethylene using silica supported $Me_2SiInd_2ZrCl_2$ catalysts. According to them the active centers of a supported catalyst act as a surface fixed microreactor, which produce polymer, independent of other microreactors. Therefore the deactivation of such as active center is not a function of the active center concentration. The kinetic measurement of the gas phase polymerization lead to the conclusion that the

deactivation is proportional to the rate of polymerization, which can be influenced by a number of parameters, like temperature and pressure. The most probable reason for deactivation is due to the fact that certain amount of insertions lead to deactivated sites due to the blocking of the active site by polymer chain or a complex activation and reactivation mechanism.

1.2.2.3: Mechanism of ethylene polymerization using silica supported metallocenes

To understand the mechanism of olefin polymerization on a solid surface poses formidable challenges. One possible approach is to study a homogeneous system that mimics the silica as a support for metallocene catalysts. Silisesquioxane complex (c-$C_5H_9)_7Si_8O_{12}$(OH) is an appropriate system for such a study (62). Duchateau et al. (63,64) prepared the mono and bis-silsesquioxane complex of monocyclopentadienyl titanium (IV) (Fig **1.6**). Both these complexes showed ethylene polymerization activity with MAO as cocatalyst. This implied that the titanium siloxy bond was cleaved in presence of MAO. However, reaction of $B(C_6F_5)_3$ with both the above complexes did not show any cleavage of the titanium siloxy bond as monitored by ^{19}F NMR spectroscopy.

In a more recent publication (65) it has been reported that an aluminosilsesquioxane is formed as a result of the reaction between trimethylaluminum and a silsesquioxane (Scheme **1.2**). This in turn reacts reversibly with Cp_2ZrMe_2 to form a species, which does not polymerize ethylene. The authors concluded that the aluminosilsesquioxane is not a strong enough Lewis acid, which can abstract the methide ion from the zirconocene to form the cationic species. This observation is inconsistent with the real system, where Cp_2ZrMe_2 supported onto silica, pretreated with trimethylaluminum, shows polymerization activity. The difference is attributed to the fact that these models of silica-supported catalysts are homogeneous in nature, which aggregate into a thermodynamically stable product unlike the heterogeneous systems. In other words the reaction of silica with metallocenes is kinetically controlled, whereas, the reaction of silsesquioxanes is thermodynamically controlled.

When silica is first pretreated with MAO, and then treated with a metallocene solution, there is no direct interaction between the support and catalysts. The free hydroxyls of silica first react with the MAO. The chemically tethered MAO acts as a bridge between the silica surface and the metallocene. Soga and Nakatani (66) and Soga and Kaminaka (67) proposed that the metallocene interacts with the anchored MAO, which can be activated by common alkylaluminum or MAO, as shown in Scheme **1.3**.

Chen and Rausch (68) proposed that the cationic metal center is trapped and stabilized by the multi-coordinating crown aluminoxane complexes (Scheme **1.4**). It was proposed that the cationic zirconium species floats over the solid surface, much like in solution, as the surface of silica is already covered by MAO. Consequently, the polymers obtained from homogeneous catalysts and the pretreated catalysts are similar in nature.

However supporting zirconocene on silica results in the enhancement in the catalytic lifetime and the polymer molecular weight. This phenomenon is observed due to the enhanced stability of the catalyst in the support matrix and suppression of the chain termination mechanism, commonly observed in homogeneous systems. Kaminsky and Strubel (69) have proposed that in case of the MAO pretreated silica support the enhancement of stability of the catalysts can be studied by monitoring the methane evolution during the supporting of the metallocene. In the case of homogeneous catalysts deactivation of the cationic species occurs due to a side reaction involving alpha hydrogen transfer between MAO and the metallocene, leading to the evolution of methane gas (Scheme **1.5**). It was observed that when TMA was used to study the methane evolution, no extra methane was evolved due to supporting of metallocene onto silica/MAO. The relatively low extent of deactivation in case of supported metallocene was manifested on the lifetime of the catalyst.

When the metallocene is directly supported on the silica surface, there exists a probability of a reaction between metallocene and the free hydroxyls on silica surface. Under these conditions the catalytic activities are reduced. For example Collins et al. (70) showed that $Et(Ind)_2ZrCl_2$ contacted with partially hydroxylated silica or alumina and then reacted with MAO exhibit no activity for propylene polymerization due to the decomposition of the catalyst on the silica surface (Scheme **1.6**). Another interesting observation is the change in the insertion mechanism upon supporting. For

example, $Me_2Si(Cp)(Flu)ZrCl_2$ polymerizes propylene in the homogeneous phase to produce syndiotactic polymers, but when supported on silica and activated by methylaluminoxane produces isotactic polypropylene (71).

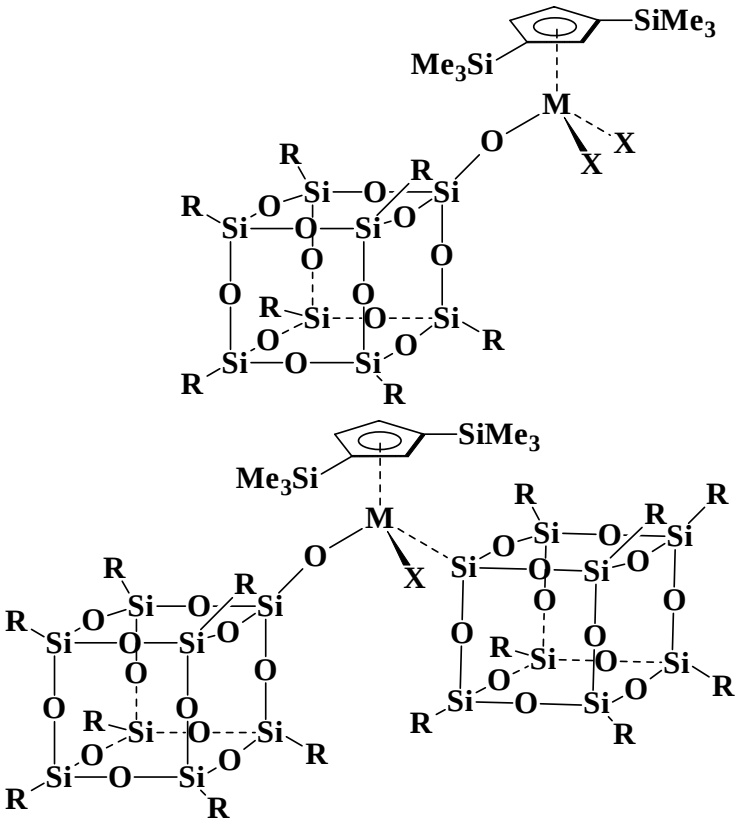

Fig 1.6: The mono (a) and the bis (b) silsesquioxane complex of monocyclopentadienyl Ti (IV)

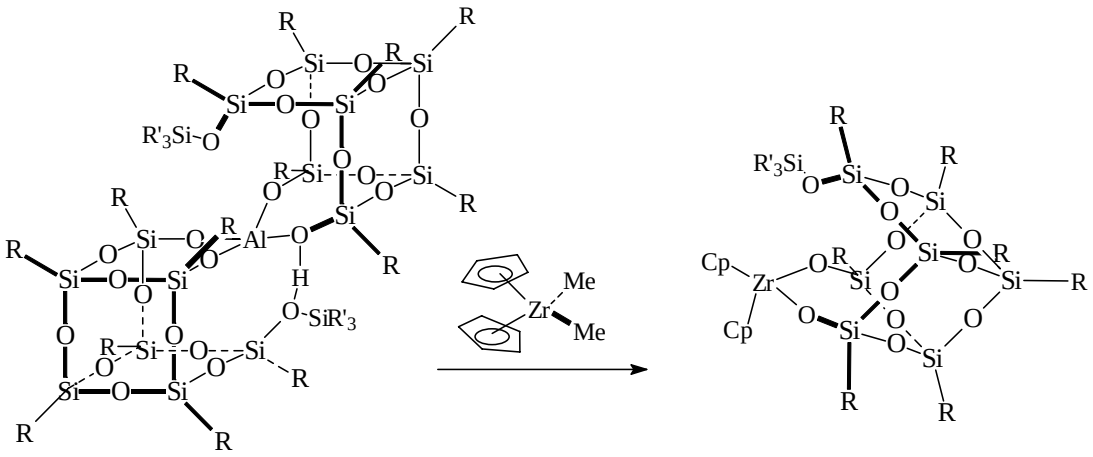

Scheme 1.2: Reaction of Aluminosesquisiloxane with Cp_2ZrMe_2

$$-\overset{|}{\underset{|}{Si}}-OH \;+\; MAO \longrightarrow -\overset{|}{\underset{|}{Si}}-O-MAO \;+\; CH_4 \qquad (1)$$

$$-\overset{|}{\underset{|}{Si}}-O-MAO \;+\; Cp_2ZrX_2 \longrightarrow -\overset{|}{\underset{|}{Si}}-O-(MAO)^{\delta-}(Cp_2ZrX_2)^{\delta+} \qquad (2)$$

Scheme 1.3: Possible interaction between MAO and metallocene in MAO pretreated silica

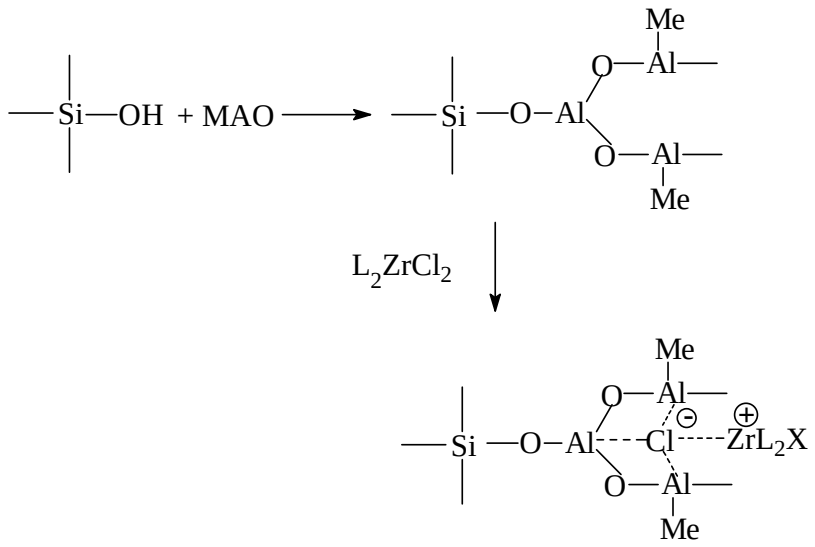

Scheme 1.4: Possible reaction between metallocene with silica pretreated with MAO as proposed by Chen and Rausch (68)

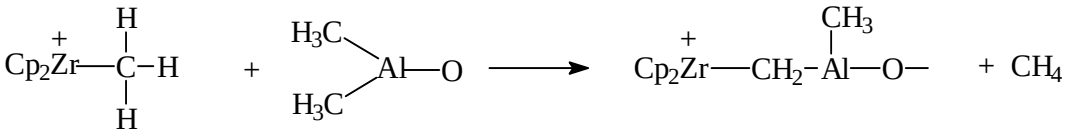

Scheme 1.5: Deactivation mechanism of metallocene with methylaluminoxane

While proposing the mechanism of ethylene polymerization using metallocene directly reacted with the silica surface some authors have suggested that part of metallocenes, tethered to the silica is displaced by methylaluminoxane (Scheme **7**) and become catalytically active (72). Dos Santos et al showed that when silica, evacuated at room temperature, is treated to $(n\text{-BuCp})_2ZrCl_2$ the catalytic activity is very low (55). This is attributed to the formation of unreactive chloride-free species (structure **II**, Fig. **1.7**). The structure **I** (Fig. **1.7**) is considered to be the active species, since in this case the chloride can be replaced by a methide ligand. However, it is known that the requirements for an active species are a metal-carbon bond and a vacant site. Structure **I** does not fulfill these requirements.

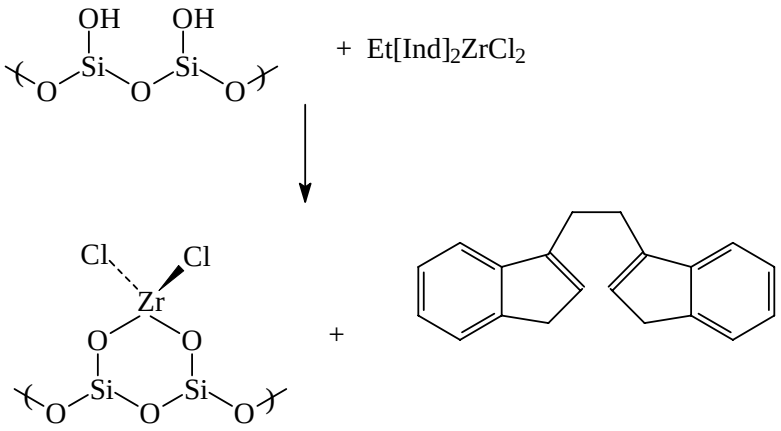

Scheme 1.6: Deactivation of metallocene on silica surface

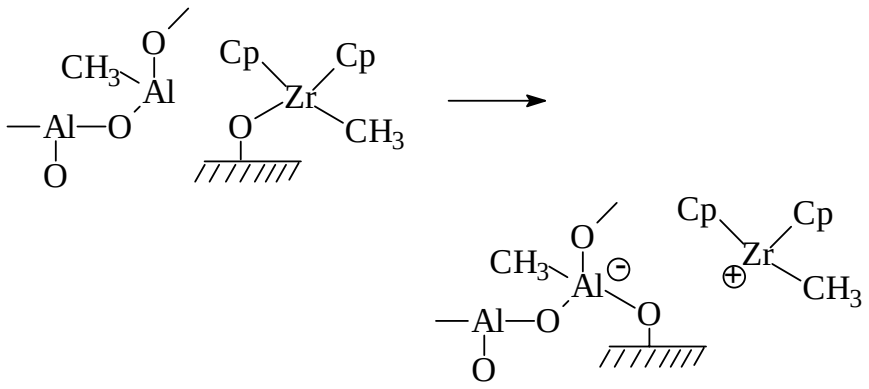

Scheme 1.7: Possible desorption of the metallocene from the silica surface in presence of MAO

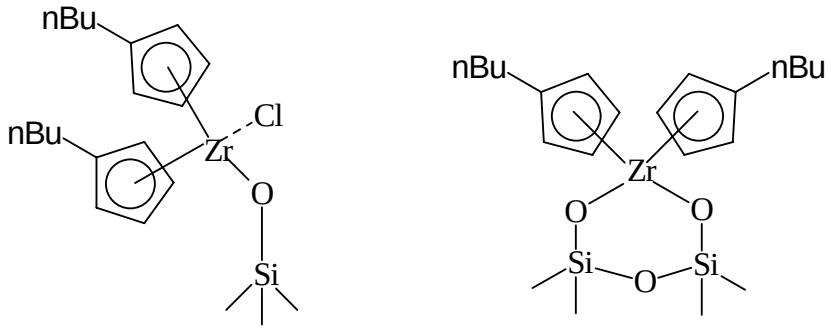

(I) **(II)**

Fig 1.7: Possible structures can be obtained by reacting $(nBuCp)_2ZrCl_2$ with the silica surface

Thus, it can be seen that many features of the mechanism of polymerization using supported metallocene catalysts still remains unclear.

1.2.3. Silica supported late transition metal catalysts

Late transition metal catalysts have emerged as another useful class of olefin polymerization catalysts. One particular feature of these catalysts is that they are less oxophilic and, thus, are less susceptible to polar impurities. Also these catalysts have the potential to polymerize polar monomers like acrylic esters.

For many practical applications late transition metal catalysts also needs to be heterogenized. Although several reports about supported late transition metal catalysts can be found in the patent literature, very few examples are available in the published literature. Vaughan and co-workers supported nickel 1,2-diimine complexes on silica, pretreated with methylaluminoxane (73). Based on earlier results obtained with homogeneous catalysts the authors calculated that the branching of the polymers will increase at the rate of 0.431/1000C branches per one psig increase in the pressure and 1.88/1000C branches per °C rise of the temperature. The authors performed the polymerizations at 220 psi and 63°C and expected a branching frequency 53/1000C and a Tm = 63°C. However they obtained a polymer with branching frequency of

34/1000C and a Tm = 91°C. The authors concluded that branching frequency decreases when supported catalysts are used. Hong et al supported [(2,6-di-iPrPh)$_2$DABAn]NiBr$_2$ and (2-py-CH=N-2,6-di-iPrPh)NiBr$_2$ on silica, pretreated with MAO or TIBAL (74). They observed that with an increase in the polymerization temperature in the range 0-50°C, the branching of the polymers increased, whereas the molecular weight of polymer decreased.

Semikolenova et al. reported the preparation of supported bis-(imino)pyridyl iron (II) complex on silica (75). Silica calcined at 800°and the Fe (II) complex was supported directly. In another approach silica was calcined at 450°C, pretreated with MAO, and Fe (II) complex supported on silica. The supported catalysts thus obtained could be activated even with triisobutylaluminum and showed high polymerization activity even at 70°. The polymerizations exhibited a steady state kinetics. The authors proposed that 'the fixation of the iron complex on the silica surface occurs by multiple bonding of LFeCl$_2$ with silica surface via interaction of pyridyl and phenyl groups of the ligand L with the OH group of silica'.

In another report (76) the catalyst 2,6-bis[iminopyridyl] iron(II) dichloride catalyst was supported on silica, previously pretreated with MAO. X-ray photoelectron spectroscopy of the metal center of the supported catalysts showed that a cation was formed after the reaction between the catalyst and the supported MAO. Compared with the homogeneous catalyst the supported catalyst showed lower activity. However the morphology of the polymer obtained was better in case of the supported catalyst.

Recently Alt and co-workers have reported a series of bis[iminopyridyl] iron(II) dichloride catalyst supported on silica, containing a small amount of water (77). The support was pretreated with TMA, which partially hydrolyzed on the surface of silica. A number of parameters like the effect of Al/Fe ratio, the effect of water content on the support, effect of the Al/silica molar mass ratio, influence of hydrogen concentration, reactor residence time and the steric and electronic effect of the catalyst, were examined.

A summary of patent literature concerning silica supported early and late transition metal catalysts is given in the Table **1.3**.

Table 1.3: Patent literature of silica supported metallocene and late transition metal catalysts (1996 – 2002)

No	References:	Catalyst	Support conditions	Polymerization conditions	Polymer properties.
1.	WO 9507939 123:199681 (1995)	$(nPrCp)_2ZrCl_2$	Silica dehydrated at 200°C, TMA added at 5°C in heptane. Catalyst added at 20°C, MAO added to the slurry, stirred and dried.	Ethylene+1-butene polymerization, T = 85°C, Comonomer feed 5%., t = 1 h,	Activity = 7.7 KgPE/mol/ Zr/h. at 10.2 bar, d = 0.9102 g/cc
2.	US 5240894 120:135396 (1993)	$Me_2Si(IndH_4)_2ZrCl_2$,	MAO+ metallocene in PhMe, ethylene prepolymerized in isopentane	Ethylene polymerization in hexane in presence of the solid and Et3Al, T = 60°C and P = 12.2 bar	Mw =281,000, activity = 51 kg/molZr/h and bd 0.307 g/mL.
3.	WO 9611960 125:59377 (1996)	$(1\text{-Me-}3\text{-}BuCp)_2ZrCl_2$	SiO_2 + MAO + metallocene reacted for 1 h and dried for 3 h	Ethylene/hexane polym. Modifier Kemamine AS 990-[octadecylbis(polyoxyethyl ene) amine] added , Added TMA	Reduced fouling of the reactor
4.	WO963242 3 125:329748 (1996)	$(nBuCp)_2ZrCl_2$, $(Ind)_2ZrCl_2$	Silica dehydrated at 600°C, preated by MAO. Catalyst added to the dry solid,	Ethylene polymerization at T = 70°C, $P(C_2H_4)$ and $P(H_2)$ = 10 bar, solvent pentane, t = 1 h.	yield = 308 g, MI = 0.72

5.	WO 9421691 123:144916 (1994)	$(nBuCp)_2ZrCl_2$	Silica dehydrated at 600°C, treated to TMA, dried, treated to to MAO + catalyst, dried till free-flowing	Ethylene-hexane copoly-merization, T = 70°C, Solvent pentane, added hexane 100 mL and TIBAL, P= 8.5 bar	Activity = 1.6 KgPE/mmolZr/h at 6.8 bar d = 0.914 g/cc,
6.	WO 9613530 125:58382 (1996)	$(nBuCp)_2ZrCl_2$ + $TiCl_4$	TMA added to silica containing 12.2% of water at 10°C, metallocene added followed by Bu_2Mg + $TiCl_4$, stirred at 74°C for 1 h, dried.	Ethylene-hexane copoly merization, T = 85°C, solvent hexane, added TIBAL, 1-hexene 1 ml, $P(H_2)$ = 0.13 bar, $P(C_2H_4)$ =10.5 bar, t = 30 min.	yield = 73 g, MWD = 40.8
7.	WO 9600245 124:261987 (1996)	(1-Me-3-$BuCp)_2ZrCl_2$	MAO + catalyst mixed, added to silica (preheated to 800°C) in toluene. Solid dried.	Ethylene-hexane copolymn. T= 70°C, solvent hexane, added TEAL, P= 10.2 bar,	MI = 1.98 g/10min, d = 0.917 g/cc. bd = 0.426 g/cc.
8.	EP 643100 123:144929 (1995)	1. Me_2Si(2-Mebenz Ind)$_2ZrCl_2$. 2. Et(4,7-Me_2IndH_4) $ZrCl_2$	Silica pretreated to MAO, catalyst added.	Propylene polymerization, in gas phase using two catalytic system in the same reactor zone	Activity = 27.5 KgPE/mol Zr/h, T_m = 145°C, G-modulus = 600 N/m^2.

9.	WO 9616093 125:87480 (1996)	1. (1-Me-3-BuCp)$_2$ $ZrCl_2$,	MAO + catalyst premixed, added to silica under nitrogen pressure.	Ethylene-hexane copoly - merization In a continuous fl-bed gas phase reactor, Solvent isopentane, added TEAL, P = 20.4 bar.	MI = 1.67 g/10min, d = 0.9118 g/cc
10.	WO 9618661 125:143540 (1996)	(nBuCp)$_2$$ZrCl_2$	MAO + catalyst premixed, added to silica (preheated at 600°C) in toluene, stirred under nitrogen pressure, dried.	Ethylene polymerization, solvent heptane, added TIBAL, T = 85°C, P = 10.2 bar, t = 30 min.	--
11.	WO952187 4 123:287194 (1995)	(nPrCp)$_2$$ZrCl_2$	Silica (pretreated at 850°C) added to catalyst in toluene, stirred for 1 h, dried.	Ethylene/butene copoly merization, semi-batch gas phase reactor, T = 100°C, 1-butene 5%, t = 1 h.	yield = 2g, Mw = 27,682
12.	WO 9604318 124:318150 (1996)	(1-Bu-3-MeCp)$_2$ $ZrCl_2$	Silica, containing 12.5% water is treated to TMA, catalyst added in heptane,, washed with hexane, dried.	Ethylene-hexene copoly merization, solvent hexane, added TIBAL and 20 mL 1-hexene, T = 70°C, P = 6.5 bar, t = 30 min.	yield = 45 g

13.	US 5238892 120:108036 (1993)	$(nBuCp)_2ZrCl_2$	Metallocene + TMA mixed in heptane. Added to silica containing 12.5% water. Heated to 65°C, dried.	Ethylene polymerization at 5 bar pressure, for 30 min.	yield = 9.2 g
14.	WO 9515216 123:287181 (1995)	Cp_2ZrCl_2	Silica (calcined at 280°C) is treated to catalyst.	Ethylene polymerization with MAO, T = 70°C, t = 1 h.	Mw = 72,000.
15.	WO 9530708 124:148195 (1995)	rac-Me_2Si(2-Me-4,5-Benz Ind)$_2ZrCl_2$	Catalyst + MAO mixed in toluene, added to silica (preheated at 800°C), dried, heated to 70°C for 9 h. Ethylene prepolymerized in isopentane	Propylene polym. In liquid phase, temp 65°C, propylene fed @ 60 Kg/h, hydrogen added, time 4 h.	Mainly isotactic polypropylene.
16.	EP 697419 124:261996 (1996)	(1,3-nBu(Me)Cp)$_2$ $ZrCl_2$	Silica (preheated at 250°C) pretreated by MAO in toluene, Catalyst added, stirred at 80°C fiiltered, washed with hexane, prepolymerized with hexene	Ethylene-hexene copolym. Solvent hexane, added TIBAL, 1-hexene 40 ml, T = 80°C, P = 8 bar-G, t = 2 h.	d = 0.924 g/cc, bd = 0.45 g/cc, MI = 0.15 g/10 mim

17.	WO 9426793 123:144877 (1994)	$(n\text{-}BuCp)_2ZrCl_2$	Silica containing 12.5% water treated to TMA, catalysts in heptane added at 74°C for 1 h. Solid dried.	Ethylene polym. In heptane + TIBAL, P = 10.2 bar, T = 80°C, t = 30 min.	yield = 79 g, d = 0.95 g/cc, MI = 0.6 dg/10min.
18.	EP 704461 125:11744 (1996)	rac-Me_2Si(2-Me-4-PhInd)$_2$ $ZrCl_2$	MAO reacted to silica (preheated at t200°C). Catalyst added + TIBAL. Propylene prepolymerized, washed.	E-P copolymerization, solvent hexane, added TIBAL, T=50°C, P = 2 bar, t = 1 h.	MI = 20 g/10 min, MWD = 2.4, ethylene 2.4%, T_m = 127°C.
19.	EP 619326 122:266294 (1994)	$Et(Ind)_2ZrCl_2$	Silica (calcined at 700°C) pretreated to MAO.Catalyst added, prepolymerized with ethylene, washed with hexane.	Ethylene polymerization, solvent toluene+TIBAL+ $PhNHMe_2^+[B(C_6F_5)^-]$, T= 70°C, P= 4 bar, t = 30 min.	MI = 0.819 g/10 min, bd. = 0.34g/mL.
20.	WO 9702297 126:186527 (1997)	Me_2Si(2-Me-4-Ph Ind)$_2ZrCl_2$	Silica (calcined at 600°C) pretreated to MAO, catalyst added, stirred, dried. Prepolymerized with propylene	Propylene/hexane polym. Solvent hexane, added TEAL, T = 60°C, t = 20 min.	$\%C_6$ = 3.5%, T_m = 128°C.

21.	EP 780402 127:109333 (1997)	Me_2Si(2-Me-4-Ph Ind)$_2ZrCl_2$	Catalyst treated to MAO, in toluene added to silica, stirred dried.	Propylene polymerization, T = 65°C, Added TEAL.	Activity = 122 gPE/molZr./h. MWD = 2.3, isotactic.
22.	WO 9729138 127:206059 (1997)	1.Cp_2ZrCl_2, 2.$Me_2SiInd_2ZrCl_2$	Catalyst pretreated to MAO, added to silica (dried at 800°C). Prepolymerized with ethylene in case of latter catalyst.	Ethylene polymerization in NaCl bed+ TMA, T =110°C, P = 2.7 bar, t = 60 min.	1. Mw = 72,000, MWD = 4.4, 2. Mw = 48,000, MWD = 4.3.
23.	WO 9635729 126:75340 (1996)	1. $EtInd_2ZrCl_2$ 2.$Me_2SiInd_2ZrCl_2$ 3. $iPrCpFluZrCl_2$	Catalyst pretreated to MAO, added to silica, solvent toluene, dried.	Ethylene, propylene polymeriza-tion solvent toluene, added TIBAL, T =100°C, t = 90 min.	Varied results.
24.	WO 9724375 127:136146 (1997)	(1-Me-3-BuCp)$_2$ $ZrCl_2$	Silica (calcined at 600°C) pretreated with MAO, Catalyst added solvent toluene, vacuum dried at 79°C.	Ethylene/hexane, ethylene/ butene polymerization solvent butane, T = 75°C, P = 20.4 bar, t = 40 min.	d = 0.9133 g/mL, free flowing powder.
25.	WO 9705178 126:225666 (1997)	Me_2Si(2-MeBenz Ind)$_2ZrCl_2$	Catalyst pretreated with MAO, added to silica (heated at 800°C), stirred, dried.	Propylene polymerization, liq. propylene+ TEAL, T =65°C, t = 60 min.	T_m = 143.2°C, Mw = 200,000.

26.	WP 9634020 126:8806 (1996)	$(1\text{-Me-3-BuCp})_2ZrCl_2$	Silica (heated at 800°C) pretreated to TMA, Catalyst+$[DMAH]^+[B(C_6F_5)_4]^-$ added in toluene, T =25°C, dried.	Ethylene/hexane copolymerization Solvent isopentane +TEAL, T = 65°C, P = 20.4 bar,	MI = 15.22 g/10 min, d = 0.9107, bd = 0.449 g/mL
27.	WO 9729134 127:206057 (1997)	$(1\text{-Me-3-BuCp})_2ZrCl_2$	Catalyst pretreated with MAO, added to silica (preheated at 600°C), solvent toluene, dried at 75°C.	Ethylene/hexane polymerization solvent isobutene/TEAL, T = 85°C, P = 22.1 bar, t = 40 min.	bd = 0.40 g\mL
28.	WO 9731035 127:234740 (1997)	$Me_2Si(IndH_4)_2ZrCl_2$	Metallocene added to silica (preheated at 200°C), dried. Metallocene treated to MAO added to solid, dried.	Propylene polymerization, in liq. propylene, T = 70°C, t = 1 h.	MI = 25 g/10min, T_m = 147°C, %soluble =2.4%
29.	WO 9634898 126:31801 (1996)	$(nBuCp)_2ZrCl_2$	Silica calcined at 500°C, catalyst+ MAO added. Solvent toluene T = 25°C, time 1 h.	Ethylene/hexane copolymerization Solvent isobutene, P = 5 bar, T = 80°C, 1-hexene 40 ml, t = 1 h.	MI = 2.7 kg/10 min, bd = 0.39 g/mL, av. particle size 0.37 mm.

30.	EP 790259 127:206066 (1997)	$Et(Ind)_2ZrCl_2$, $Et(IndH_4)_2ZrCl_2$.	Catalyst Treated with MAO, Added to silica, T = 110°C, t = 90 min, solvent toluene, washed, dried.	Ethylene/hexene copolymerization, solvent toluene + TIBAL, P = 2.2 Mpa, T = 70°C, t = 1 h, Hexene = 2.44 wt%	bd = 0.25 g/mL MI = 0.06 MWD = 7.4
31.	WO 9732905 127:248528 (1997)	$(nBuCp)_2ZrCl_2$	Catalyst treated with MAO, added to silica (calcined at 600°C), solvent toluene, dried.	Ethylene polymerization, initially with a chromium catalyst (Philips type), quenched with IPA, commenced with supported metallocene.	--
32.	US 6124229	$(nBuCp)_2ZrCl_2$	Silica (spray dried) pretreated with TMA+H_2O, solvent toluene. Catalyst added using spray-drier, T = 100°C	Ethylene/hexene copolymerization, T = 85°C, P = 13.8 bar, t = 60 min.	--
33.	WO 9634895 126:19434 (1996)	$(nBuCp)_2ZrCl_2$	Catalyst treated with MAO, added to silica (calcined at 600°C), solvent toluene,	Ethylene/hexene copolymerization Solvent hexane, P = 10 bar, T = 70°C, t = 1 h.	Mw = 100,000, MWD = 2.65, d = 0.93 g/mL, hexene content = 2.5 wt%.

34.	US 5643847 127:122104 (1997)	(Cp)(Cp*)$ZrMe_2$	Silica (calcined at 600°C), treated with $B(C_6F_5)_3$ in toluene, followed by catalyst, solvent toluene,	Ethylene polymerization, Solvent toluene + TEAL, T = 60°C, P = 5.17 bar, t = 30 min.	Mw = 261, 000. MWD = 2.49.
35.	US 5629253 127:34630 (1997)	$(nBuCp)_2ZrCl_2$	Silica (containing 12.5% H_2O) reacted to TMA, solvent heptane. Catalyst added, T = 74°C, t = 1 h, dried.	Ethylene polymerization, Solvent hexane + TIBAL, P = 10.2 bar, T = 80°C, t = 30 min.	yield = 79 g, d = 0.95 g/cc, MI = 0.6 dg/10 min.
36.	US 5602067 126:186526 (1997)	Cp_2ZrCl_2 + $TiCl_4$	Silica (calcined at 600°C) treated with Bu_2Mg, then $TiCl_4$. Mixture of catalyst + MAO added, T = 59°C, t = 10 min.	Ethylene/hexene copolymeriza-tion, Solvent heptane + TMA, T = 85°C, $P(C_2H_4)$ = 13.8 bar, $P(H_2)$ =10 psi, t = 1 h.	Polymer with bimodal distribution.
37.	WO 9717136 127:51113 (1997)	$(nBuCp)_2ZrCl_2$ + $TiCl_4$	Silica (calcined at 600°C) treated with Bu_2Mg, then $TiCl_4$, solvent isopentane, T = 50°C. Metallocene added, solvent toluene, T = 45°C, dried.	Ethylene/hexene polymerization, fluidized bed reactor, T = 90°C, $P(C_2H_4)$ = 12.2 bar, added H_2.	d = 0.949 g/cm^3

38.	EP 816394 128:128398 (1998)	$Me_2Si(Me_4Cp)(N bu^t)TiMe_2$	Silica (calcined at 500°C) pretreated with TMA, solvent hexane. $B(C_6F_5)_3$, catalyst added, solvent toluene, dried. Prepolymerized with ethylene	Ethylene/hexene copolymerization, P = 6.5 bar, T = 70°C, t = 127 min, added H_2 + TIBAL	Activity 22.5 gPE/molTi./h/bar
39.	US 5719241 128:154527 (1998)	1.Cp_2ZrCl_2, 2. $Et(Ind)_2ZrCl_2$	Silica pretreated with MAO, solvent toluene, catalyst added, washed, dried.	Ethylene/hexene copolymerization, with a mixture of supported catalyst 1. and 2. in 2:1, solvent isobutene, P = 40 bar, added H_2 + TIBAL	Polymer with broad MWD (~35)
40.	WO 9802246 128:115374 (1998)	$(nBuCp)_2ZrCl_2$	Catalyst treated with MAO in toluene, added to silica (calcined at 250°C), T = 45°C, t 16 h. dried.	Ethylene/hexene copolymerization, solvent heptane, T = 70°C, P = 8.7 bar, t = 1 h. hexene 100 ml + TIBAL.	Activity = 12 kg/molZr/h. MI = 19.6, d = 0.922 g/cm^3, $\%C_{69o}$= 1.9%
41.	WO 9805422 128:141185 (1998)	$(nBuCp)_2ZrCl_2$ + $TiCl_4$	Silica (calcined at 250°C) treated with catalyst+ MAO. Silica treated to Bu_2Mg, two components mixed, $TiCl_4$ added, in pentanol/heptane, dried.	Ethylene/hexene copolymerization, solvent heptane+ TEAL, T = 90 °C, P = 13.6 bar, t = 1 h, added H_2.	Bimodal distribution.

42.	EP 839835 129:4980 (1998)	[(Bu^t)(Cp)SiMeCl]-TiCl2	Silica (calcined at 400°C) treated to catalyst, solvent toluene, T = 40°C, dried.	Ethylene polymerization, solvent heptane, P = 4 bar, Cocat. $[Me_2NH_2]^+[B(C_6F_5)_4]^-$, t = 15 min.	Mw = 337220, MWD = 7.2, bimodal distribution.
43.	WO 9813393 128:230835 (1998)	Me_2Si(2-Me-4-Ph Ind)$_2ZrCl_2$	Catalyst treated with silica (heated at 600°C), solvent hexane, dreid.	Propylene polymerization, solvent heptane + TEAL+ liq. Propylene, T = 70°C, P = 32.6 bar, t = 1 h.	Yield = 29 g.
44.	US 5605578	(Cp)(2,7-(PhC≡C)$_2$ Flu)$ZrCl_2$	Catalyst treated with MAO, added to silica pretreated with TMA, solvent toluene, t = 3 h.	Ethylene polymerization, solvent isobutane, T = 90°C, P = 30.6 bar, t =1 h.	MI = 100 dg/10 min, Mw = 8260, MWD = 3.53.
45.	WO 9742228 128:23277 (1997)	[$C_5Me_4(CH_2)_2NMe_2$]$TiCl_2$	Silica (dried at 400°C) treated with MAO in toluene, dried. Catalyst added in hexane slurry, t = 12 h, dried.	Ethylene/octene copolymerization, solvent hexane, P = 8 bar.	Bimodal distribution, MWD = 15, MW = 400,000.
46.	EP 849286 129:95833 (1998)	$Ph_2MeC(CpFlu)_2$ $ZrCl_2$	Silica pretreated with MAO, T = 115°C catalyst added in toluene, t 3 h, wshed dried.	Propylene polymerization, in liq. propylene + TIBAL, T = 60°C, t = 1 h, added H_2	bd = 0.36g/cc, MI = 11.5g/10min Mw = 114108, MWD = 4.3.

47.	US 5786291 129:149365 (1998)	a.$Me_2Si(IndH_4)ZrCl_2$ b.$Me_2Si(Me_2Ind)_2$ $ZrCl_2$	Silica (calcined 200°C) catalyst a added in toluene, dried. Catalyst b +MAO added to solid obtained.	Propylene polymerization, in liq. propylene + TMA, T = 75°C, t =1 h.	PP with no reactor fouling, MI > 1000 dg/min, T_m = 134.6°C.
48.	US 5763547 129:54717 (1998)	[(Bu^tN)(Me_4Cp)Si Me_2]$TiMe_2$	Silica (calcined at 600°C) pretreated with MAO, catalyst added t = 70 h.	Ethylene/octene copolymerization, T = 120°C, added H_2.	d = 0.91 g/cc,
49.	EP 853091 129:122990 (1998)	[(Bu^tN)(Me_4Cp)Si Me_2]$TiMe_2$	Silica (heated at 500°C) pretreated with TEAL, in hexane. Catalyst added in toluene, followed by $B(C_6F_5)_3$, dried.	Ethylene/hexene copolymerization, solvent pentane, T = 70°C, P = 6.5 bar, t = 233 min.	Activity = 10.9 Kg/molcat.h.bar, d = 0.9175 g/cc, MI = 2.10 dg/ min
50.	EP 824113 128:180767 (1998)	$Me_2Si(2\text{-}MeInd)_2$ $ZrMe_2$	Silica treated to catalyst in toluene, dried, suspended in Exxol	Bulk polymerization of propylene, T = 60°C, t = 1 h. cocat. p-(C_6F_4) $[B(C_6F_5)_2]_2$	Activity = 12.6 kgPP/molZr/h, no reactor fouling.
51. .	WO 9828350 129:109422 (1998)	$CpIndZrCl_2$	Catalyst treated to MAO in toluene, added to silica (calcined at 600°C), surface modifier AS 990 added, dried.	Ethylene/hexane copolymerization in fluidized bed reactor, T = 79C, P = 21.7 bar.	d = 0.9293 g/cc, bd = 0.334 g/cc, MI = 232 dg/10 min.

52.	WO 9747662 128:75794 (1997)	$Et(Ind)_2ZrCl_2$ + $TiCl_4$	Silica (heated to 200C) added to MAO treated catalyst, in heptane, reacted to Bu_2Mg + Et_3SiOH. $TiCl_4$ in heptane + pentanol added. Pre-polymerization with hexene.	Ethylene/hexane copolymerization in heptane + $Bu^i{}_2AlH$, T = 90°C, P = 13.6 bar., t = 30 min.	Polymer with bimodal distribution.
53.	WO 9818842 128:322590 (1998)	$(nBuCp)_2ZrCl_2$	Catalyst treated to MAO, added to silica heated at (250°C), dried.	Ethylene/hexane copolymerization, in Fluidized bed reactor, T = 84°C, P = 15 bar, t = 2.5 h, added isopentane + ash.	Polymer with d = 0.918 g/cc.
54.	WO 9845337 129:302956 (1998)	$Me_2Si(Me_3CN)(Me_4Cp)TiMe_2$	Silica (heated at 200°C) treated to TEAL + H_2O in toluene, catalyst + $B(C_6F_5)_3$ added, solvent removed.	Ethylene/butene copolymerization, T = 79°C, $P(C_2H_4)$ = 16 bar, P(C4) =5.4 psi, t = 30 min.	--
55.	EP 870779 129:276513 (1998)	Mixture of isospecific + syndio-specific metallocene	Silica (pretraeted with MAO), catalyst mixture of diff. ratio + MAO added.	Propylene polymerization in liq. propylene, T = 60°C, t = 1 h, added TIBAL + H_2	In case of 50: 50 mixture: bd = 0.31g/cc , MI = 4.2 g/10min, Mw = 217,000

56.	US 5789502 126:161961 (1998)	$Me_2Si(2\text{-}MeInd)_2ZrCl_2$	Silica pretreated with MAO, catalyst added solvent heptane.	EP copolym. T = 60°C, Propylene = 4 L/min, Ethylene = 20 L/min, H_2 = 80 L/min, t = 1 h, solvent heptane	Higher degree of C2 randomness in case of supported catalyst, in comp. To unsupported catalyst.
57.	WO 9747662 128:75794 (1997)	$Me_2Si(2\text{-}MeBenz Ind)_2ZrCl_2$.	Silica (pH = 5.5) treated to MAO, catalyst added in toluene, dried.	Propylene polymerization, T = 65°C, P = 25 bar, t = 90 min, added TIBAL.	Activity = 120 Kg/molZr.h, MI = 4.8 g/10min, PD = 1.8, xylene-soluble fraction = 0.3%
58.	WO 9844011 129:276521 (1998)	$Me_2Si(IndH_4)_2ZrCl_2$	Catalyst treated with MAO, added to silica, in toluene, washed, dried.	Ethylene/hexene copolym. In fluidized bed reactor, T = 79.4°C, P = 20.4 bar. added H_2.	Activity = 554 KgPE/molcat/h, d = 0.9190g/cc, Mw = 92,200, MWD =5.02.
59.	WO 9852686 130:38795 (1998)	MeC(Cp)(Flu)-1-(But-3-enyl)$ZrCl_2$	Catalyst traeted to MAO, added to silica treated to toluene, T = 20°C, prepolymerized with ethylene.	Pilot plant scale slurry loop reactor.	d = 0.941g/cc, MI = 17.2 dg/10 min.

60.	WO 9903580 130:139771 (1999)	$(nBuCp)_2ZrCl_2$	Silica (calcined at 600°C) treated to MAO, added to catalyst, traeted with TMA, solvent heptane, dried.	Ethyelene/hexene copolymeriza-tion, solvent hexane, T = 75°C, P = 14.2 bar, t = 1 h, added H_2	Activity = 2410 g/g h, MI = 18.1 dg/10 min, mol% Hexene = 1.9%
61.	WO 9902570 130:110751 (1999)	(!, 3-$Me_2Cp)_2Zr(CF_3SO_3)_2$.	Silica (calcined at 800°C) treated to TIBAL, T = 120°C. Catalyst treated to $B(C_6F_5)_3$, added to support, solvent toluene, dried.	Gas phase ethylene polymerization, added toluene, P = 8 bar, T = 75°C, t = 125 min.	yield = 27 g.
62.	WO 9909079 130:168800 (1999)	1. $Et(Ind)_2ZrCl_2$ 2. $(nBuCp)_2ZrCl_2$	Silica (calcined at 600°C) treated to Bu_2Mg, isopentane/butanol, $TiCl_4$ added. Catalyst treated to MAO, added to support, T = 50°C.	Ethylene/hexene copolymeriza-tion in heptane + TMA, T = 95°C, P = 13.7 bar, t = 1 h, added H_2.	HMW fraction: 1: 0.18; 2: 0.71. Activity: 1: 82900 kgPE/molZr/h 2: 32800 kgPE/molZr/h
63.	WO 9909076 130:154107 (1999)	$Me_2Si(2$-Me-4-Ph $Ind)_2ZrCl_2$	Catalyst treated to MAO in toluene, added to silica, dried	Propylene polymerization in presence of TEAL + H_2	MWD = 16.4, T_m = 147.1°C, MI = 260 g/10 min.

64.	GB 2323846 130:111252 (1999)	$(nBuCp)_2ZrCl_2$	Silica (calcined at 250°C) treated to MAO, T = 95°C, catalyst added in hexane, prepolymerized with ethylene.	Ethylene/hexene copolymeriza-tion In afluidized bed reactor.	% C6 = 9.5%, d = 0.93g/cc, MI = 0.9 g/10 min, T_m = 129°C, MWD = 3.5.
65.	WO 9914270 130:223980 (1999)	$Me_2Si(2,3,5\text{-}Me_3Cp)$ (2',4',5'-$Me_3Cp)ZrCl_2$	Silica treated to MAO, in toluene, catalyst added, dried.	Propylene polymerization in liq. propylene + TEAL, cocat. MAO.	mmmm = 0.941, Mw =133,800, MWD = 2.3
66.	WO 9931147 131:45238 (1999)	1. $nBuCp)_2ZrCl_2$ 2. $Me_2Si(2\text{-}MeInd)_2ZrCl_2$	Silica pretreated to MAO, catalyst added.	Ethylene/hexene copolymerization.	
67.	WO 9926989 131:5714 (1999)	$(nBuCp)_2ZrCl_2$	Catalyst treated to MAO, added to silica, calcined at 600°C, T + 79°C.	Ethylene/norbornene polymerization, solvent hexane + TMA, T = 90°C, t = 1h, P = 3.4 bar.	NB = 6.9 mol%, yield = 13 g, Mw = 73,700, MWD = 3.3

68.	WO 9952951 131:286952 (1999)	$Cp_2Zr(Cl)(Me)$, Cp_2ZrBz_2, $Cp_2Zr(Me)(OPhMe)$	Silica treated with aquous solution of CrO_3, reduced by CO at T = 380°C. Metallocene added, slurried, dried.	Ethylene polymerization, in i-Butane, T = 90-100°C, P = 31 bar, t = 20-40 min.	In case of Cp_2ZrBz_2: Activity = 95 Kg/molZr/h, MI = 0.9 g/10min, D = 0.993g/cc.
69.	US 5939347 131:158094 (1999)	Cp_2ZrMe_2	Silica (calcined at 500°C0 treated to $B(C_6F_5)_3$, BuLi and Ph_3CCl. TEAL, metallocene added to the catalyst.	--	--
70.	US 5968864 131:272349 (1999)	$Ph_2C(Cp\text{-}Flu)ZrCl_2$ $Me_2Si[2\text{-}MeInd]_2ZrCl_2$	Silica pretreated with MAO, in toluene, catalysts added, washed with hexane, dried.	Propylene polymerization in liq. propylene + TIBAL, T = 60°C, t = 1h.	yield = 322 g
71.	WO 9952949 131:299822 (1999)	$[(EtO)(Me)_2Si(CH_2)_6\ Cp]ZrCl_2$	Silica (calcined at 800°C) catalyst added in hexane, stirred for 18 h. Chemically tethered metallocene.	Ethylene polymerization in hexane, P = 27.2 bar, T = 80°C, t = 1 h . Cocat. MMAO-3.	Activity = 136.8 kgPE/molZr/h, Mw = 189,000, MWD = 2.64

72.	US 5965477 131:272341 (1999)	Cp_2ZrCl_2	Silica (calcined at 550°C) traeted to $MgCl_2$ in THF, catalyst added in THF, T = 65°C, washed, dried.	--	--
73.	US 5972823 131:310941 (1997)	$(Cp)(Cp^*)ZrMe_2$	Silica (calcined at 8--°C) treated to $B(C_6F_5)_3$ in toluene, washed dried. Catalyst added in toluene, washed dried.	Ethylene polymerization, T = 60°C, P = 5.1 bar, t = 30 min,	Mw = 261,000, MWD = 2.9.
74.	WO 9943717 131:200269 (1999)	$Me_2Si(2\text{-}Me\text{-}4\text{-}Ph\ Ind)_2ZrCl_2$	Catalyst added to silica in toluene, stirred, dried.	Propylene polymerization in liq. propylene + TIBAL, T = 60°C, t =1 h,	Activity = 23466 kgPE/ molZr/.h
75.	WO 9940131 131:144987 (1999)	$(nBuCp)_2ZrCl_2$	Commercially available Cr-SiO_2 calcined at680°C, is treated with MAO pretreated metallocene, dried.	Ethylene/hexene polymerization in isobutane, %C6 = 0.16, T = 94°C, P = 22 bar, t = 1 h.	Activity = 800 kg/molZr.h, Mw =135,000, MWD = 5.1

76.	WO 9958587 131:351822 (1999)	Me_2Si(2-Me-4-Ph Ind)$_2ZrCl_2$	Silica (calciend at 600°C) treated to metallocene pretreated to MAO, T = 50°C, t = 16 h	Propylene polymerization in stirred tank reactor, C3 = 80 kg/h, Added H_2 + TEAL in hexane.	T_m = 151°C, MWD = 3.7, %soluble = 0.5%, T_c = 111°C.
77.	WO 9948934 131:243761 (1999)	$(nBuCp)_2ZrCl_2$	Silica (calcined at 600°C) treated to Bu_2Mg in hexane, added BuOH + $TiCl_4$, metallocene added.	Ethylene polymerization in isobutane + TEAL, T = 85°C, P = 40.8 bar, H_2 added.	Mw = 501,000. MI = 1.59 g/10 min, Die swell = 22%,
78.	WO 9933563 131:88306 (1999)	$(nBuCp)_2ZrCl_2$	Silica (calcined at 600°C) treated by Bu_2Mg in heptane. BuOH + $TiCl_4$ added, T = 55°C, Catalyst + TMA added, T = 50°C, dried.	Ethylene/hexene copolymeriza-tion in hexane + TMA + MMAO, T = 95°C, P = 13.6 bar, t = 1 h, 1-hexene = 30 mL.	At TMA:MMAO = 2:0.3: Activity = 1856 KgPE/molZr/h
79.	WO 9967302 132:50396 (1999)	$(nBuCp)_2ZrCl_2$	Silica (calcined at 130°C) treated to TIBAL in toluene, $[Me_2NHPh]^+ [B(C_6F_5)_4]^-$ + catalyst added, T =- 80°C	Ethylene polymerization in isobutane + $BuMgC_8H_{17}$, T = 70°C, P =38 bar, t = 30 min.	Activity = 200 KgPE/molZr/.h

80.	WO-200012565	$Me_2Si(2\text{-}MeInd)_2ZrCl_2$	Silica, mixed with NH_4SiF_6, heated at 500°C for 4 h. Metallocene treated to MAO, added to the fluorinated silica.	Propylene polymerization, in liq. propylene, T = 75°C, t = 1h, added H_2	Activity = 200 kgPP/mmolZr/h, MI = 25.8, Mw = 149532, MWD = 1.82.
81.	WO 9961489 132:23271 (1999)	$Et(2\text{-}Bu^tMe_2SiOInd)_2ZrCl_2$	Silica (calcined at 100°C) treated to TMA in pentane, MMAO added, catalyst added in pentane, t = 15 min.	Ethylene polymerization in isobutane, T = 80°C, P = 5 bar, t = 1 h.	Activity = 610kg/molZr/h
82.	WO-200004059 133:89746 (2000)	$Me_2Si(2\text{-}Me\text{-}4\text{-}Ph\ Ind)_2ZrMe_2$	Silica (calcined at 600°C) treated to $HB(C_6F_5)_2$ in toluene, t = 1 h, washed, dried. Catalysts added, stirred, 30 min, washed, dried.	Slurry phase propylene polymerization in toluene + TIBAL + liq. propylene. T = 70°C, t = 10 min.	yield = 10.6 g, Mw = 553,000, MWD = 1.86
83.	WO 9965949 132:50404 (1999)	$(nBuCp)_2ZrCl_2$	Metallocene, treated with MAO, added to silica calcined at 600°C. stirred for 3 h. dried.	Ethylene/hexane copolymerization in a loop reactor, T = 85°C, P = 65 bar, added liq. propylene + H_2	--

84.	WO 9960032 132:3599 (1999)	$Me_2Si(Me_4Cp)(MeCp)ZrCl_2$	Metallocene reacted to MAO in toluene+ added to silica, t = 20 min, dried.	Ethylene/hexane copolymerization in fluidized bed reactor. T = 79.5°C, p = 20.4 bar, C6 = 1.07mol%, + H_2.	d = 0.9192 g/cc, MI = 8.8 dg /10 min. Mw = 128,500, MWD = 6.91.
85.	WO-200011047	$(1,3\text{-Me-BuCp})_2ZrCl_2$.	Metallocene treated to MAO in toluene, added to silica (calcined at 600°C), stirred, dried for 18 h.	Ethylene/hexane copolymerization in i-butene + TEAL, T = 85°C, P = 8.8 bar, t = 40 min,	Activity = 1619 KgPE /molZr/h
86.	WO-200004058	$(1,3\text{-BuMeCp})_2ZrCl_2$	Silica (calcined at 600°C) treated with $Al(C_6F_5)_2$. Catalyst in toluene added, stirred, dried.	Ethylene/hexane copolymerization in i-butane + TEAL = TIBAL, T = 85°C, P = 8. 8 bar, t = 40 min.	yield = 16.8 g.
87.	WO-200002931	$Me_2Si(IndH_4)_2ZrCl_2$	Metallocene pretreated with MAO at 80°C, added to silica, calcined at 600°C. Surface modifier Kemamine AS-990 added, T = 79°C, dried	Ethylene/hexene copolymerization in isobutane + TEAL, C6 = 20 cc, T = 85°C, P = 22.1 bar, t = 40 min.	Activity = 832.9 KgPE /molZr/h

88.	WO 9961486 132:23288 (1999)	$(1,3\text{-Me-nBuCp})_2ZrCl_2$	Silica, calcined at 600°C, is treated to MAO, at 66°C, catalyst added in toluene, dried.	Ethylene/hexene copolymerization In i-butane + TEAL, T = 85°C, P = 22.1 bar, t = 40 min, added kemamine AS-990.	Activity = 737.3 KgPE /molZr/h
89.	WO-200015671	$Me_2Si(N^tBu)(Me_4Cp)$ Ti (1,3-pentadiene)	Silica, calcined at 250°C, treated to TMA in hexane, catalyst added, stirred, dried.	Ethylene/butene copolymerization in hexane, T = 75°C, P = 1.3 bar, added H_2.	d = 0.944 g/cc, MI = 2.5 g/10min die swell< 175%.
90.	US 6239060	$Me_2Si(IndH_4)_2ZrCl_2$	Silica, modified with borax, treated with TMA in toluene, added to catalyst pretreated with MAO, dried.	Ethylene polymerization at 80°C.	Increased activity in case of borax modified catalyst.
91.	WO-200049748	$[Cp^*Ti]_2[Me_2C(C_6H_4O)_2]$	Silica, calcined at 250°C, treated to MAO, added to silica calcined at 700°C and treated to styrene-acrylonitrile, catalyst added, dried.	Styrene polymerization in toluene + TIBAL + MAO, T = 70°C, t = 2 h.	Conversion = 46.7%, highly syndiotactic, Mw = 540,400, MWD =2.22.

92.	WO-200019758	a. $Me_2Si(2\text{-}MeInd)_2 ZrCl_2$. b. $Me_2Si(nPrCp)_2 ZrCl_2$	Metallocene (a) treated to MAO, added to silica, calcined at 600°C, in toluene. Kemamine AS-990 added, dried. (b) added in toluene, dried.	Ethylene/hexene copolymerization in hexane + TIBAL, T = 85°C, P = 10.2 bar, t = 30 min.	At a:b = 0.33: Mw = 143,092, MWD = 12, d = 0.9457 g/cc.
93.	US 6221981 134:311553 (2001)	[(Ind)(Flu)C(Me)] $ZrCl_2$	Metallocene treated with MAO, added to silica treated with TMA, then prepolymerized with ethylene.	Ethylene polymerization in isobutane, T = 90°C	d = 0.93 g/cc, Mw = 105,000, MWD = 2.3.
94.	WO-200078827	$[Bu^t\text{-}O\text{-}(CH_2)_6Cp]_2 ZrCl_2$	Silica, heated at 800°C, reacted to catalyst in hexane, washed, dried. Chemically tethered catalyst.	Catalyst prepolymerized with ethyene + MAO. Polymerization at 80°C, P = 8.8 bar, t = 1 h, solvent hexane.	bd = 0.36 g/ml, Mw = 226,000, MWD = 2.6.
95.	WO 200153356	$Me_2Si(2\text{-}Me\text{-}4Ph\ Ind)_2ZrCl_2$	Silica treated to TIBAL in heptane, $[Me_2NHPh]^+ [B(C_6F_5)_4]^-$ + catalyst added, T = 80°C, dried.	Propylene polymerization in liq. propylene, T = 63°C.	Activity = 1891 KgPP /molZr.h

96.	US-2001000789 6 135:93034 (2001)	$Me_2Si(2\text{-}Me,4\text{-}Ph\ Ind)_2ZrCl_2$	Metallocene treated to MAO, is added to silica (calcined at 600°C), dried.	Propylene polymerization, in liq. propylene, added TEAL + decadiene, T = 70°C, t = 1 h.	MI = 26 dg/10 min, Mw = 167,000 , MWD = 8.8, T_m = 153.3°C.
97.	WO-200206357	$Me_2Si(N^tBu)(Me_4Cp)Ti(1,3\text{-}pentadiene)$	Silica (calcined at 250°C) treated to TEAL in hexane, washed, dried. Ionic activator $[NHMeC_{18}H_{37}][B(C_6F_5)_2(C_6H_4OH)]$ added, catalyst +TEAL added, dried.	Ethylene/hexane copolymerization in gas phase, T = 75°C, P = 9 bar, added H_2.	d = 917.3 kg/m^3, MI = 1.2 g/10min, productivity = 3400 g/gcat
98.	US-2002001344 0	$Me_2Si(2\text{-}Me,4\text{-}Ph\ Ind)_2ZrCl_2$	Metallocene treated to MAO, added to silica, washed, dried.	Propylene/1,9-decadiene polymerization in liq. propylene, T = 70°C, t = 1 h.	MI = 26 dg/ 10 min, Mw = 167,000 , MWD = 8.8, T_m = 153.3°C.
99.	WO-200110227	$Et(Ind)_2ZrCl_2$	Metallocene added to MAO, added to silica calciend at 600°C, dried.	Ethylene/hexane copolymeriza-tion T = 80°C, P = 16.2 bar, added TIBAL + H_2.	MI = 0.5, D = 0.918g/cc.

100.	US 6380328	{[2,4,6-$Me_3C_6H_2$)N CH_2CH_2]NH}$_2$Hf $(CH_2Ph)_2$. $Me_2Si(nPrCp)_2ZrMe_2$	Silica (calcined at 600°C) treated to $Al(C_6F_5)_3$. Catalysts added in toluene, dried.	Ethylene polymerization in isobutane + TIBAL. T = 85°C, P = 8.4 bar, t = 40 min.	Activity = 1656 KgPE /molHf/bar/h
101.	WO 200196419	Et[2-(Bu^tMe_2SiO) Ind]$_2ZrCl_2$	Catalyst treated to MAO, added to silica, dried.	Ethylene/hexene copolymeriza-tion in a gas phase reactor, T =75°C, P = 15 bar, added H_2.	Activity = 11kg/h, MI = 31g/10 min, Mw =49,000, MWD = 4.1
102.	WO-200226842	$Me_2C(Bu^tN)(Me_4$ Cp) Ti(1, 3-pentadiene)	Silica (calcined at 500°C) treated to TEAL, washed dried. Quinuclidine + catalyst added, $B(C_6F_5)_3$ added.	Ethylene/1-butene polymerization in gas phase T = 69°C, P = 16.32 bar, t = 30 min. added H_2.	yield = 45 g, Activity = 474 Kg copolymer/molTi/.h.
103.	WO-200220156	$Me_2Si(2\text{-}MeInd)_2$ $ZrCl_2$	Silica (calcined at 600°C) treated to TEAL, treated to isobutylaluminoxane, dried, catalyst added, dried.	Propylene polymrization in liq. propylene, T= 65°C, t = 1h.	Activity = 1243Kg/molZr/h, bd = 0.37 g/ml, T_m = 144.58°C,

104.	WO 200198380	(Cp)(1-MeC_5H_4B) $ZrCl_2$	Silica treated to hexamethyldisilazane, dried, Et_3B added, stirred dried. Catalyst + $B(C_6F_5)_3$ added in toluene dried.	Ethylene/hexene copolymeriza-tion in isobutane added hexene = 20 ml, TEAL + fatty amine. T = 70°C, P = 23.8 bar, t = 30 min.	Activity = 589 kgPE/molZr/.h, bd = 0.34 gm/mL.
105.	EP 1234837 137:186003 (2002)	Me_2Si(2-Me,4-Ph Ind)$_2ZrCl_2$	Silica (calcined at 150°C) treated to MAO in toluene, T = 150°C, washed, dried, catalyst added, stirred, washed, dried	Propylene polymerization in liq. Propylene + TIBAL, T = 60°C, t = 1 h.	Activity = 7100 KgPP/molZr/.h. bd = 0.46 g/cc, MI= 1.4 g/ 10min, Tm = 150.1°C, Mw = 431,000, MWD =2.8.
106.	WO 200296420	Me_2Si(2-Me,4-Ph Ind)$_2ZrCl_2$	Silica treated with NH_4SiF_6, heated to 500°C, $C_6H_5NEt_2$ + $B(C_6F_5)_3$ added in toluene, stirred. Catalyst added stirred, dried.	Propylene polymerization in hexane + TEAL, T = 65°C, C3 feed = 32 kg/h	MI= 100 g/10 min, Mw = 167,000 MWD = 2.2, MP = 152°C.
107.	WO 2002066524	(Bu^t_3PN)(Ind)$TiCl_2$	Silica treated to $(NH_4)_2SO_4$, dried at 600°C, treated to MAO in toluene, catalyst added.	Ethylene polymerization in fluidized bed reactor, T = 90°C, P = 13.6 bar, t = 1 h, added TIBAL.	Activity = 71,699 g PE/mmol.Ti/h

108.	EP 1213304 137:6599 (2002)	Cp_2ZrCl_2	Silica (calcined at 600°C) treated to MAO in toluene, catalyst treated to THF +LiCl, MAO added, mixed with silica, dried.	Ethylene/hexene polymerization in hexane, T = 70°C, t = 200 h.	No fouling, bd = 0.39g/cc, Tm = 123°C, MWD = 2.3.
109.	WO 9946304 131:214732 (1999)	2, 6 diacetyl pyridine bis (2, 6 diisopropyl anil)$FeCl_2$	Catalyst treated with MAO in toluene, treated to silica (calcined at 700°C), stirred T = 50°C, washed, dried.	Ethylene/hexene copolymeriza-tion in gas phase, added TIBAL, P = 8.1 bar, T = 80°C, t = 60 min.	Broad MWD polymers.
110.	WO 9946303 131:214731 (1999)	2, 6 diacetyl pyridine bis (2, 6 diisopropyl anil)$FeCl_2$	Catalyst treated with MAO in toluene, treated to silica (calcined at 700°C), stirred T = 50°C, washed, dried.	Ethylene/hexene copolymeriza-tion in gas phase, added TMA + H_2, P = 8 bar, T = 80°C, t = 60 min.	Mw = 892,000, MWD = 8.2
111.	WO 200024788	2, 6 diacetyl pyridine bis (2, 4, 6 trimethyl phenylanil)$FeCl_2$	Silica (calcined at 600°C) treated to MAO +toluene, washed, dried. Catalyst added in toluene, washed, dried.	Ethylene polymerization in gas phase, added TEAL + H_2, P = 0.8 bar, t = 1 h 18 min.	Activity = 3374 Kg/mol Fe/h/bar, MI = 3.74g/10min.

112.	WO 200015646	2, 6 diacetyl pyridine bis (2, 6-dimethyl, 4-Bu^{t}anil)$FeCl_2$	Silica (calcined at 250°C) treated to MAO in toluene, catalyst added, shaken, solvent decanted, dried.	Ethylene/hexene copolymeriza-tion in gas phase, added TMA + H_2, P = 8 bar, T = 80°C, t = 60 min.	Mw = 328,000, MWD =11.1.
113.	US 6492473	1. (N, N'-diisopropyl anil-acenapthe quinone) $NiBr_2$. 2. Cp_2*$ZrCl_2$	Catalysts treated with MAO, added to silica (calcined at 600°C), dried.	Slurry polymerization, in hexane + TMA, T = 75°C, P = 4.1 bar, t = 30 min.	Mw = 357,000, MWD = 2.9. Two polymer components as shown in TREF.
114.	US 6303720	{2,3-[diisopropyl-phenylimino]-1,4 (dithiane)}$NiBr_2$	Catalyst treated to MAO, added to silica in CH_2Cl_2, T = 0°C	Ethylene polymerization in toluene, T = 50°C, P = 6.1 bar, t = 30 min.	Rubbery polymer, Mn = 336,000 MDW = 2.22. ^{1}H NMR = 62 branches/1000C.

1.2.4. Chemically tethered catalysts on heterogeneous supports

1.2.4.1. Introduction

One approach to linking the olefin polymerization catalysts onto the surface of silica irreversibly is through a process of chemical tethering. A large body of literature on the subject of chemically tethering metallocenes, can be found (78-100). The main advantage of a chemically tethered catalyst is that it can prevent the catalyst from leaching out of the solid support during the course of polymerization. Also, by chemically tethering a catalyst on the solid surface the catalytic center remains unaltered.

1.2.4.2. Principles of chemical tethering

A chemically tethered catalyst is one, wherein, there is a covalent link between the catalyst and the support. This can be achieved by two different methods. One, by modifying the surface of the support and, the other, by modifying the catalyst structure. In both the methods the objective is to generate functional groups on the catalyst as well as the support surface which can react with each other to form a covalent bond.

The most widely used technique for tethering a single site catalyst on a support surface is to construct the ligand structure on the surface, covalently bound to the surface, and then adding the metal salt. In case of metallocenes one typical approach is to chemically attach a ligand, containing a cyclopentadiene ring, to the surface of the silica, using a reactive coupling agent like silane. Upon addition of a suitable metal salt the active site can be generated. In another approach the entire complex, with a reactive functional group, can be generated and then linked covalently to the silica surface.

While introducing a chemical tether in an organometallic complex certain points need to be remembered. First of all the introduction of a new functional group should not disrupt significantly the stereoelectronic environment of the metal center. Also during the tethering the reaction conditions should be chosen carefully. Finally, any other byproducts, formed as a result of the tethering reaction should be removed from the system.

1.2.4.3. Chemically tethered late transition metal catalysts

Kaul et al. have reported that 2,6-bis[1-((2,6-diisopropylphenyl) imino)ethyl] pyridine iron(II) catalyst can be functionalized with various alkenyl group to yield the corresponding alkenyl-functionalized ligands having different spacer moieties (101) (Scheme **1.8**). The modified catalysts were used for ethylene polymerization and were found to be self-immobilized on the polymer chain. Before supporting the catalyst on the surface of silica, the free hydroxyl groups of silica was functionalized with Si-H surface group, by treating the silica with tetramethyldisilazane (TMDS). In the second step the alkenyl functionalized [bis(imino)pyridyl)]iron(II) complex was reacted to the surface Si-H group using Karstedt catalyst. The immobilization of the catalyst was monitored using IR spectroscopy. The supported catalysts were active for the polymerization of ethylene and produced polyethylene with high molecular weight and broad molecular weight distributions.

In a recent publication Preishuber-Pflugl et al have attached a nickel diimine complex onto the surface of silica. The catalyst was modified using hydroxyl and amine functional groups, and was reacted to the surface of silica modified by TMA (102) (Scheme **1.9**). The amino-functionalized complex showed a polymerization activity of 580 kgPE/g of Ni. The polymers obtained showed molecular weights in the range of 10^5 and polydispersities of 3.5.

1.3. Supports other than silica for olefin polymerization catalysts

The other widely used supports for olefin polymerization catalyst are anhydrous magnesium chloride and alumina. Magnesium chloride is a well-known support for titanium based Zieglar-Natta catalysts. Magnesium chloride is an ideal support for such titanium halides because of the similarity of the ionic radii of Mg^{+2} and Ti^{+4} ions (103). Magnesium chloride, however, is far less studied in case of metallocene catalysts.

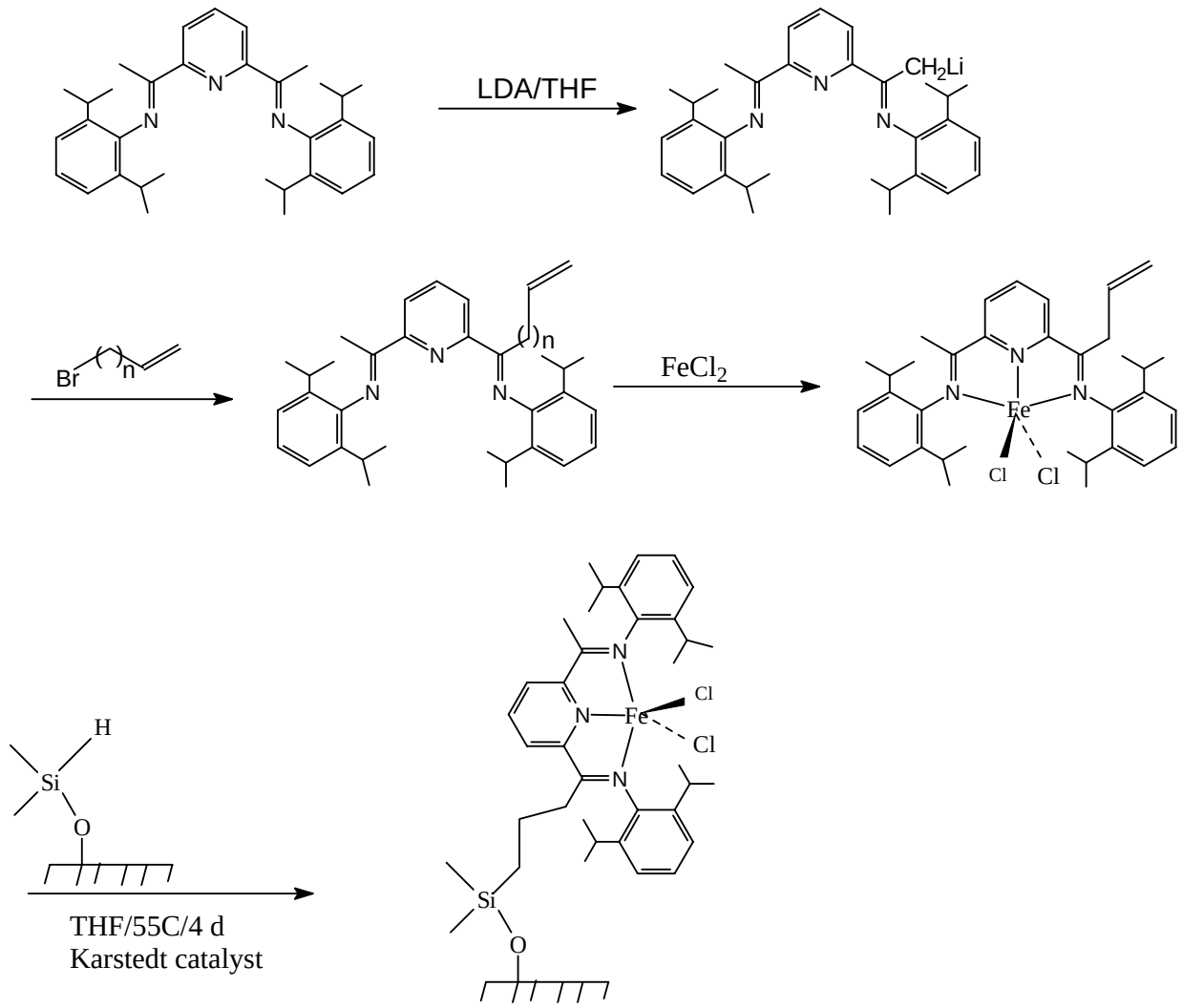

Scheme 1.8: Chemically tethered Fe (II) catalyst on the surface of silica

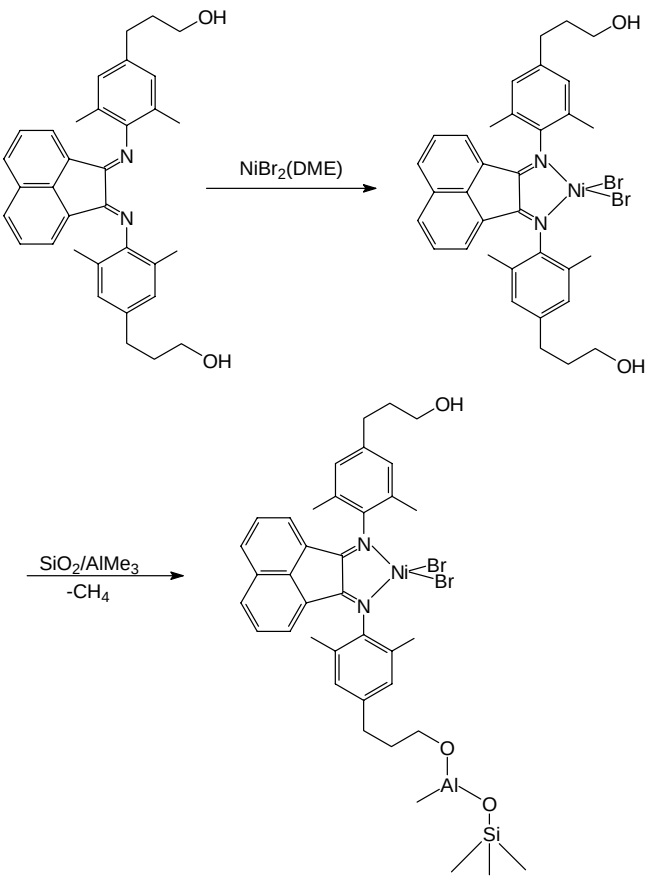

Scheme1.9: Chemically tethered Ni (II) catalyst on the surface of silica

$MgCl_2$ supported metallocenes was prepared by the reaction of BuMgCl and $SiCl_4$ in an electron donor solvent followed by supporting of metallocene (104). Satyanarayana and Sivaram reported the preparation of $MgCl_2$ supported Cp_2TiCl_2 catalyst by decomposition of a Grignard compound (105). The support was prepared by exploiting the solubility of both $MgCl_2$ and Cp_2TiCl_2 in THF. The authors showed a high rate of ethylene polymerization using a $MgCl_2$-Cp_2TiCl_2 complex. The catalyst exhibits steady state kinetics up to one hour at low Al/Ti ratios, suggesting that $MgCl_2$ confers unusually high stability to the catalysts. Soluble bivalent magnesium compounds such as Bu_2Mg, $(RO)_2Mg$, Mg-stearate are also used as a precursor for $MgCl_2$ support. Bailly and Chabrand reported the reaction of di(butyl) magnesium and t-BuCl in diisoamyl ether-hexane mixture producing $MgCl_2$ with a very narrow particle size distribution (106). Cp_2ZrCl_2 was taken in toluene in presence or absence of a proton donor such as n-butanol. Reaction with MAO formed an active

polymerization catalyst. The supported catalyst was employed for the polymerization of ethylene in a gas-phase process. Lin reported a one-pot synthesis of a $MgCl_2$ support by reacting Bu_2Mg to a mixture of MAO and *iso*-$BuAlCl_2$ followed by reaction of $(n\text{-}BuCp)_2ZrCl_2$ (107). The ethylene polymerization activity of this catalyst was double that of silica supported catalyst. Soga et al. used the metallocene $Cl_2Si(Ind)_2ZrCl_2$ and supported it on $MgCl_2$ (108). The Lewis acidity of the $MgCl_2$ was utilized to anchor the catalyst.

Sensarma and Sivaram reported a new method of preparation of $MgCl_2$ supported Cp_2ZrCl_2 by reacting magnesium with 1,2-dichloroethane in THF to produce $MgCl_2$.nTHF and adding a THF solution of metallocene (M = Zr, Ti) (109-112). The catalyst $CpTiCl_2$-MAO-$MgCl_2$ showed higher activity in xylene than the corresponding homogeneous catalyst.

Zeolites have also been explored as supports for olefin polymerization catalysts. The salient features of the zeolites are, large surface area, a well-defined pore structure and a narrow pore size distribution. In the method used by Woo et al. faujasite zeolite NaY (having a pore diameter 5 Å) was first treated with MAO, filtered, dried and then impregnated with Cp_2MCl_2 (M = Ti, Zr) to form the catalyst (113). The catalytic activities are lower than the homogeneous catalyst, but the molecular weights obtained were higher. The low activity was attributed to the small number of cages capable of accommodating both catalyst components, or due to lower rate of diffusion of the monomers to the catalyst site. Michelotti et al. have supported Cp_2ZrCl_2 onto HY zeolite and used it for polymerizing ethylene (114). A general decrease in the catalytic activity was observed, but higher activity was obtained when the support was pretreated with MAO and TMA.

In order to accommodate larger metallocenes such as $Et(Ind)_2ZrCl_2$ and to polymerize larger monomers, mesoporous molecular sieves have been explored as a support. The two most well-known mesoporous materials are MCM-41 and VPI-5 having pore size of approximately 40 and 13 Å respectively. Stereospecific polymerization of propylene was conducted using a rac-$Et[Ind]_2ZrCl_2$. The resulting polypropylene had a higher Tm (115). Rahela et al. supported Cp_2ZrCl_2 onto silica, MCM-41 and an aluminum- modified MCM-41 and compared the results (116). If was found that the aluminum-modified silica adsorbed the highest amount of catalyst. Also the incorporation of the aluminum in the MCM matrix increased the polymerization

activity of the catalyst. The order of polymerization activity of the three supported catalysts was Al-MCM-41>SiO_2>MCM-41. However there was no change in the molecular weights of the polymers obtained from various catalysts.

In a recent report TMA was partially hydrolyzed inside the cavity of a zeolite ZSM-5 by the water present inside the zeolite (117). Cp_2ZrCl_2 and $Et(Ind)_2ZrCl_2$ were heterogenized on the support surface and they were found to be active for the polymerization of ethylene even without addition of any cocatalyst. The molecular weights of the polyethylenes obtained were higher than those obtained using homogeneous catalysts.

In yet another report Costa Vaya et al. supported a zirconocene catalyst on HZSM-5 zeolite calcined at three different temperatures (118). The authors demonstrated a 'de-aluminization' of the zeolite framework, which increases with the increase in calcinations temperature, which leads to the formation of 'extra-framework aluminum' (EFAL). Higher activity of the catalyst was observed where the support was calcined at higher temperature. The authors speculated that the increase in the EFAL content increases the catalytic activity.

Various clays, like montmorillonite, hectorite, mica etc., have also been employed as supports in olefin polymerization catalysis. Clays have been extensively used as support in olefin polymerization, in the patent literature (119-125) and to some extent in the published literature (126). In the patent literature clay supported metallocenes have been used as catalyst for polymerization of olefins. The structures of clays comprise of layers of octahedral alumina sandwiched by layers of tetrahedral silica. Some of the trivalent aluminium centers are replaced by bivalent magnesium. This makes the creation of some negative charges, which is compensated by cations like Na^+. In swollen state organic ammonium salts can replace these sodium ions. This helps in the formation of organophilic layers of silicates.

The metallocene-supported clay are prepared by the following steps. First the clay layers are swollen in deionised water and thoroughly dried. This is followed by treatment of the clay with organoammonium cations or organoaluminium compounds (TMA). This modified clay is then treated with metallocenes in a slurry of organic solvents like toluene. Finally the slurry is dried and used for olefin polymerization.

Supporting of metallocene catalyst onto clay leads to the formation of nanocomposites. This involves formation of exfoliated clay in the polymer matrix. Late transition metal catalysts have also been supported on clay and used to polymerize olefin, leading to the formation of nanocomposites (127).

Inert polymers have also been employed as a support for olefin polymerization catalysis. Porous polyethylene (128) and granulated polypropylene (129) were both used for this purpose. However the most widely reported polymer support was polystyrene. Poly(styrene)-supported zirconocene was first reported by Nishida et al. (130). Styrene and divinylbenzene were copolymerized using AIBN as an initiator. The copolymer beads obtained were lithiated, using n-BuLi/TMEDA. This was then reacted with Cl_2SiInd_2 followed by addition of the metal salt. The catalyst thus synthesized obtained a structure $>Si(Ind)_2ZrCl_2$. A similar catalyst was made using $Cl(Me)Si(Ind)_2$ ligand, the structure obtained was $–Si(Me)(Ind)_2ZrCl_2$. Propylene was polymerized using the two catalysts. It was observed that the polymerization activity of the former catalyst did not change much with an increase in polymerization temperature. However in the latter case the activity increased significantly with an increase in polymerization temperature.

Kitagawa et al. reported (131) the copolymerization of 1-vinyl-4-(1-cyclopentadienyl-1-fluorenyl) ethylbenzene with styrene (Scheme **1.10**). The catalyst was obtained by metallation of the ligand framework. Different catalyst precursors were obtained by varying the comonomer content and, thereby, the metal content. Propylene polymerizations were performed using the resulting catalyst. It was observed that the syndiotacticity of the polymers decreased with the increase in the metal content in the catalysts. It was assumed that with the increase in the comonomer content the metal center could interact with more than one ligand center, due to the irregularity of the polymer chain and, thereby, produce catalytic centers capable of producing atactic or isotactic chains.

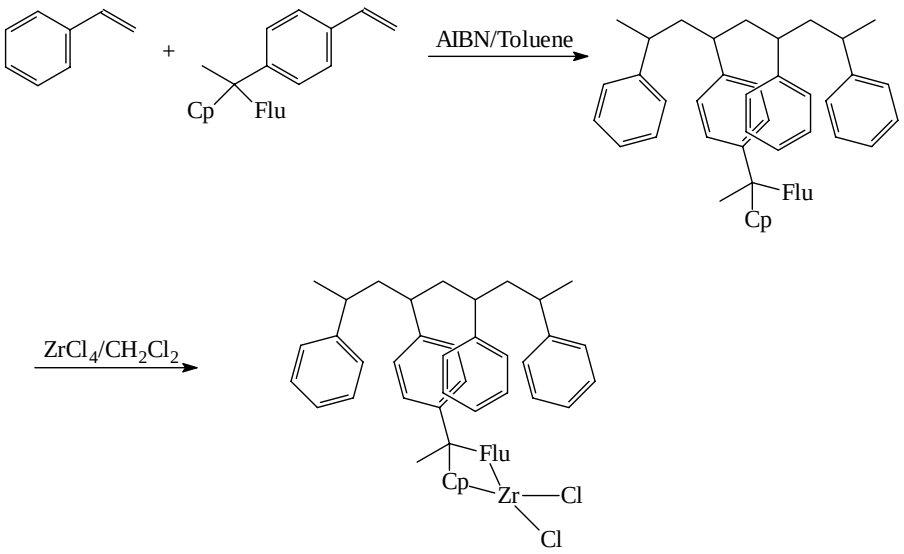

Scheme 1.10: Copolymer of 1-vinyl-4-(1-cyclopentadienyl-1-fluorenyl) ethylbenzene and styrene as support for metallocene catalyst

Roscoe et al. (132) functionalized polystyrene-co-(4-chloromethyl)styrene with a secondary amine HNRR' (Scheme **1.11**). This was then reacted with $HA^{+}[B(C_6F_5)_4^{-}]$. The resulting ionic pair was then reacted with Cp_2ZrMe_2 to generate the ion pair $[Cp_2ZrMe^{+}][B(C_6F_5)_4^{-}]$. This supported catalyst displayed excellent polymerization activity for the slurry phase copolymerization of ethylene and 1-hexene with a high comonomer incorporation. The polymer particles were found to replicate the catalyst beads.

Liu et al. reported (133) a novel polymer supported metallocene catalyst with a crosslinked poly (styrene –co-acrylamide), with a homogeneous distribution of acrylamide (32% acrylamide). It was found that the MAO interacts with the polymer through the nitrogen and the oxygen atom of the acrylamide moiety. Polymerization of ethylene and copolymerization with 1-octene were performed. The addition of comonomer lead to the lowering of the polymerization activity in comparison to that of the homogeneous catalyst, but the comonomer distribution of the copolymer obtained was similar to that obtained with homogeneous catalysts.

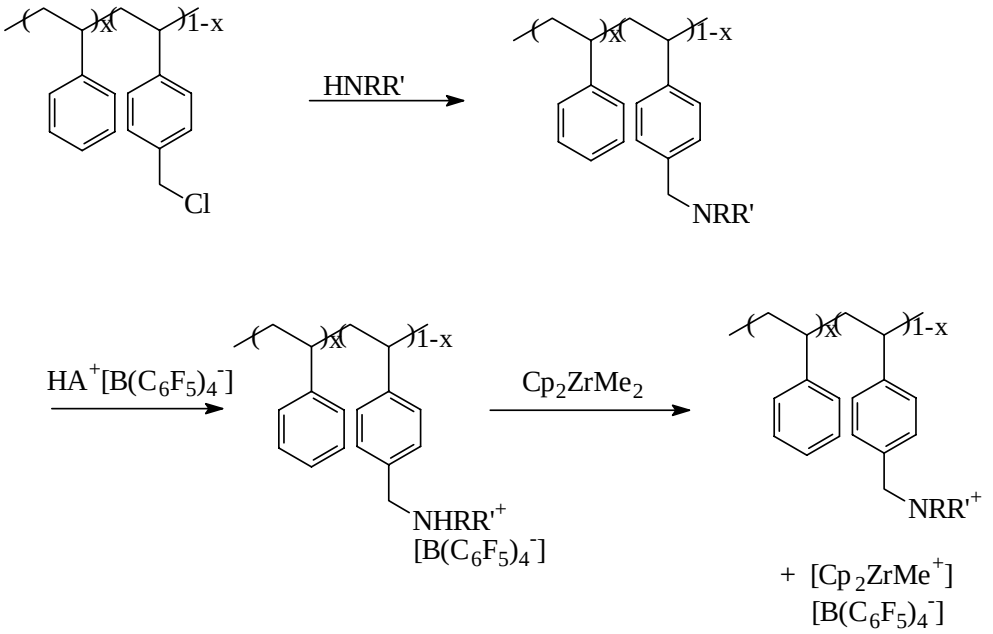

Scheme 1.11: Polystyrene-co-(4-chloromethyl)styrene as a support for metallocene catalyst

Recently Ming and Huang (134) reported crosslinked poly(styrene-co-4-vinylpyridine) supported Cp_2ZrCl_2. A strong bond between the Al center of the MAO and the pyridine nitrogen was observed by IR spectroscopy (scheme **1.12**). The activity of the catalyst was found to be dependant upon the extent of the crosslinking and the content of 4- vinylpyridine in the polymer.

Mullen and coworkers reported supporting Cp_2ZrCl_2 on a reversibly crosslinked polystyrene (135). Ethylene was polymerized using the catalyst with high polymerization activity and good control over the polymer morphology. More recently they also reported supporting $Me_2Si(2\text{-}MeBenzInd)_2ZrCl_2$ on a polypropylene support and employed it for the polymerization of propylene. The polymers obtained were highly isotactic similar to that obtained using homogeneous catalysts.

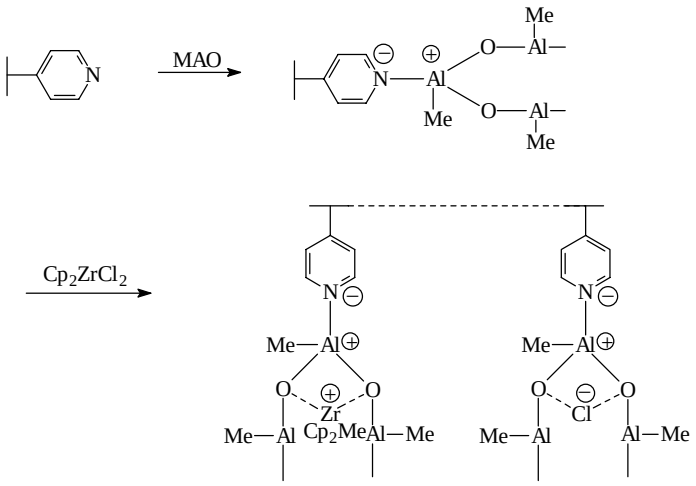

Scheme 1.12: Crosslinked poly(styrene-co-4-vinylpyridine) supported Cp_2ZrCl_2

1.5: References

1. Sinn, H.; Kaminsky, W.; Vollmer, H. J.; Woldt, R. *Angew.Chem.* **1980,** *92*(5), 396-402.
2. Wild, F. R. W. P.; Zsolnai, L.; Huttner, G.; Brintzinger, H. H. *J.Organomet.Chem.* **1982,** *232*(3), 233-247.
3. Kaminsky, W.; Kuelper, K.; Brintzinger, H. H.; Wild, F. R. W. P. *Angew.Chem.* **1985,** *97*(6), 507-508.
4. Ewen, J. A.; Jones, R. L.; Razavi, A.; Ferrara, J. D. *J.Am.Chem.Soc.* **1988,** *110*(18), 6255-6256.
5. Sinn, H.; Kaminsky, W. *Adv.Organomet.Chem.* **1980,** *18* 99-149.
6. Kaminsky, W. *J.Chem.Soc., Dalton Trans.* **1998,** *9* 1413-1418.
7. Alt, H. G.; Samuel, E. *Chem.Soc.Rev.* **1998,** *27*(5), 323-329.
8. Hlatky, G. G. *Coord.Chem.Rev.* **1998,** *181* 243-296.

9. Scheirs, J.; Kaminsky, W. *Metallocene-Based Polyolefins, Volume 1;* Wiley: Chichester, UK, 2000.

10. Peuckert, M.; Keim, W. *Organometallics* **1983,** *2*(5), 594-597.

11. Keim, W.; Kowaldt, F. H.; Goddard, R.; Krueger, C. *Angew.Chem.* **1978,** *90*(6), 493.

12. Starzewski, K. A. O.; Witte, J. Z. F. B. *Angew.Chem.* **1985,** *97*(7), 610-612.

13. Klabunde, U.; Ittel, S. D. *J.Mol.Catal.* **1987,** *41*(1-2), 123-134.

14. Johnson, L. K.; Killian, C. M.; Brookhart, M. *J.Am.Chem.Soc.* **1995,** *117*(23), 6414-6415.

15. Killian, C. M.; Tempel, D. J.; Johnson, L. K.; Brookhart, M. *J.Am.Chem.Soc.* **1996,** *118*(46), 11664-11665.

16. Small, B. L.; Brookhart, M.; Bennett, A. M. A. *J.Am.Chem.Soc.* **1998,** *120*(16), 4049-4050.

17. Birtovsek, G. J. P.; Gibson, V.; Kimberley, B. S.; Maddox, P. J.; McTavish, S. J.; Solan, G. A.; White, A. J. P.; Williams, D. J. *Chem.Commun.(Cambridge)* **1998,** *7* 849-850.

18. Bennett, A. M. A. WO 9827124 A1, **1998**.

19. Younkin, T. R.; Connor, E. F.; Henderson, J. I.; Friedrich, S. K.; Grubbs, R. H.; Bansleben, D. A. *Science (Washington, D.C.)* **2000,** *287*(5452), 460-462.

20. Gibson, V. C.; Spitzmesser, S. F. *Chem. Rev.* **2003**, *103*, 283-315.

21. Ribeiro, M. R.; Deffieux, A.; Portela, M. F. *Ind.Eng.Chem.Res.* **1997,** *36*(4), 1224-1237.

22. Ciardelli, F.; Altomare, A.; Michelotti, M. *Catal.Today*, **1998,** *41*(1-3), 149-157.

23. Alt, H. G. *J.Chem.Soc., Dalton Trans.* **1999,**(11), 1703-1710.

24. Hlatky, G. G. *Chem.Rev.(Washington, D.C.)* **2000,** *100*(4), 1347-1376.

25. Carnahan, E. M.; Jacobsen, G. B. *CATTECH* **2000,** *4*(1), 74-88.

26. Pullukat, T. J.; Hoff, R. E. *Catal.Rev.- Sci.Eng.* **1999,** *41* (3 & 4), 389-428.

27. Hogan, J. P.; Banks, R. L. US 2,825,721, **1958**.

28. Hogan, J. P. *J.Polym.Sci., A-1* **1970,** *8* 2637-2652.

29. McDaniel, M. P. *J.Polym.Sci., Polym.Chem.Ed.* **1981,** *19*(8), 1967-1976.

30. Legrand, A. P. *The Surface Properties of Silicas;* Wiley: Chichester, 1998.

31. Yermakov, Yu. I.; Kuznetsov, B. N.; Zakharov, V. A. 8 ed.; 1981; Chapter 2, pp. 59-120.

32. Burneau, A.; Barres, O.; Gallas, J. P.; Lavalley, J. C. *Langmuir* **1990,** *6*(8), 1364-1372.

33. Morrow, B. A.; McFarlan, A. J. *Langmuir* **1991,** *7*(6), 1695-1701.

34. Gallas, J. P.; Lavalley, J. C.; Burneau, A.; Barres, O. *Langmuir* **1991,** *7*(6), 1235-1240.

35. Tuel, A.; Hommel, H.; Legrand, A. P.; Kovats, E. *Langmuir* **1990**, *6*, 770.

36. Kaminaka, M.; Soga, K. *Makromol.Chem., Rapid Commun.* **1991,** *12*(6), 367-372.

37. Soga, K.; Kaminaka, M. *Makromol.Chem.* **1993,** *194*(6), 1745-1755.

38. Kaminsky, W.; Renner, F. *Makromol.Chem.* **1993,** *Rapid Commun., 14*(4), 239-243.

39. Soga, K.; Park, J. R.; Shiono, T. *Polym.Commun.* **1991,** *32*(10), 310-313.

40. Sacchi, M. C.; Zucchi, D.; Tritto, I.; Locatelli, P.; Dall'Occo, T. *Macromol.Rapid Commun.* **1995,** *16*(8), 581-590.

41. dos Santos, J. H. Z.; Greco, P. P.; Stedile, F. C.; Dupont, J. *J.Mol.Catal.A: Chem.* **2000,** *154*(1-2), 103-113.

42. Chang, M.US 5238892, **1993**

43. Burkhardt, T. J.; Brandley, W. B. WO 9705178, **1997**.

44. Kamfjord, T.; Wester, T. S.; Rytter, E. *Macromol.Rapid Commun.* **1998,** *19*(10), 505-509.

45. Rytter, E.; Ott, M. *Macromolecular Rapid Communications* **2001,** *22*(17), 1427-1431.

46. Lu, H. L.; Hong, S.; Chung, T. C. *J.Polym.Sci., Part A: Polym.Chem.* **1999,** *37*(15), 2795-2802.

47. Wang, J.; Han, L.; Zhang, L.; Li, Y. *Hebei Gongye Daxue Xuebao* **1998,** *27*(2), 1-8.

48. Soga, K.; Lee, D. H. *Makromol.Chem.* **1992,** *193*(7), 1687-1694.

49. Fischer, D.; Langhauser, F.; Kerth, J.; Schweier, G.; Lynch, J.; Goertz, H.-H. EP 700935, **1996**.

50. Mealares, C. M.-C.; Taylor, M. J. WO 0206357, **2002**.

51. Dufrenne, N. G.; Blitz, J. P.; Meverden, C. C. *Microchem.J.* **1997,** *55*(2), 192-199.

52. Quijada, R.; Rojas, R.; Narvaez, A.; Alzamora, L.; Retuert, J.; Rabagliati, F. M. *Appl.Catal., A* **1998,** *166*(1), 207-213.

53. Kallio, K.; Wartmann, A.; Reichert, K. H. *Macromolecular Rapid Communications* **2001,** *22*(16), 1330-1334.

54. Quijada, R.; Rojas, R.; Alzamora, L.; Retuert, J.; Rabagliati, F. M. *Catal.Lett.* **1997,** *46*(1-2), 107-112.

55. Dos Santos, J. H. Z.; Larentis, A.; Da Rosa, M. B.; Krug, C.; Baumvol, I. J. R.; Dupont, J.; Stedile, F. C.; Camargo Forte, M. *Macromol.Chem.Phys.* **1999,** *200*(4), 751-757.

56. Dos Santos, J. H. Z.; Krug, C.; Da Rosa, M. B.; Stedile, F. C.; Dupont, J.; Camargo Forte, M. *J.Mol.Catal.A: Chem.* **1999,** *139*(2-3), 199-207.

57. Dos Santos, J. H. Z.; Da Rosa, M. B.; Krug, C.; Stedile, F. C.; Haag, M. C.; Dupont, J.; Forte, M. d. C. *J.Polym.Sci., Part A: Polym.Chem.* **1999,** *37*(13), 1987-1996.

58. Lin, C. H.; Sheu, C. Y. *Macromol.Rapid Commun.* **2000,** *21*(15), 1058-1062.

59. Kim, J. D.; Soares, J. B. P.; Rempel, G. L. *Macromol.Rapid Commun.* **1998,** *19*(4), 197-199.

60. Kim, J. D.; Soares, J. B. P.; Rempel, G. L. *J.Polym.Sci., Part A: Polym.Chem.* **1999,** *37*(3), 331-339.

61. Roos, P.; Meier, G. B.; Samson, J. J. C.; Weickert, G.; Westerterp, K. R. *Macromol.Rapid Commun.* **1997,** *18*(4), 319-324.

62. Feher, F. J.; Budzichowski, T. A. *Polyhedron* **1995,** *14*(22), 3239-3253.

63. Duchateau, R.; Abbenhuis, H. C. L.; van Santen, R. A.; Thiele, S. K. H.; van Tol, M. F. H. *Organometallics* **1998,** *17*(24), 5222-5224.

64. Duchateau, R.; Cremer, U.; Harmsen, R. J.; Mohamud, S. I.; Abbenhuis, H. C. L.; van Santen, R. A.; Meetsma, A.; Thiele, S. K. H.; van Tol, M. F. H.; Kranenburg, M. *Organometallics* **1999,** *18*(26), 5447-5459.

65. Skowronska-Ptasinska, M. D.; Duchateau, R.; van Santen, R. A.; Yap, G. P. A. *Organometallics* **2001,** *20*(16), 3519-3530.

66. Soga, K.; Nakatani, H. *Macromolecules* **1990,** *23*(4), 957-959.

67. Soga, K.; Kaminaka, M. *Makromol.Chem., Rapid Commun.* **1992,** *13*(4), 221-224.

68. Chen, Y.-X.; Rausch, M. D. *J.Polym.Sci., Part A: Polym.Chem.* **1995,** *33*(13), 2093-2108.

69. Kaminsky, W.; Strubel, C. *J.Mol.Catal.A: Chem.* **1998,** *128*(1-3), 191-200.

70. Collins, S.; Kelly, W. M.; Holden, D. A. *Macromolecules* **1992,** *25*(6), 1780-1785.

71. Kaminsky, W. *Macromol.Symp.* **1995,** *89* 203-219.

72. Semikolenova, N. V.; Zakharov, V. A. *Macromol.Chem.Phys.* **1997,** *198*(9), 2889-2897.

73. Vaughan, G. A.; Canich, J. A. M.; Gindelberger, D. E.; Squire, K. R. PCT Int. Appl. WO 9748736, **1997**.

74. Hong, D. S.; Seo, T. S.; Woo, S. I. *Studies in Surface Science and Catalysis* **2000,** *130D*(International Congress on Catalysis, 2000, Pt. D), 3867-3872.

75. Semikolenova, N. V.; Zakharov, V. A.; Talsi, E. P.; Babushkin, D. E.; Sobolev, A. P.; Echevskaya, L. G.; Khysniyarov, M. M. *Journal of Molecular Catalysis A: Chemical* **2002,** *182-183* 283-294.

76. Ma, Z.; Sun, W. H.; Zhu, N.; Li, Z.; Shao, C.; Hu, Y. *Polymer International* **2002,** *51*(4), 349-352.

77. Schmidt, R.; Welch, M. B.; Palackal, S. J.; Alt, H. G. *Journal of Molecular Catalysis A: Chemical* **2002,** *179*(1-2), 155-173.

78. Iiskola, E. I.; Timonen, S.; Pakkanen, T. T.; Haerkki, O.; Seppaelae, J. V. *Appl.Surf.Sci.* **1997,** *121/122* 372-377.

79. Iiskola, E. I.; Timonen, S.; Pakkanen, T. T.; Haerkki, O.; Lehmus, P.; Seppaelae, J. V. *Macromolecules* **1997,** *30*(10), 2853-2859.

80. Lee, D. H.; Lee, H. B.; Noh, S. K.; Song, B. K.; Hong, S. M. *J.Appl.Polym.Sci.* **1999,** *71*(7), 1071-1080.

81. Patsidis, K.; Peifer, B.; Palackal, S. J.; Alt, H. G.; Welch, M. B.; Geerts, R. L.; Fahey, D. R.; Deck, H. R. USA US 5466766, **1995**.

82. Suzuki, N.; Yu, J.; Shioda, N.; Asami, H.; Nakamura, T.; Huhn, T.; Fukuoka, A.; Ichikawa, M.; Saburi, M.; Wakatsuki, Y. *Applied Catalysis, A: General* **2002,** *224*(1-2), 63-75.

83. Lee, B. Y.; Oh, J. S. *Macromolecules* **2000,** *33*(9), 3194-3195.

84. Soga, K.; Kim, H. J.; Shiono, T. *Macromol.Chem.Phys.* **1994,** *195*(10), 3347-3360.

85. Soga, K.; Aria, T.; Nozawa, H.; Uozumi, T. *Macromol.Symp.* **1995,** *97* 53-62.

86. Soga, K.; Ban, H. T.; Arai, T.; Uozumi, T. *Macromol.Chem.Phys.* **1997,** *198*(9), 2779-2787.

87. Soga, K.; Arai, T.; Hoang, B. T.; Uozumi, T. *Macromol.Rapid Commun.* **1995,** *16*(12), 905-911.

88. Stork, M.; Koch, M.; Klapper, M.; Mullen, K.; Gregorius, H.; Rief, U. *Macromol.Rapid Commun.* **1999,** *20*(4), 210-213.

89. Peifer, B.; Alt, H. G.; Welch, M. B.; Palackal, S. J. US 5473020, **1996**.

90. Hong, S. C.; Ban, H. T.; Kishi, N.; Jin, J.; Uozumi, T.; Soga, K. *Macromol.Chem.Phys.* **1998,** *199*(7), 1393-1397.

91. Antberg, M.; Herrmann, H. F.; Rohrmann, J. EP 496193, **1992**.

92. Chabrand, C. J.; Little, I. R.; McNally, J. P. US 5714425, **1998**.

93. Jung, M.; Alt, H. G.; Welch, M. B. US 5854363, **1998**.

94. Jung, M.; Alt, H. G.; Welch, M. B. US 5856547, **1999**.

95. Peifer, B.; Milius, W.; Alt, H. G. *J.Organomet.Chem.* **1998,** *553*(1-2), 205-220.

96. Uozumi, T.; Toneri, T.; Soga, K.; Shiono, T. *Macromol.Rapid Commun.* **1997,** *18*(1), 9-15.

97. Galan-Fereres, M.; Koch, T.; Hey-Hawkins, E.; Eisen, M. S. *J.Organomet.Chem.* **1999,** *580*(1), 145-155.

98. Juvaste, H.; Iiskola, E. I.; Pakkanen, T. T. *J.Organomet.Chem.* **1999,** *587*(1), 38-45.

99. Nagy, S.; Tyrell, J. A.; Cribbs, L. V. WO 9741157, **1998**.

100. dos Santos, J. H. Z.; Ban, H. T.; Teranishi, T.; Uozumi, T.; Sano, T.; Soga, K. *Applied Catalysis, A: General* **2001,** *220*(1-2), 287-302.

101. Kaul, F. A. R.; Puchta, G. T.; Schneider, H.; Bielert, F.; Mihalios, D.; Herrmann, W. A. *Organometallics* **2002,** *21* (1) 74-82.

102. Preishuber-Pflugl, P.; Brookhart, M.; *Macromolecules* **2002,** *35* (16) 6074-6076.

103. Barbe, P. C.; Cecchin, G.; Noristi, L. *Adv. Polym. Sci*. **1986,** *81* 1-81.

104. Kioka Mamoru; Kashiwa Norio JP JP 1006004, **1989**.

105 Satyanarayana, G.; Sivaram, S. *Macromolecules* **1993,** *26*(17), 4712-4714.

106. Bailly, J.-C. A.; Chabrand, C. J. EP 435514, **1991**.

107. Lin, Z. WO 9921898, October 27, 1998; **1999**.

108. Soga, K.; Arai, T.; Uozumi, T. *Polymer* **1997,** *38*(19), 4993-4995.

109. Sarma, S. S.; Sivaram, S. *Macromol.Chem.Phys.* **1997,** *198*(2), 498-503.

110. Sensarma, S.; Sivaram, S. *Macromol.Chem.Phys.* **1999,** *200*(2), 323-329.

111. Sensarma, S.; Sivaram, S. EP 878484, **1998**.

112. Sensarma, S.; Sivaram, S. EP 878486, **1998**.

113. Woo, S. I.; Ko, Y. S.; Han, T. K. *Macromol.Rapid Commun.* **1995,** *16*(7), 489-494.

114. Michelotti, M.; Arribas, G.; Bronco, S.; Altomare, A. *J.Mol.Catal.A: Chem.* **2000,** *152*(1-2), 167-177.

115. Ko, Y. S.; Han, T. K.; Park, J. W.; Woo, S. I. *Macromol.Rapid Commun.* **1996,** *17*(11), 749-758.

116. Rahiala, H.; Beurroies, I.; Eklund, T.; Hakala, K.; Gougeon, R.; Trens, P.; Rosenholm, J. B. *J.Catal.* **1999,** *188*(1), 14-23.

117. Meshkova, I. N.; Ushakova, T. M.; Ladygina, T. A.; Kovaleva, N. Y.; Novokshonova, L. A. *Polym.Bull.(Berlin)* **2000,** *44*(5-6), 461-468.

118. Costa Vaya, V. I.; Belelli, P. G.; dos Santos, J. H. Z.; Ferreira, M. L.; Damiani, D. E. *Journal of Catalysis* **2001,** *204*(1), 1-10.

119. Maehama, S.; Yano, A.; Sato, M. EP 0881232, **1998**.

120. Hamura, S.; Yasuda, H.; Yoshida, T.; Sato, M. EP 0849288, **1998**.

121. Yano, A.; Sato, M. EP 0658576, **1998**.

122. Suga, Y.; Maruyama, Y.; Isobe, E.; Suzuki, T.; Shimizu, F. EP 0511665, **1998**.

123. Kaneko, T.; Yano, A. EP 0849292, **2002**.

124. Suga, Y.; Uehara, Y.; Maruyama, Y.; Isobe, E.; Ishihama, Y.; Sagae, T. US 5928982, **1999**.

125. Hamura, S.; Yasuda, H.; Yoshida, T.; Sato, M. US 5906955, **1999**.

126. Heinemann, J.; Reichert, P.; Thomann, R.; Mülhaupt, R. *Macromol.Rapid Commun.* **1999,** *20*(8), 423-430.

127. Bergman, J. S.; Chen, H.; Giannelis, E. P.; Thomas, M. G.; Coates, G. W. *Chem.Commun.(Cambridge)* **1999,** *21* 2179-2180.

128. Sugano, T. JP 08208733, **1996** .

129. Sugano, T.; Takahama, T. J P 07233220, **1995**.

130. Nishida, H.; Uozumi, T.; Arai, T.; Soga, K. *Macromol.Rapid Commun.* **1995,** *16*(11), 821-830.

131. Kitagawa, T.; Uozumi, T.; Soga, K.; Takata, T. *Polymer* **1997,** *38*(3), 615-620.

132. Roscoe, S. B.; Frechet, J. M. J.; Walzer, J. F.; Dias, A. J. *Science* **1998,** *280*(5361), 270.

133. Liu, S.; Meng, F.; Yu, G.; Huang, B. *J.Appl.Polym.Sci.* **1999,** *71*(13), 2253-2258.

134. Meng, F.; Yu, G.; Huang, B. *J.Polym.Sci., Part A: Polym.Chem.* **1999,** *37*(1), 37-46.

135. Koch, M.; Stork, M.; Klapper, M.; Müllen, K. *Macromolecules* **2000,** *33*(21), 7713-7717.

2. Scope and objective of the thesis

Metallocenes are generally supported on silica after pretreatment using aluminum alkyls like methylaluminoxane and trimethylaluminum. This, however, does not allow the catalyst to anchor directly onto the surface of silica. On the contrary it is believed that the active site 'floats' over the surface and the characteristics of such catalysts are similar to homogeneous catalyst (1-3). Metallocenes can also be directly reacted with silica surface (4-6). These two different methods of reaction of metallocene with silica could, in principle, lead to different catalytically active sites on the surface of silica. The silica used for supporting metallocene is calcined at specific temperatures to remove the adsorbed moisture and to reduce the free hydroxyls groups present on the surface of silica. The free hydroxyls groups of silica are of various kinds, namely isolated and paired. The paired hydroxyls can be vicinal and geminal (7). It is well documented in the literature that by heating at different temperature it is possible to control the ratio of the different kind of free hydroxyls present on the surface of silica. It is also known that the paired hydroxyls, present on the silica surface has a detrimental effect on the activity of the catalyst because of the fact that it generates inactive sites on reacting with the metallocene (8).

2.1 Objectives

The objective of the present thesis is to study a catalyst which can react with the free hydroxyl of silica and compare its catalytic behavior with a catalyst which is expected to not to react with the free hydroxyls of the silica. Ethylene polymerization using such catalyst systems are performed and properties like polymerization activities and the kinetics of polymerization are studied. The properties of the polymers produced, like molecular weights and molecular weight distributions, are also studied.

In another study late transition metal catalyst was supported on clay. Clays are known to be useful support for olefin polymerization catalyst. In recent years there has been a large interest in the area of clay polymer nanocomposite formation using *in-situ* polymerization methods, wherein, the catalyst is first introduced into the galleries of the clay followed by polymerization, leading to intercalation/exfoliation of the clay particles into the polymer matrix.

The objective of the present work are described in the following paragraphs.

2.1.1. Silica supported dicyclopentadienyl zirconium (IV) dimethyl

In this study Cp_2ZrMe_2 is supported on silica, calcined at different temperatures

The following issues are addressed:

1. The stoichiometry of the reaction between silica, preheated at different temperature, and the metallocene.

2. The nature of sites generated upon reacting Cp_2ZrMe_2 with silica, preheated at different temperatures.

3. The effect of different catalytic sites on the activity of the catalysts.

4. The effect of different catalytic sites on the properties of the polymers.

5. An understanding of the difference in catalytic behavior of silica supported zirconocenes prepared by different methods.

2.1.2. Silica supported 2,6-diacetylpyridine-bis-(2,6 diisopropylphenylamine) iron (II) dichloride

In another study, 2,6-diacetylpyridine-bis-(2,6-diisopropylphenylamine) iron (II) dichloride is supported on silica.

The objective of the study is to support the Fe (II) catalyst directly onto silica and compare its catalytic behavior with the two other methods frequently mentioned in the literature, namely, silica pretreated with MAO, and pre-contacting the catalyst with MAO and then supporting it on silica.
The issues addressed in this studies, are:

1. Examine the nature of interaction, if any, between the silica surface and the catalyst complex.

2. Examine the effect of calcination temperature of silica on the catalyst properties.

2.1.3. Synthesis of polyethylene-clay nanocomposites by In-situ polymerization with late transition metal catalysts

Polyolefin-clay nanocomposites are attracting significant attention, both, in industrial and academic research, due to their immense potential as improved material (9,10). In the present study two catalysts, namely, [bis(2, 6-diisopropylanil) acenapthequinone] nickel (II) dibromide and 2,6-diacetylpyridine-bis-(2,6-diisopropylphenylamine) iron(II) dichloride are supported onto modified montmorillonite C-20A. Ethylene polymerization was performed at 6 bar pressure at 30°C with MAO as the co-catalyst. The objectives of the investigation are:

1. Examine the catalytic activities of the two clay-supported catalysts.

2. Examine the ability of the two catalysts to intercalate/exfoliate the clay after polymerization.

3. Examine the properties of polymers obtained using the above clay supported catalysts.

The nickel catalyst used in this study is known to produce a branched polymer, whereas, the iron catalyst is known to produce high molecular weight linear polymers.

2.2. Approach

2.2.1. Silica supported dicyclopentadienyl zirconium (IV) dimethyl

Cp_2ZrMe_2 was treated with silica calcined at 200, 400 and 600°C. The methane evolution, as a result of the reaction between the free hydroxyls of silica and the

metallocene was estimated. The possible generation of cyclopentadiene was also detected using gas chromatography. The amounts of free hydroxyls present on the surface of silica, before and after supporting the catalysts were estimated. The depletion of the free hydroxyls was balanced with the quantity of methane evolved during the process of supporting. The amount of methyl group retained by the catalysts after the supporting process was also estimated. The metal loading on the support was estimated using Inductively Coupled Plasma Spectroscopy. Carbon and zirconium X-ray photoelectron spectroscopies of the supported catalysts were performed to gain an understanding of the nature of sites generated on the silica surface. Ethylene polymerizations were performed using the supported metallocene catalysts, using MAO as the co-catalyst. The effect of silica calcination temperature upon the catalytic activity as well as polymer properties is studied. These results are compared with a supported Cp_2ZrMe_2, prepared using a silica pretreated with MAO..

2.2.2. Silica supported 2,6-bis[1-(2,6-diisopropylphenylimino) ethyl] pyridine iron (II) dichloride catalyst

2,6-diacetylpyridine-bis-(2,6-diisopropylphenylamine) iron (II) dichloride is supported on silica previously calcined at 200, 400 and 600°C. The amounts of free hydroxyls present on the surface of silica, before and after supporting the catalysts are estimated. The metal loading on the support was estimated by Inductively Coupled Plasma Spectroscopy. X-ray photoelectron spectroscopy of the metal centers were performed and compared with those of the homogeneous catalyst. Polymerization of ethylene was performed using the catalysts, in conjunction with MAO as the co-catalyst. The effect of silica calcination temperature on the catalytic activity and polymer properties were studied. Two additional catalysts were prepared, namely, silica pretreated with methylaluminoxane followed by supporting the catalyst and pre-contacting the catalyst with methylaluminoxane followed by supporting on silica. A comparative evaluation of all the catalysts was made.

2.2.3. Polyethylene-clay nanocomposites by in-situ polymerization with late transition metal catalysts

Two catalysts were supported on a hydrophobically modified montmorillonite clay C-20A. The clay was pretreated with MAO prior to contacting the clay with the solution of the catalyst. In case of the 2,6-diacetylpyridine-bis-(2,6-diisopropylphenylamine) iron (II) dichloride catalyst the concentration of the clay was varied keeping the concentration of the catalyst constant. Ethylene polymerizations was performed at 6 bar pressure for one hour using MAO as the cocatalyst. Wide angle X-ray diffraction of the clay-polymer composite was used to examine the extent of exfoliation of the clay. The molecular weight and the molecular weight distribution of the polymers were examined after extracting the clays from the polymer. Transmission electron microscopies of the polymer samples were performed to examine the dispersion of clay in the polymer.

2.2.4. References

1. Chen, Y.-X.; Rausch, M. D. *J.Polym.Sci., Part A: Polym.Chem.* **1995,** *33*(13), 2093-2108.

2. Soga, K.; Nakatani, H. *Macromolecules* **1990,** *23*(4), 957-959.

3. Soga, K.; Kaminaka, M. *Makromol.Chem., Rapid Commun.* **1992,** *13*(4), 221-224.

4. Kaminaka, M.; Soga, K. *Makromol.Chem., Rapid Commun.* **1991,** *12*(6), 367-372.

5. Kaminsky, W.; Renner, F. *Makromol.Chem.* **1993,** *Rapid Commun., 14*(4), 239-243.

6. Soga, K.; Kaminaka, M. *Makromol.Chem.* **1993,** *194*(6), 1745-1755.

7. Yermakov, Yu. I.; Kuznetsov, B. N.; Zakharov, V. A. *Stud.Surf.Sci.Catal.* **1981,** *8*(2), 59-120.

8. Collins, S.; Kelly, W. M.; Holden, D. A. *Macromolecules* **1992,** *25*(6), 1780-1785.

9. Heinemann, J.; Reichert, P.; Thomann, R.; Mulhaupt, R. *Macromol.Rapid Commun.* **1999,** *20*(8), 423-430.

10. Bergman, J. S.; Coates, G. W.; Chen, H.; Giannelis, E. P.; Thomas, M. G. *Chem.Commun.(Cambridge)* **1999,**(21), 2179-2180.

3. Experimental methods

3.1. General prerequisites

The field of olefin polymerization catalysis deals with materials which are either pyrophoric or highly air (moisture and oxygen) sensitive. Consequently, the field of olefin polymerization catalysis requires all manipulations to be performed under stringent inert atmosphere. All the experiments were thus, performed under an argon atmosphere using standard bench-top Schlenk techniques. The argon, used to maintain the inert atmosphere, was further purified by passing it through activated molecular sieves (3 and 4Å). The purified argon was analyzed for moisture and oxygen using mBraun oxygen and moisture analyser and was found to contain >2 ppm of moisture and oxygen. All the solids catalysts were stored inside M Braun model Labmaster-100 inert atmosphere glove-box. All the solvents used in different experiments are purified and dried according to established methods.

3.2. Reagents and materials

Polymerization grade ethylene was used for all the experiments. The ethylene was collected from the Gas Cracker Complex of Indian Petrochemicals Ltd., Nagothane and used without further purification. Methylaluminoxane was procured from Witco GmbH (Germany).

3.3. Analysis of MAO

The aluminum content in MAO was estimated by back titration method using standard zinc sulphate and EDTA solutions and dithizone indicator. The typical aluminum concentration in the MAO was found to be around 4.5-6 mmol/mL of MAO.

The methyl content of the MAO was estimated using the following method:

I mL of MAO solution was injected, using a hypodermic syringe, into a glass reactor containing a mixture of heptane and 2 (N) H_2SO_4. The mixture was stirred and the methane evolved was estimated using a gas burette, connected to the reactor. The first

two measurements were discarded, in order to allow the heptane to get saturated with methane. The typical methyl group content in MAO is around 6-9 mmol/ ml of MAO. The typical methyl: aluminum ratio is around 1.5-1.6.

3.4. Analyses of polymers

Intrinsic viscosities of polymer samples were determined using an Ubbelohde viscometer in decahydronapthalene as solvent at 135^{o}C The molecular weight and the molecular weight distribution of the polymers were determined by Gel Permeation Chromatograph (GPC) PL-GPC 220 at 160°C using 1,2,4-trichlorobenzene as the solvent and polystyrene as standard. A 0.3-0.4 % w/v solution was used at a flow rate of 1.0 mL/min.

3.5. Ethylene polymerization at atmospheric pressure

3.5.1. Description of the apparatus

A glass tube of capacity 3000 mL with a glass jacket, a three way stop cock and a supporting parallel glass tube was fabricated. The fabricated unit was mounted on a wooden platform. Upon calibration, it was found that 1 cm of the length of the tube corresponds to 30 mL of ethylene. The calibrated glass tube was used as a gas burette for measuring the differences in displacement of volume of ethylene during the polymerization. A three-necked flat bottomed jacketed glass vessel of capacity 100-150 mL was used as the polymerization cell.An oil reservoir of capacity 4000 mL filled with silicone oil was connected through a PVC tubing to the gas burette. The reaction cell was mounted on a magnetic stirrer, which was connected to the gas burette via a T-shaped stopcock using pressure tubing. Two paraffin bubblers were also connected for evacuation purpose to the reaction assembly and gas burette as shown in the diagram. The reaction cell was dried at 150°C, overnight and thoroughly checked for leaks by running a blank experiment under one atmosphere pressure for 2-3 hours. The silicone oil was saturated with ethylene gas before the start of experiment.

3.5.2. Polymerization of ethylene

Polymerization was performed with the assembly described above at one bar ethylene pressure in xylene and n-hexane. A diagram of ethylene polymerization setup for 1 bar is shown in Fig **3.1**. A gas burette with a reservoir containing silicone oil was used to feed ethylene continuously to the reaction cell. The reaction cell was dried at 155^{o}C at least for two hours and cooled under ethylene. The required amount of catalyst was transferred into the cell inside the glove-box. Solvent was introduced into the cell using a hypodermic syringe. The solvent was saturated with ethylene. Polymerization was initiated by the addition of cocatalyst (MAO). The reaction temperature was maintained by circulating water from a thermostat through the jacket of the cell and the gas burette. Ethylene uptake was measured as a function of time. The reaction was terminated by addition of acidified methanol. The polymer was filtered, washed with methanol and dried at 40^{o}C under vacuum.

3.5.3. Standard ethylene polymerization

In order to check the quality of the MAO, standard ethylene polymerizations were performed using Cp_2ZrCl_2 catalyst. The following conditions were used, Cp_2ZrCl_2 2.6×10^{-8} mol, the Zr:Al ratio = 100,000, temperature = 70°C and toluene = 30 mL. The typical catalyst activity obtained under this condition was 800-950 kg PE/g Zr/ h.

3.6. Polymerization of ethylene at higher pressure

High-pressure polymerizations were performed into a glass made Buchi Miniclave reactor with a capacity of 50 and 200 mL, equipped with a magnetic needle (Fig **3.2**). The reactors were baked in an oven at 150°C for at least 2 h and then taken out and quickly fitted to the ethylene supply line and subsequently cooled under ethylene pressure. The solid catalysts were taken out from the glove-box and introduced into the reactor via a glass vial. The soluble catalysts were introduced into the reactor in the solution form through hypodermic syringe. 50 mL of toluene (dried over sodium and freshly distilled) were injected and was saturated with ethylene. Finally required amount of MAO were injected, to commence the polymerization. The pressure was maintained at the required level. At the end of the stipulated time the reactions were terminated by adding acidified methanol. The polymer was filtered, washed and dried at 40-50^{0}C under vacuum.

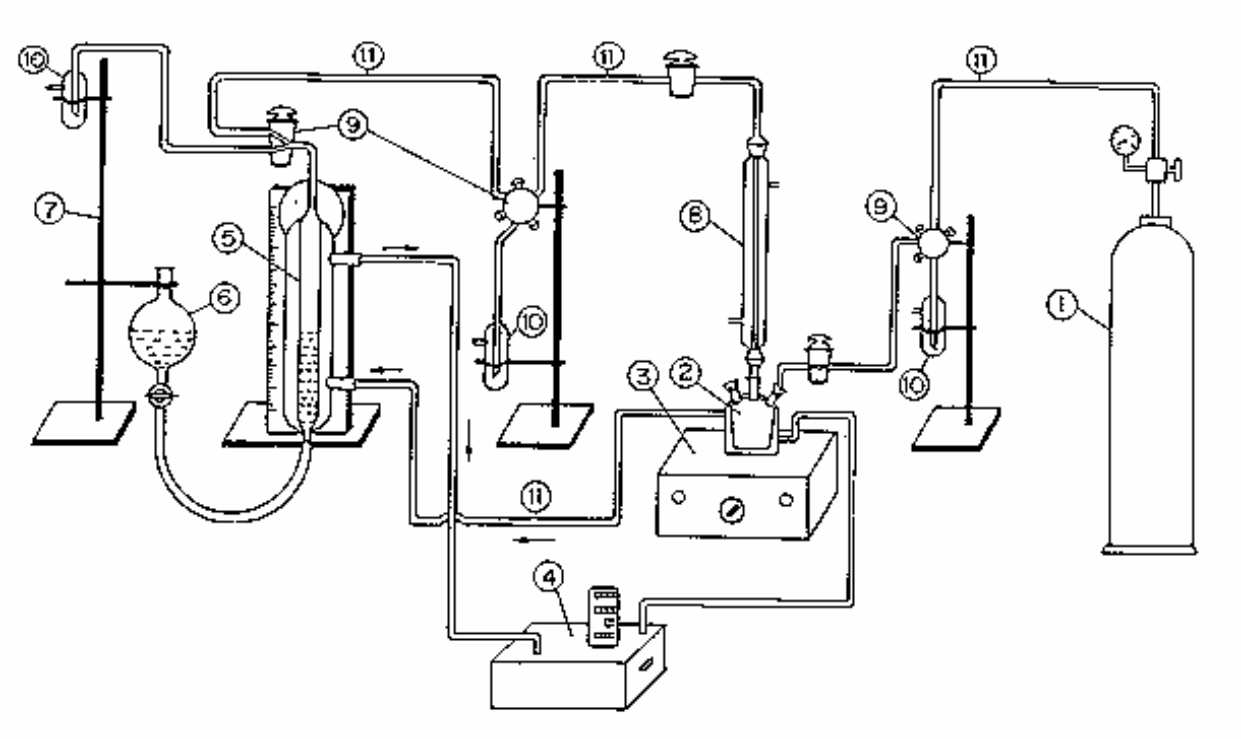

Fig 3.1. Ethylene polymerization set up at one atmosphere pressure

1 - Ethylene gas cylinder	6 - Separating funnel with silicone oil
2 - Glass reactor	7 - Iron stand
3 - Magnetic stirrer	8 - Glass condenser
4 - Haake water bath	9 - Three way stop cocks
5 - Calibrated gas burrette on wooden	10 - Silicone oil bubbler

3.7. Estimation of metal content in heterogeneous catalysts

The metal content of the solid supported catalyst were estimated by using Perkin Elmer-P100 inductively coupled plasma ionization spectrometer.

3.7.1. Sample preparation

100 mg of the solid supported catalyst was taken out from the glove-box in a beaker and boiled in 50 mL 2(N) H_2SO_4 and 0.5 mL of conc. HNO_3 for 30 min. The content

was then cooled and filtered into a 100 mL standard flask and the volume of the content made up to the mark using de-ionized water. The solution was then diluted 10 times. A blank solution is also made using the same method.

3.7.2. Analysis

The solutions thus prepared were subject to ICP analysis. Before the sample analysis was performed, the instruments were calibrated procured from Aldrich. The metal concentration of the sample solutions were adjusted in order to keep it within the range of 2-20 ppm, which is the best detection range for the instrument.

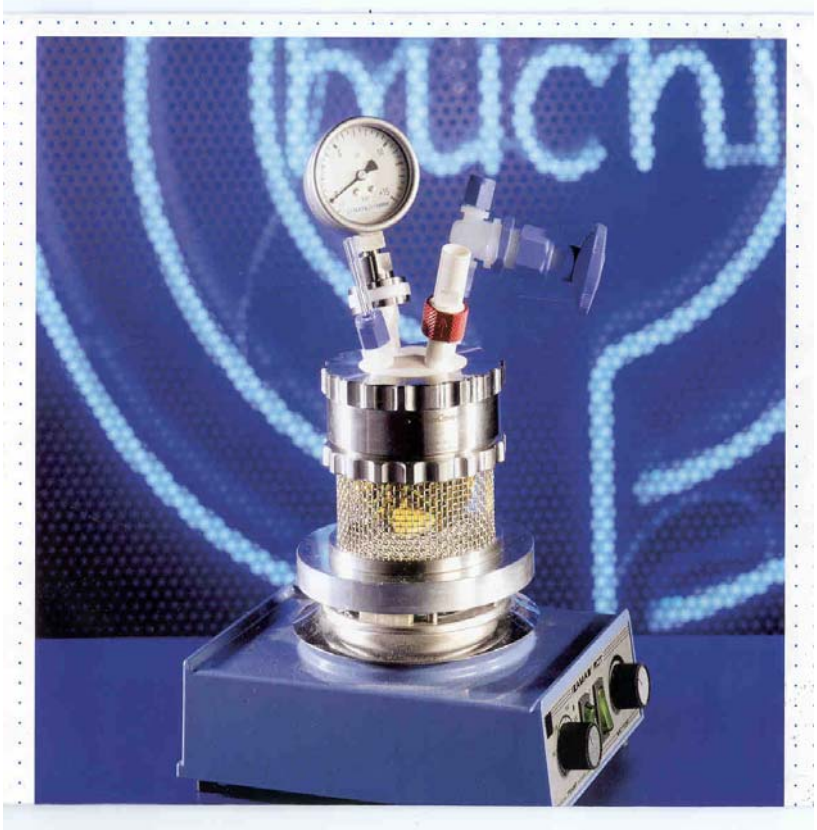

Figure 3.2. Buchi Miniclave – the glass pressure reactor for polymerization of olefins

4. Silica supported bis-(cyclopentadienyl) zirconium (IV) dimethyl. Nature of metal support interactions

4.1. Introduction

Significant interest has been evinced in the study of supported metallocene catalysts In view of its tremendous practical applications. Homogeneous metallocene catalysts can be heterogenized by supporting it on an inert carrier. Such supported catalysts provide better control of polymer powder morphology, improve the powder bulk density and minimize fouling of industrial reactors. Furthermore they consume lesser organoaluminum compounds for activation and are active for longer period of time in comparison with their homogeneous counterparts. Several supports are known to be useful for this purpose of which silica is the most widely used (1-5). Generally, supported catalysts are prepared by treating silica with a solution of an organoaluminum compound, such as trimethylaluminum (TMA) or methylalominoxane (MAO) in toluene, followed by treatment with a solution of the metallocene in toluene. Under these conditions the free hydroxyl groups present at the surface of silica react with the Al-R bond. The metallocene then interact with the support ionically (6-11). The metallocene can also directly react with the free hydroxyls of silica, provided a suitable functional group is available for reaction (6,9,12-14). When the latter procedure is used, the polymerization activities of the supported catalysts are reported to drop substantially.

The free hydroxyls of silica are either isolated or hydrogen bonded (geminal or vicinal), the relative ratio of which can be controlled by the temperature of calcination (15,16). It has been postulated that paired hydroxyls on the surface of silica generate catalytic sites, which are inactive for polymerization (17,18). The catalytic activity is also reported to be related to the calcination temperature of silica (18). Dos Santos et al (18) showed that upon supporting $(nBuCp)_2ZrCl_2$ on silica which has been subject to evacuation at room temperature, the resulting supported catalysts showed only minor polymerization activity. This was attributed to a large amount of inactive centers resulting from a high surface density of OH on silica. However, when a silica, calcined at temperatures between 373-723K was used as the support the catalyst showed polymerization activity. The highest activity was obtained with silica calcined at 723K.

Jezequel et al (19) examined the reaction of Cp^*ZrMe_3 and Cp_2ZrMe_2 with partially dehydroxylated silica, calcined at 500°C, using *in-situ* infrared spectroscopy, surface microanalysis, solid state ^1H and ^{13}C NMR using ^{13}C enriched compounds and EXAFS. They observed that both the metallocenes react with the OH of the silica by a simple protonolysis of one Zr-Me bond with the formation of a single well-defined neutral species, $(CpMe_2)Zr\text{-}OSi$ and $(Cp_2Me)Zr\text{-}OSi$ respectively. The first species showed ethylene polymerization activity, but the second species was inactive. This was explained by the fact that the grafted biscyclopentadienyl species simultaneously cannot accommodate one σ-bonded oxygen, two Cp ligands, one methyl group and one cationic charge. In other words it can be said that the two sites necessary of polymerization, one for coordination of the incoming monomer and another for the insertion of the monomer to the growing polymer chain is possible by the monocyclopentadienyl species supported on silica and not by the biscyclopentadienyl species.

However there are evidences that the cylcopentadienyl ligands can open up on reaction with the free hydroxyls of silica, as shown in Scheme **4.1**, reported by Collins et al (17).

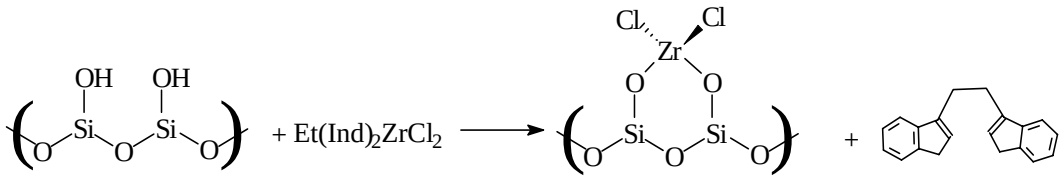

Scheme 4.1. Reaction between the silica and the ligand leading to deactivation of the site

Also there are numerous examples of other metallocenes that react with the silanols, producing cyclopentadienyl species as a byproduct (20). The most important example is the chromocene Cp_2Cr supported on silica. This is one of the most efficient catalysts for ethylene polymerization. The kind of reactive groups generated are shown in Scheme **4.2**.

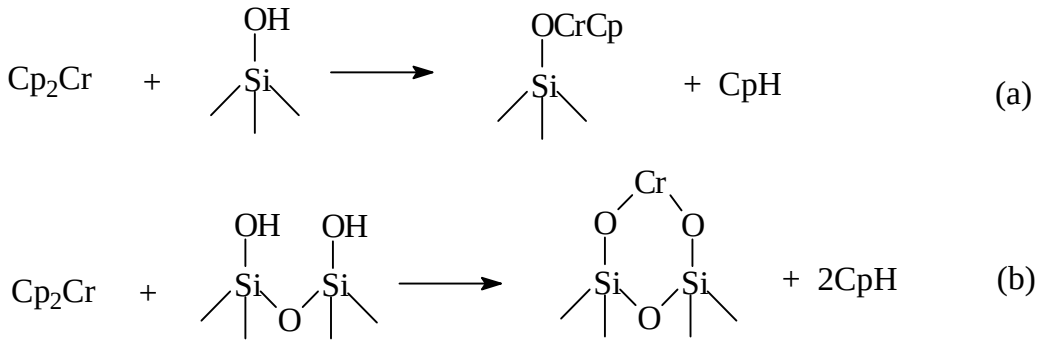

Scheme 4.2. Reaction of silica with the dicyclopentadienylchromium

Also, other metallocenes like $MgCp_2$ and $FeCp_2$ are known to react in this manner.

The objective of this study is to investigate the nature of the reaction between the metallocene and silica, preheated at different temperatures. The effect of the preheating temperature of silica on the nature of sites generated and their relative ratio as well as the effect of these sites on the activity of the catalysts in ethylene polymerization is examined. The results are compared with a supported catalyst prepared by preheating silica with MAO following by reaction with Cp_2ZrMe_2. X-ray photoelectron spectroscopy (XPS) is used to probe the nature of active sites present in the catalysts (21,22).

4.2. Experimental part

4.2.1. Reagents and materials

All operations were performed as described in Chapter **3**. SiO_2 (grade 952) with a surface area of approx. 230 m^2/g was obtained from Davison Chemicals (USA). The catalyst precursor namely, zirconocene dichloride was procured from Aldrich, USA and used without purification.

4.2.2. Synthesis, characterization and purification of bis(cyclopentadienyl) zirconium (IV) dimethyl

The synthesis of Cp_2ZrMe_2 was done using reported method (23). Cp_2ZrCl_2, 3.0 g, was slurried in 20 mL of diethylether, cooled to -20°C. MeLi, 13 mL (1.45 mmol) was added dropwise to the slurry over 45 min. The temperature was allowed to rise at 0°C and maintained for 30 min. White crystalline solid appeared on the wall of the flask. The solvent was evaporated and the crude solid was subjected to sublimation at approx. 10^{-5} mbar of pressure at 70°C. Pure white crystals of Cp_2ZrMe_2 appeared at the surface of the cold finger which was collected under a positive nitrogen flow and preserved inside the glove box in a Schlenk flask under vacuum. Anal. $C_{12}H_{16}Zr$ 251.22 Calcd. C 57.20, H 6.4; Found C 57.05, H 6.3. ^1H NMR (C_6D_6) δ = 0.04 (s, 6 H, Zr-CH_3), 5.79 (s, 10 H, C_5H_5).

4.2.3. Calcination of silica

Silica samples were calcined at three different temperatures, 600°C, 400°C and 200°C under vacuum for different periods of time. A cylindrical quartz tube with vacuum stopcock was used for this purpose. The silica samples were placed into a quartz bobbin, inside the tube. The tube was kept inside a cylindrical furnace and heated at the desired temperature.

4.2.4. Pretreatment of silica with methylaluminoxane

The silica used in this experiment was calcined at 400°C for 4 h under vacuum. Approximately 1g of calcined silica was taken in a 100 mL round bottom flask to which 20 mL of dry toluene was added. A solution of MAO in toluene was added to the mixture. The amount of methane evolved was estimated using a gas burette. The total aluminum concentration taken for the pretreatment was about 3 mmol. The mixture was stirred for 50°C for 2 h. The slurry was filtered and washed with 10 mL of toluene thrice. The solid was dried under vacuum at 25°C for 2 h.

4.2.5. Pretreatment of silica with dimethylcarbonate

The pretreatment of silica with dimethylcarbonate was performed according to a reported method (24). The silica used in this method was preheated at 400°. Silica (1

g) was taken in a 100 mL round bottom flask, fitted with a septum adaptor, and 10 mL of dry hexane was added. 0.42 g of tributylamine (2.3 mmol) was added to the reaction flask and allowed to stir for 2 h. Thereafter 2.16 g (24 mmol) of dimethylcarbonate was added to the flask and stirred for 24 h. The reaction slurry was finally dried under vacuum.

4.2.6. Characterization of silica

4.2.6.1. Estimation of free hydroxyl content

The free hydroxyl content of silica, calcined at different temperature, was estimated by treating silica with methyl magnesium iodide and subsequently estimating the evolved methane gas, due to the reaction of the hydroxyl groups with methyl magnesium iodide, using a gas burette.

Approximately 100 mg of calcined silica was taken in a 50 mL round bottom flask containing a magnetic needle, fitted with a septum adapter, which was connected to a 50 mL capacity of gas burette with a pressure equalizer and a oil reservoir. 5 ml of dry butyl ether was added to the silica through a syringe. The flask was then cooled to 0°C. and the pressure inside the gas burette was adjusted to atmospheric pressure. The burette was then disconnected from the flask, with the help of the septum adapter. Then 2 mL of 2 M methyl magnesium iodide solution, in butyl ether, was quickly added to the flask by a syringe. The mixture is then allowed to stir for 5 min. Then the burette was connected to the flask by opening the stopcock and the methane generated was allowed to flow to the burette. Once the flow of methane ceased the level of the oil was adjusted to the atmospheric pressure and the volume of methane recorded. This same experiment was then repeated without adding silica, to record a blank reading. The moles of methane evolved per g of silica was then calculated from the volume of methane gas generated.

4.2.7. Synthesis of the silica supported bis (cyclopentadienyl) zirconium (IV) dimethyl catalysts

Approximately 1 g of calcined silica was taken in a 100 mL round bottom flask and slurried with 10 mL of dry toluene. In another flask 85 mg (0.35 mmol) of the

Cp_2ZrMe_2 was taken in 10 mL of dry toluene. The Cp_2ZrMe_2 solution was added to the slurry of silica slowly while stirring and the amount of methane evolved was recorded using a gas burette. The mixture was stirred at 50°C for 3 h. The slurry was filtered, washed with 10 mL of dry toluene thrice. The filtrate was dried under vacuum at 25°C for 2 h.

4.2.8. Characterization of the catalyst

4.2.8.1. Extraction of the metal from the solid support

Approx. 100 mg of the supported catalyst was taken in a round-bottomed flask and stirred with 10 mL of toluene at 80°C for 4 h. The toluene was separated by filtration. This experiment was repeated in presence of MAO. The toluene filtrate obtained was evaporated to dryness, the residue dissolved in 2(N) sulfuric acid, and used for the measurement of the zirconium content by ICP.

4.2.8.2. X-ray photoelectron spectroscopy

The X-ray photoelectron spectra (XPS) were recorded on a V. G. Scientific (U.K.) ESCA 3000, using MgK$\propto$ (1253.6eV) as the exciting source. The X-ray source operated 12 mA and 14.5 kV. The residual gas pressure in the spectrometer chamber during data acquisition was less than 10^{-9} Torr. All spectra were recorded with pass energy of 50 eV and 4 mm slit. The spectrometer was calibrated by determining the binding energy of Au $_{4f7/2}$ (84.0 eV), Ag $_{3d5/2}$ (368.3 eV) and Cu $_{2p3/2}$ (932.4 eV) levels using spectroscopically pure metals (M/s Johnson and Matthey). These values are in good agreement with the literature values (25). The accuracy of the value was within +0.2 eV. The X-ray photoelectron spectra were referred to the C_{1s} (285.0 eV).

Pellets of 10 mm×1 mm dimension were made from solid catalysts with the help of a die and subjected to hydrolic press under nitrogen flow. They were then introduced into the fast entry air-lock chamber while retaining the base pressure of the analysis chamber at a base pressure of 10^{-10} mbar. From the air-lock chamber the samples were transferred to the analysis chamber. The samples were degassed for approximately 15-16 h for before the analyses were done.

The data analysis of the spectra were done using the standard methods like background subtraction, smoothing and non-linear (Gaussian) least square curve fitting. The peak position and the intensity were roughly assigned on the spectra, and were used as the crude value for the curve-fitting program.

The XPS peaks corresponding to the C(1S) and Zr(3/2d) and Zr(5/2d) are recorded. In case of the carbon nonlinear curve fitting using a Gaussian equation does the deconvolutions of the spectra.

$$Y = P1*\exp(-0.5*((x-P2)/P3)^2) + P4*\exp(-0.5*((x-P5)/P3)^2)$$

Where P1 and P4 are the intensities, P3 is the half line width; P2 and P5 are the binding energy values. This is done with the anticipation of each sample contains two peaks. This is done with anticipation that each of the spectra contains two peaks.

In case of the Zirconium the deconvolution of the spectra was performed using the following equation:

$$Y = P1*\exp(-0.5*((x-P2)/P3)^2) + (2*P1/3)*\exp(-0.5*((x-P2-2.4)/P3)^2) + P4*\exp(-0.5*((x- P5)/P3)^2)+(2*P4/3)*\exp(-0.5*((x-P5-2.4)/P3)^2).$$

The modification in this equation is necessary due to the fact that in case of zirconium each chemical shift is accompanied by two peaks, 3d5/2 and 3d3/2.

4.2.8.3. Residual methyl groups attached to the catalysts in the silica support

The residual methyl group in the supported catalysts was estimated by hydrolyzing the catalysts with 10% H_2SO_4 and measuring the amount of methane evolved in a gas burette.

100 mg of the supported catalyst was taken in a 50 mL round bottom flask, containing a magnetic needle and connected to a gas burette via a septum adaptor. 5 mL of dry butyl ether is added to the flask and the content of the flask was brought to 0°C. The pressure inside the burette was adjusted to atmospheric pressure and the burette was disconnected from the flask. Then 2 mL of 10% H_2SO_4 solution was added to the flask and stirred for 10 min. The burette was connected to the flask once again and the

volume of methane evolved was measured in the burette after adjusting the pressure inside the burette to atmospheric pressure.

The mol of methyl group per g of catalysts was estimated as follows:
Considering x mL of methane gas is evolved at room temperature and at atmospheric pressure for 100 mg of silica supported catalyst the mol of methyl groups per g of the catalyst will be given by

$$= \quad x\left(\frac{273 \times 10}{298 \times 22400}\right) \text{ mol Me/g catalyst}$$

4.2.8.4. Detection of cyclopentadiene as a product of the reaction between Cp_2ZrMe_2 and silica using gas chromatography

In order to check if cyclopentadiene is a product of the reaction between Cp_2ZrMe_2 and silica, the supernatant liquid was analyzed by gas chromatography. Gas chromatography of synthetic samples of dicyclopentadiene and dodecene (which was used as an internal standard) in toluene was performed for purposes of calibration. Different concentrations of dicyclopentadiene (100-30 ppm) were taken with a constant concentration of dodecene (50 ppm). The area ratio of the two peaks versus the mole ratio was plotted and a straight line passing through the origin was obtained (Fig **4.1**). The slope obtained for this curve is 1.31.

Silica used for this experiment was calcined at 200°C. Approximately 85 mg (0.35 mmol) of Cp_2ZrMe_2 was dissolved in 5 mL of toluene and added to approximately 1 g silica in 5 mL of toluene. The methane evolution was estimated and the reaction was carried out for 2 h at 50°C.

The supernatant liquid and the first washings were collected and analyzed by gas chromatography. 0.5 mL of 100 ppm dodecene solution was added to 0.5 mL of the supernatant liquid as an internal standard. Thus the concentration of dodecene in the solution was 50 ppm. Cyclopentadiene was observed in both the supernatant liquid and the first washing. The total Cp detected was approx. 0.04 mmol/g of silica of the metallocene.

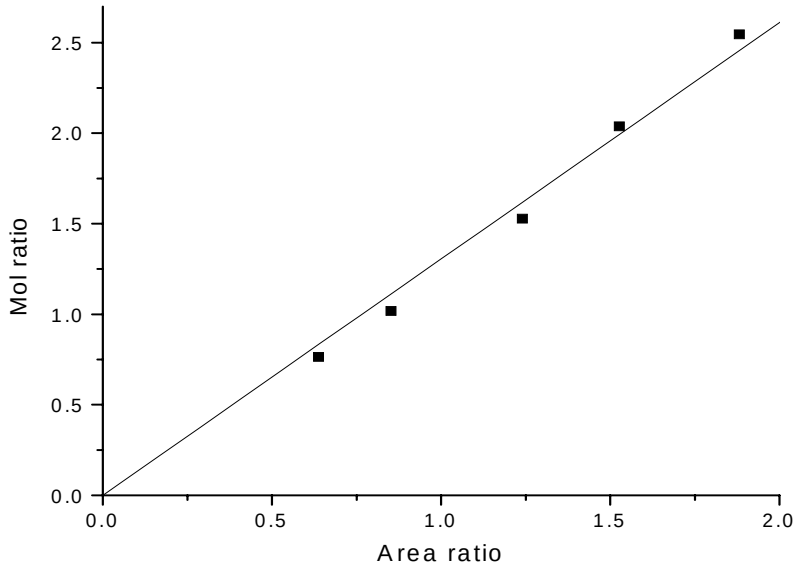

Fig 4.1: Calibration curve of area ratio vs. mol ratio of dicyclopentadiene and dodecene

4.3. Result and discussion

4.3.1. Nature of silica

The silica used in the experiments had a surface area of approximately of 230 m^2/g. The surface of silica contains free hydroxyl groups, paired and isolated. The paired hydroxyls can be either geminal or vicinal. This apart, silica contains a substantial quantity of hydrogen bonded water molecules (Fig. **1.1**). The silica samples were heated at three different temperatures, 200°C, 400°C and 600°C under vacuum and for 4 h and 8 h. It is known that when silica is heated at 200°C it looses all its hydrogen bonded water molecules, keeping all its hydroxyls intact. At 400°C the paired hydroxyls starts depleting and at 600°C most of the paired hydroxyls gets depleted and majority of the free hydroxyls left on the surface are isolated. So heating at 400°C will lead to a mixture of paired and isolated hydroxyls and at 600°C essentially all the hydroxyls are isolated.

Silica was heated at 600ºC for 8 h (catalyst **1**) and 4 h (catalyst **2**) and 400ºC for 8 h (catalyst **3**) and 4 h (catalyst **4**) and 200°C for 4 h (catalyst **5**), all under vacuum (Table **4.1**). As expected, the quantities of free hydroxyls in the silica were found to be higher in silica heated at lower temperature and for lesser time. The total free hydroxyl content of silica was estimated by treating the silica with methyl magnesium iodide and estimating the amount of methane gas evolved. The results are shown in table **4.2**.

Table 4.1: Designation of the silica supported Cp_2ZrMe_2 catalysts

Catalyst Designation	Method of preparation
1	Cp_2ZrMe_2 + Silica (calcined at 600°C for 8 h)
2	Cp_2ZrMe_2 + Silica (calcined at 600°C for 4 h)
3	Cp_2ZrMe_2 + Silica (calcined at 400°C for 8 h)
4	Cp_2ZrMe_2 + Silica (calcined at 400°C for 4 h)
5	Cp_2ZrMe_2 + Silica (calcined at 400°C for 4 h)
6	Silica (calcined at 400°C for 4 h) + MAO + Cp_2ZrMe_2

It is known that the free hydroxyl groups of silica are capable of reacting with the aluminum alkyls. In most of the earlier literature relating to silica supported metallocene catalysts, the silica was first pretreated with methylaluminoxane and then reacted with the metallocene (Catalyst **6,** Table **4.1**). On reacting silica with MAO, all the free hydroxyl groups of silica is consumed and Si-O-Al group is generated along with a mol of methane. Aluminum loading in the solid was ~9% by weight. The

amount of methane evolution during the treatment of MAO to silica was equal to the amount of free hydroxyls on the silica surface.

In another experiment silica was treated with dimethylcarbonate with the intention of completely removing the hydroxyls from the silica surface. The primary objective of this experiment was to observe the behavior of the metallocene on a surface which is completely devoid of any reactive functional group. Dimethylcarbonate is reported to react with the free hydroxyls of silica according to Scheme **4.3** (24)**.** However, in our hands the reaction between the silica free hydroxyls and dimethylcarbonate failed to deplete the free hydroxyls of silica completely. In fact the free hydroxyl content was found to be very high, as high as that of the silica dehydroxylated at that particular temperature (Table **4.2**, catalyst **4**). The surface adsorbed methanol formed during the reaction between the hydroxyl and the dimethylcarbonate could account for the abnormally high value of methane liberated. For this reason no further attempt was made to use silica modified with dimethylcarbonate.

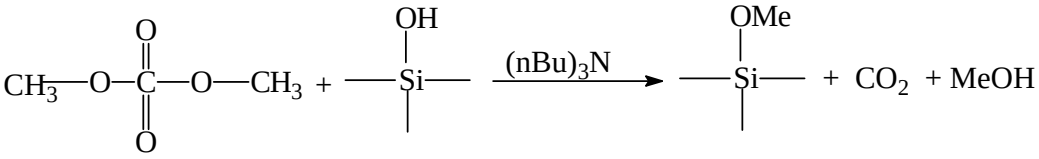

Scheme 4.3: Reaction between the silica free hydroxyls and dimethylcarbonate

4.3.2. Nature of metal-support interaction

4.3.2.1. Stoichiometry of the reaction

Reaction of the calcined silica with Cp_2ZrMe_2 is accompanied by the evolution of methane as a byproduct of the reaction of Cp_2ZrMe_2 with silica is dependant on the calcining temperature of silica. Amount of zirconium incorporated, methane evolved, the amount of residual hydroxyl and methyl group on the supported catalysts are shown in Tables **4.2** and **4.3** and Figs. **4.2** and **4.3**. As expected, the quantity of methane evolved is lower at higher silica calcination temperature.

Table 4.2: Depletion of free hydroxyls and % Zr of various silica supported Cp_2ZrMe_2 catalyst

Cat No.	Temp (°C)/time (h) of calcination	Free hydroxyl before supporting[1]	Free hydroxyl after supporting	%Zr	
				Obtained	Theoretical[2]
Cat 1	600/8	1.79	1.41	1.9	3.5
Cat 2	600/4	1.78	1.40	2.1	3.5
Cat 3	400/8	2.19	1.76	2.0	4.3
Cat 4	400/4	2.37	1.89	1.9	4.8
Cat 5	200	2.49	1.97	2.4	5.2
Cat 6	400/4	2.20	Nil	2.3	--

[1]mmol/g silica,

[2] % Zr expected from the free hydroxyl content of silica

When silica is pretreated with MAO, all the hydroxyl groups on silica are lost by the reaction with MAO (catalyst **6,** Table **4.2**). The Al content of silica is ~9% by weight. The quantity of methane evolved during the treatment of MAO with silica is equal to the amount of silanol in the silica (2.2 mmol/g of silica). In spite of the near absence of hydroxyl group on silica, reaction with Cp_2ZrMe_2 results in evolution of large quantities of methane. This is intriguing. It is a well known fact that metallocene can react with MAO to generate methane, through α-hydrogen transfer, and forming an inactive species. Also MAO is known to self-condense forming methane and Al-CH_2-Al bonding (26). Such reactions are probably responsible for the observed generation of methane (Scheme **4.4**).

Table 4.3: Amount of zirconium incorporation and methyl groups retained by different silica supported Cp_2ZrMe_2 catalyst

Catalyst designation	Temp (°C)/ time (h) of calcination	Zr found (mmol)	Methane evolved (mmol)	Residual methyl group on supported catalyst (mmol)
Cat 1	600/8	0.21	0.15	0.27
Cat 2	600/4	0.23	0.23	0.21
Cat 3	400/8	0.21	0.28	0.12
Cat 4	400/4	0.21	0.35	0.18
Cat 5	200	0.28	0.43	0.12
Cat 6	400/4	0.25	0.78	Nil

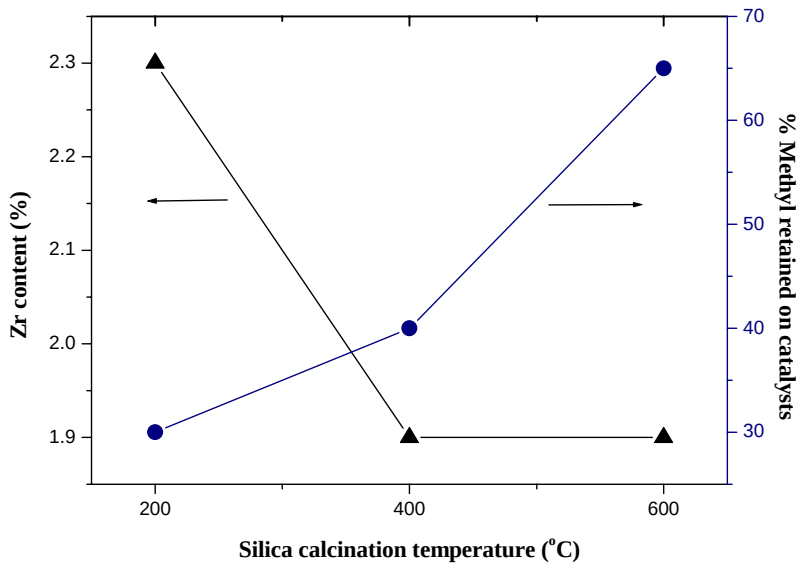

Fig 4.2: % Zr content and % Me retained as a function of silica calcination temperature

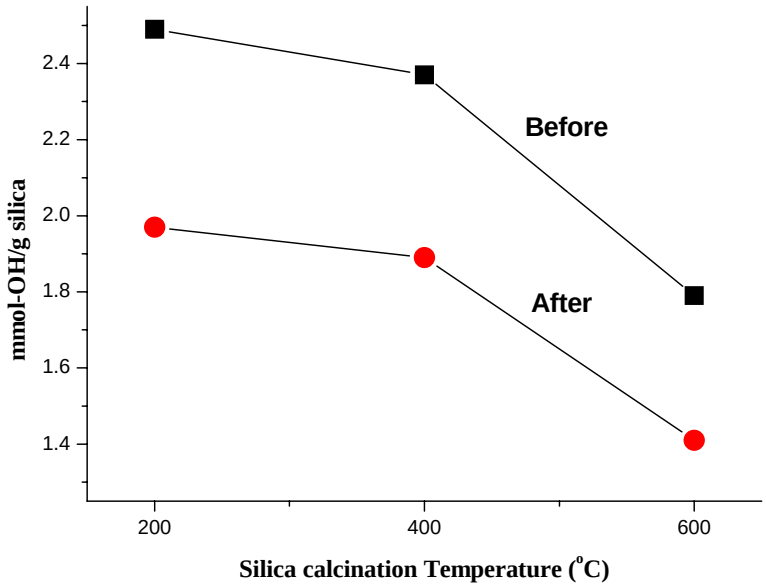

Fig 4.3: Free hydroxyl of silica before and after reaction with Cp_2ZrMe_2

Activation

$$Cp_2ZrMe_2 + MAO \rightleftharpoons [Cp_2ZrMe]^+ + [MAO\text{-}CH_3]^-$$

Deactivation

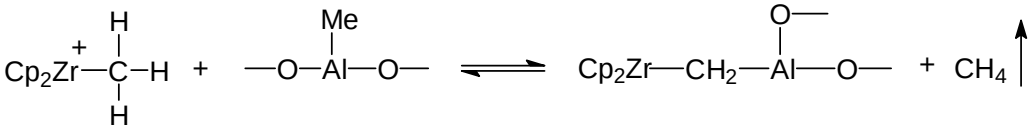

MAO self condensation

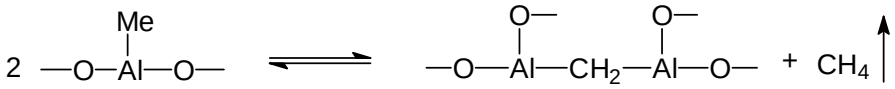

Scheme 4.4: Reaction of Zirconocene with MAO

Estimation of zirconium content reveals that catalysts **1-4** contain, approximately the same amount of metal (1.9-2.1% by weight), whereas catalyst **5** contains slightly higher quantity (2.4% by weight) of zirconium (Table **4.3**) (18). This can be correlated with the free hydroxyl content of silica. The zirconium content of catalyst **6** is higher than catalyst **4**. This is due to the fact that in case of the catalyst **6** the metallocene is anchored to the silica surface through the MAO.

Attempts to extract the catalyst from the solid support did not result in any detectable amount of zirconium even when the extraction was done at 80°C and in presence of MAO. This shows that in all the catalysts (**1-5**) metallocene is truly bonded to the silica surface. In case of the catalyst **6** ~6% of zirconium could be extracted.

4.3.2.2. Nature of the active sites

Possible structures that can result from the reaction of Cp_2ZrMe_2 with silica are shown in Scheme **4.5**. Structures **1** and **2** result from the reactions of the isolated hydroxyls of silica, structure **3**, **4** and **5** from the paired hydroxyls of silica. Of these, only structure **1** is likely to be active in polymerization since it can lead to the formation of the cation (by abstraction of one methide anion by the co-catalyst) and insertion (into the other Zr-Me bond). Thus, the loss of cyclopentadiene is a necessary prerequisite for the generation of the active site. This conclusion is also supported by recent results of Jazequel et al (19) who showed by using solid-state ^{1}H and ^{13}C NMR, that site 2 was inactive in polymerization. Supporting $CpZrMe_3$ onto silica resulted in the formation of site 1 which was found to be active in polymerization.

In the present study loss of cyclopentadiene was experimentally confirmed by gas chromatography. Approximately 85 (0.35 mmol) mg of Cp_2ZrMe_2 was dissolved in 5 mL of toluene and added to approximately 1 g silica, calcined at 200°C for 5 h, in 5 mL of toluene. The methane evolution was estimated, and the reaction was carried out for 2 h at 50°C. The filtrate and the first washing were collected after keeping the solvent for two days over supported silica under nitrogen atmosphere. Gas chromatography of the two samples was performed with an internal standard, dodecene. 0.5 ml of 100 ppm dodecene solution was added to 0.5 ml of the supernatant. Thus the concentration of dodecene in the solution was 50 ppm.

Cyclopentadiene was observed in both the filtrate and the first washing. The total Cp detected was approx. 0.04 mmol for 1 g of silica.

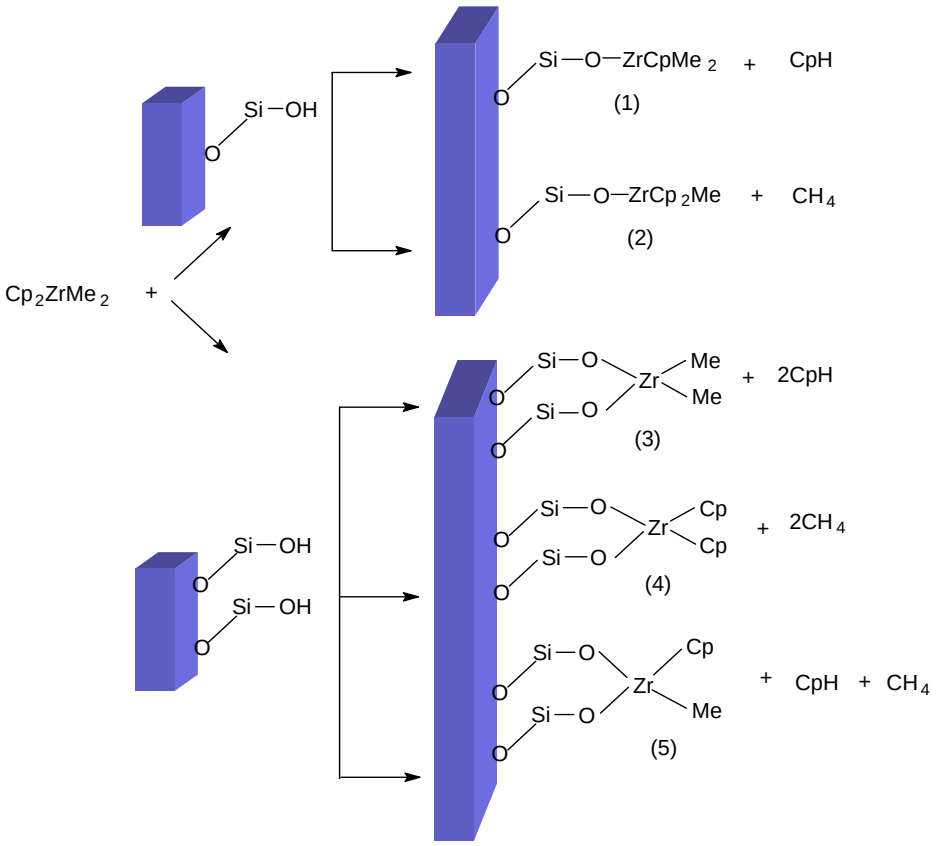

Scheme 4.5: Five possible structures that can arise from supporting Cp_2ZrMe_2 onto silica

4.3.2.3. XPS analyses of the catalysts

XPS of the carbon and zirconium were recorded for all the catalysts (Figs. **4.4** and **4.5**). XPS of silicon did not provide any desired information since the change in the silicon environment was rather insignificant.

Fig 4.4: Zr 3d(5/2) and 3d(3/2) of the silica supported Cp_2ZrMe_2. A to F catalysts **1** to **6**

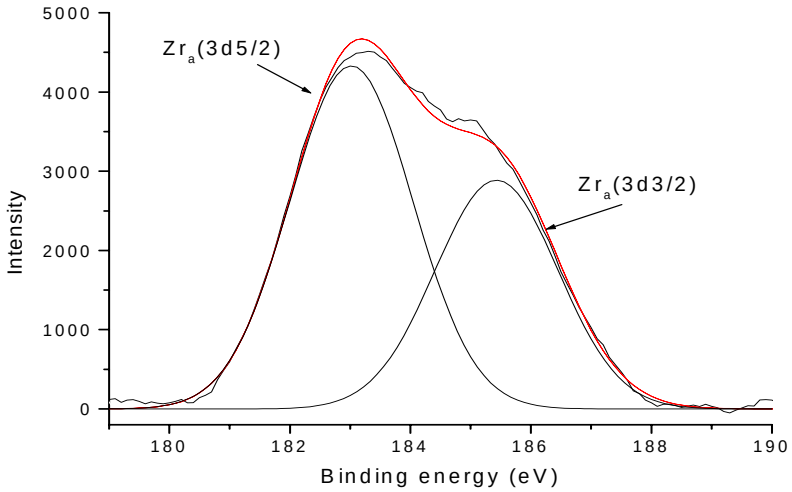

(A)

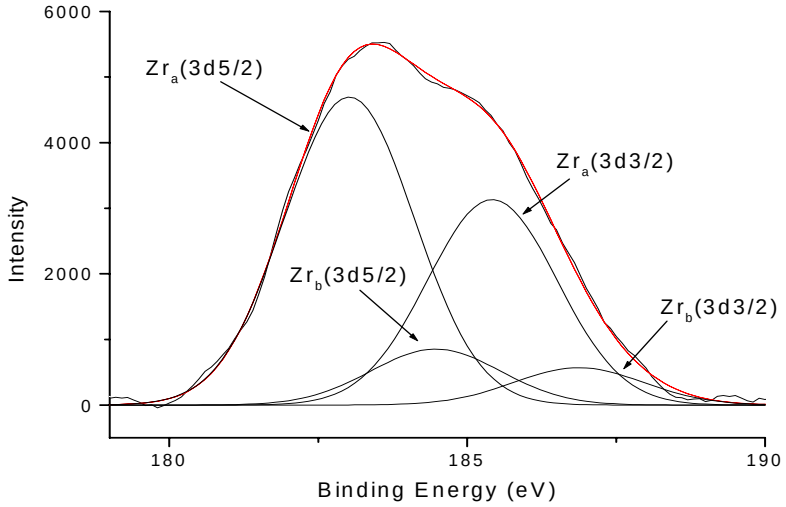

(B)

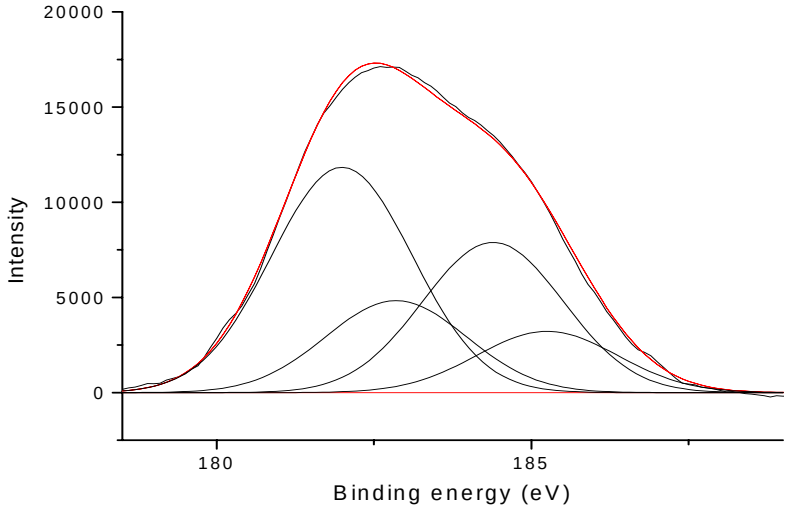
20000
15000
10000
5000
0
Intensity
180
185
Binding energy (eV)

(C)

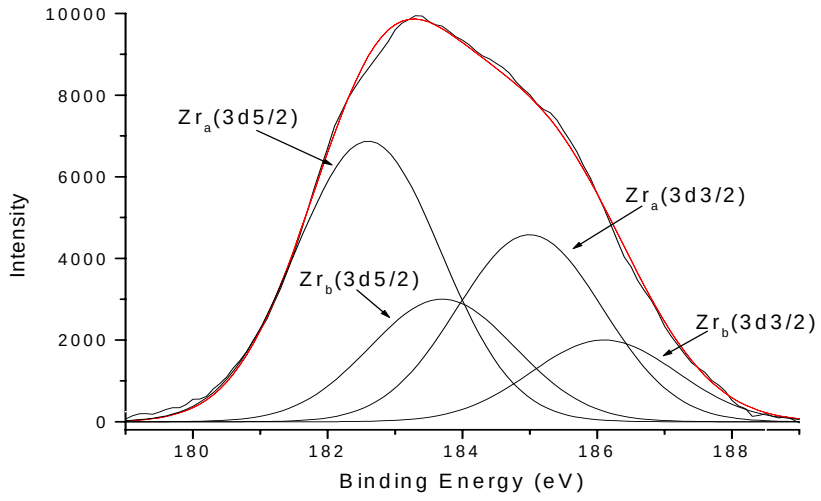
10000
8000
6000
4000
2000
0
Intensity
Zr$_a$(3d5/2)
Zr$_a$(3d3/2)
Zr$_b$(3d5/2)
Zr$_b$(3d3/2)
180
182
184
186
188
Binding Energy (eV)

(D)

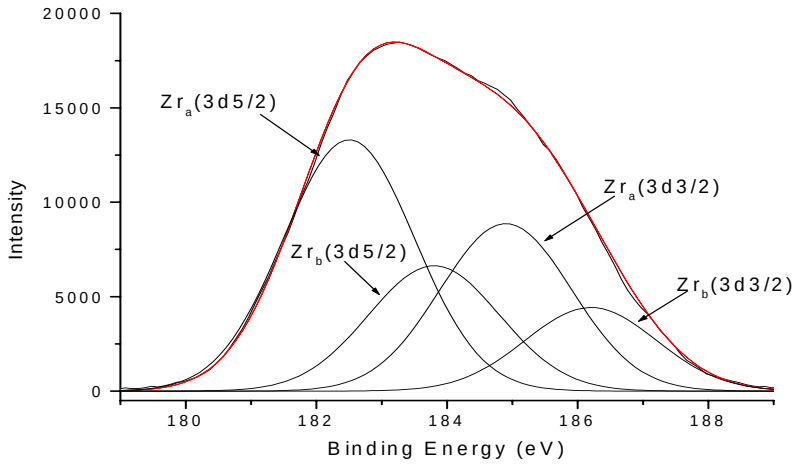
20000
15000
10000
5000
0
Intensity
Zr$_a$(3d5/2)
Zr$_a$(3d3/2)
Zr$_b$(3d5/2)
Zr$_b$(3d3/2)
180
182
184
186
188
Binding Energy (eV)

(E)

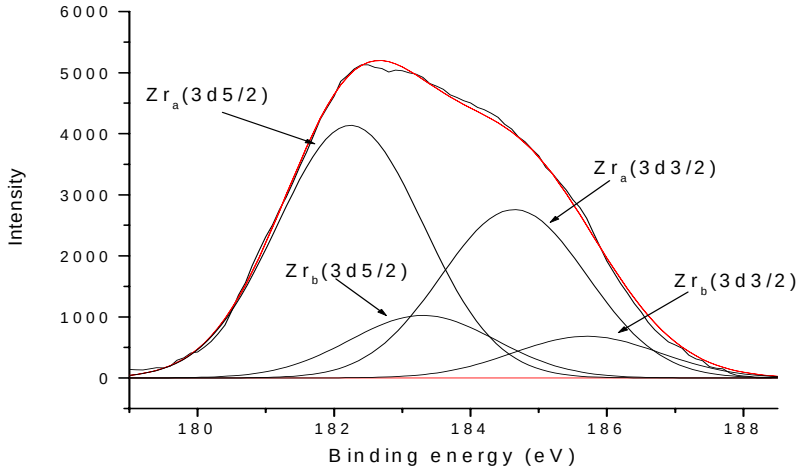
6000
5000
4000
3000
2000
1000
0
Intensity
Zr$_a$(3d5/2)
Zr$_a$(3d3/2)
Zr$_b$(3d5/2)
Zr$_b$(3d3/2)
180
182
184
186
188
Binding energy (eV)

(F)

Fig 4.5: C 1S spectra of silica suported Cp_2ZrMe_2. A to F catalysts **1** to **6**

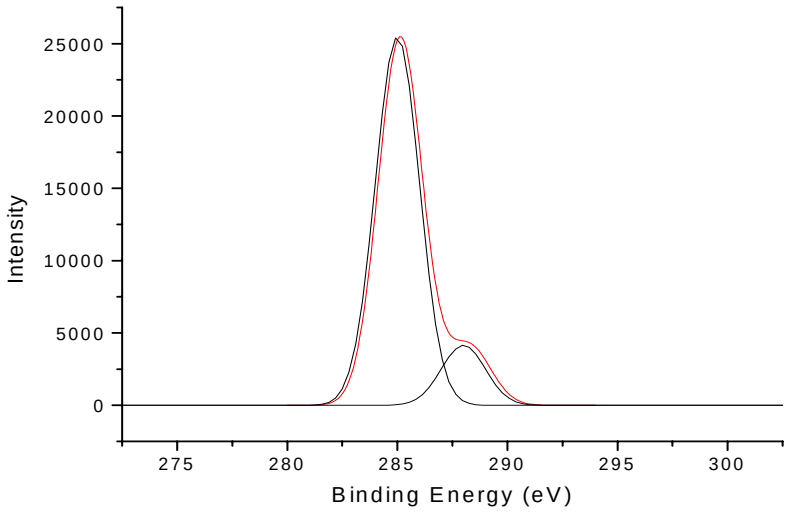

(A)

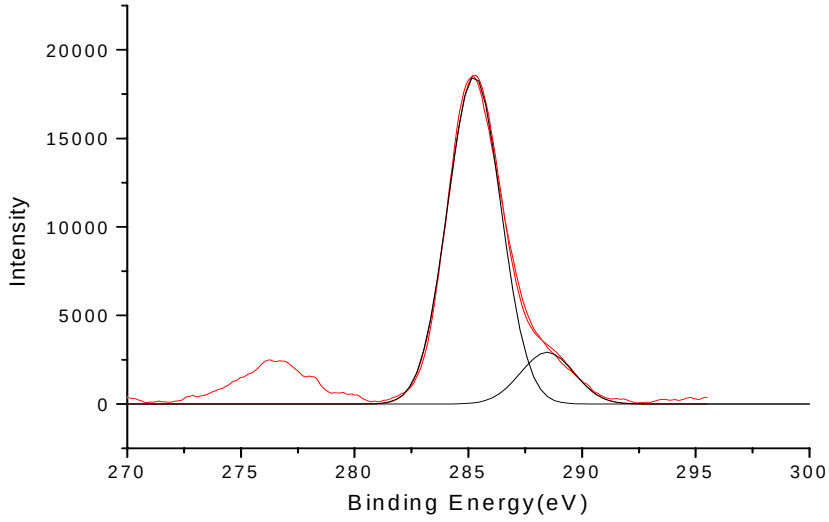

(B)

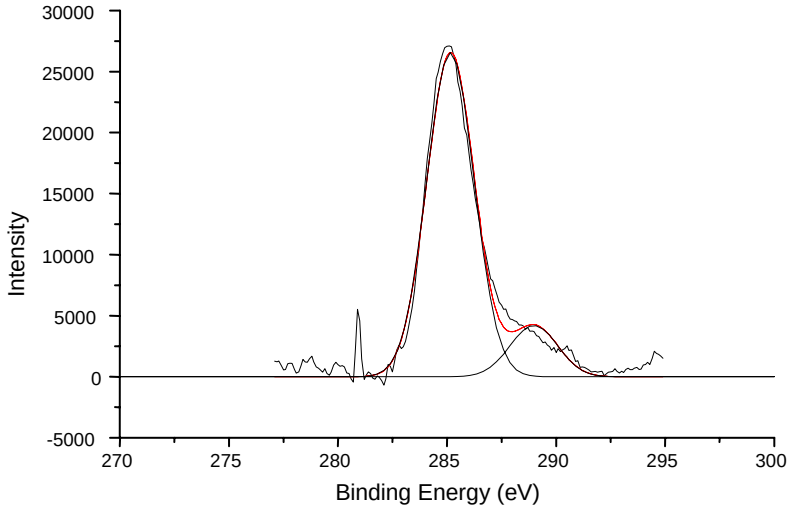
30000
25000
20000
15000
10000
5000
0
-5000
Intensity
270
275
280
285
290
295
300
Binding Energy (eV)

(C)

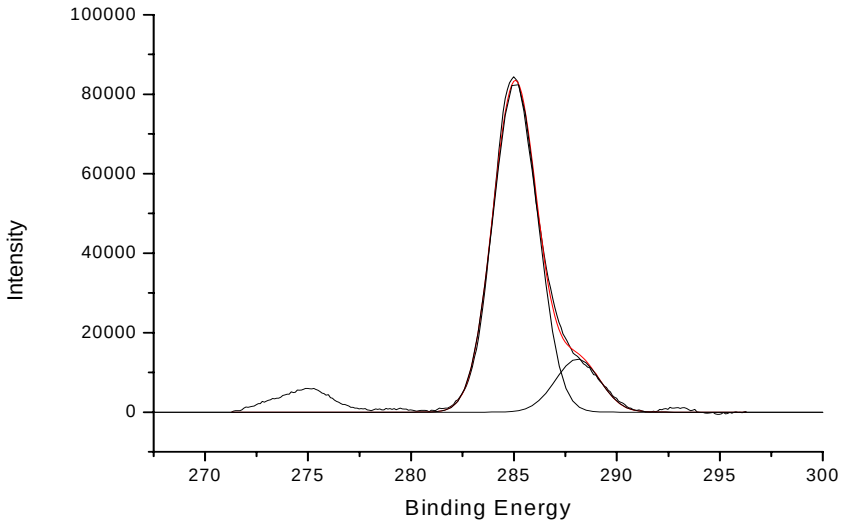
100000
80000
60000
40000
20000
0
Intensity
270
275
280
285
290
295
300
Binding Energy

(D)

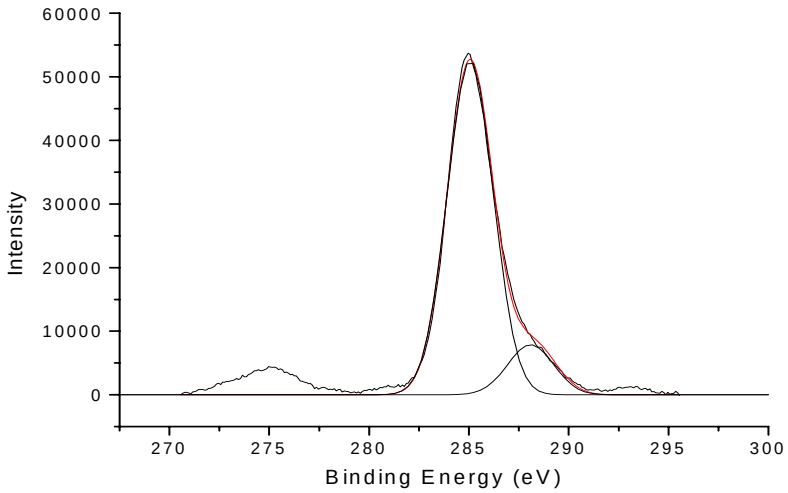
60000
50000
40000
30000
20000
10000
0
Intensity
270
275
280
285
290
295
300
Binding Energy (eV)

(E)

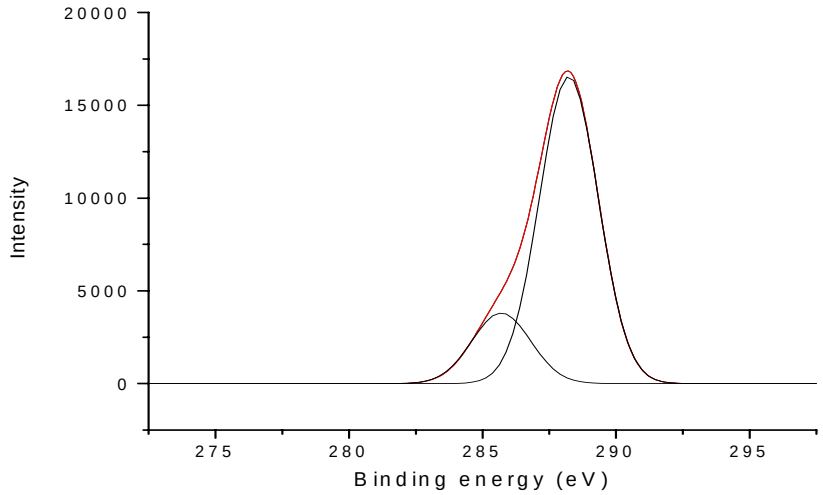
20000
15000
10000
5000
0
Intensity
275
280
285
290
295
Binding energy (eV)

(F)

It is observed that the C(1s) XPS of all the catalysts show two peaks after deconvolution. They are due to the carbons in the cyclopentadienyl ring and the methyl groups in the catalyst. The ratio of the area of the two carbon species present in the catalysts also confirms that in some cases the cyclopentadienyl ligand is lost. The minimum area ratio of Cp/Me is expected to be 10 considering the structure **2** as shown in the scheme **4.5** an even higher if structure 4 is considered. However the Cp:Me ratios that are obtained are in the range 6-7, which suggests the presence of other structures such as **1**,**3** and **5**. It can be seen that the ratio of two carbons is higher for the catalysts where silica is calcined at lower temperature.

However the amount of cyclopentadiene detected by gas chromatography is lower by ~ 65% than what was expected from the XPS data. This could be attributed to the fact that cyclopentadiene, produced, is not completely extracted out of the silica surface. But when the degassing of the sample is done at a very high vacuum (~10^{-9} to 10^{-10} mbar) during XPS analysis cyclopentadiene is completely lost from the surface.

The depletion in the mol of free hydroxyls of the silica after supporting the catalyst also does not correspond to the mol of methane evolved. This can also be explained based on carbon XPS analyses, which shows that a part of the cyclopentadienyl ligand is removed during the process of supporting.

The XPS of 3d(5/2) and 3d(3/2) of zirconium shows the evolution one of zirconium species at 3d5/2 ~ 182 in catalyst **1**. In catalyst **2** to **5,** an additional zirconium species is seen at a higher binding energy (~184 eV). The two species are ascribed to Zr-O and Zr-O_2 species. The zirconium center at Zr-O_2 appears at higher binding energy, as it is more de-shielded. However the change in the ligand environment (Cp and Me) around the zirconium center is not detectable. It can also be seen that the relative quantity of the Zr-O_2 species is higher in catalyst **5** (silica is calcined at 200°C), than in catalyst **3** and **4** (silica is calcined at 400°C). Also there is a small quantity of Zr-O_2 species present at silica calcined at 600°C for 4 h (catalyst **2**). The XPS of Zr(3d5/2) and (3d3/2) of catalyst **6** shows the presence of two species in the catalyst, the ratio of which is 4:1. Although the precise environments of the two zirconium species are not obvious, certain conclusions can still be drawn. It was postulated that MAO anchored to the surface of silica generate the cationic site and stabilize the cation in multi-coordinate crown aluminoxane complexes (7). In that case there is a possibility of formation of two species Zr-O-Al or Zr-$(O\text{-}Al)_2$.

The XPS of C(1s) in case of catalyst **6** shows a different pattern. In addition to Cp and the Zr-Me there is a large quantity of Al-Me in the catalyst. The binding energy values of Al-Me and Zr-Me are similar and thus the two peaks could not be deconvoluted. The observed ratio Cp-carbon/Me-carbon and of ZrO/ZrO_2 for various catalysts is summarized in Table **4.4**.

Table 4.4: Ratio of C_{Cp}/C_{Me} and $Zr\text{-}O/ZrO_2$ in various catalysts as obtained from the XPS analysis

Catalysts	Ratio of C_{Cp}/C_{Me}	Ratio of ZrO/ZrO_2
Catalyst 1	6.14	Nil
Catalyst 2	6.20	5.5
Catalyst 3	6.30	2.5
Catalyst 4	6.25	2.3
Catalyst 5	6.75	2.0
Catalyst 6	Nil	4.1

4.3.3. Polymerization of ethylene

Ethylene polymerization was performed using catalysts **1**-**6**. All catalysts show moderate activities (Table **4.5** and **4.6**). As expected the polymerization activity was higher using catalyst in which silica was calcined at higher temperatures. It can be seen that there is a relationship between the ratio of Zr-O: $Zr\text{-}O_2$ in the catalyst system and the polymerization activities (Fig. **4.6**). Higher the relative quantity of $Zr\text{-}O_2$ in the catalysts lower is the polymerization activity.

Table 4.5: Ethylene polymerization using the silica-supported Cp_2ZrMe_2 catalysts: Effect of temperature[1]

Catalyst No.	Entry No.	Calcination Conditions (°C/h)	Polym Temp. (°C)	Activity[2]	$R_p^3 \times 10^3$	PDI	$\overline{M_w}$
1	1.	600/8	70	21	1.61	2.4	51,200
	2.		60	19	0.93	3.0	119,400
	3.		50	11	0.87	3.3	325,700
2	4.	600/4	70	20	1.42	2.5	97,600
	5.		60	14.5	0.78	3.1	227,400
	6.		50	7	0.61	3.2	328,600
3	7.	400/8	70	15	1.35	2.6	112,300
	8.		60	11	0.72	2.9	278,200
	9.		50	7	0.58	2.9	335,200
4	10.	400/4	70	11	0.59	2.9	88,900
	11.		60	13	0.40	3.0	228,700
	12.		50	5.5	0.32	3.5	303,200
5	13.	200/4	70	15	1.02	2.5	78,300
	14.		60	11	0.74	3.0	181,700
	15.		50	4	0.54	3.3	212,800
6	16.	400/4	70	12	0.52	2.6	140,000
	17.		60	7	0.45	3.1	209,000
	18.		50	1.5	0.16	3.1	278,800

[1]Conditions: [Al]/[Zr] = 500, P = 1 atmosphere, t = 30 min.

[2]KgPE/gZr/h

[3]Initial Rp in $M.sec^{-1}$

Table 4.6: Ethylene polymerization using the silica-supported Cp_2ZrMe_2 catalysts: Effect of [Al]/[Zr][1].

Catalyst No.	Entry No.	Calcination Conditions (°C/h)	[Al]/[Zr]	Activity[2]	$R_p^3 \times 10^3$	PDI	$\overline{M_w}$
1	1.	600/8	1000	28.5	1.82	2.6	64,800
	2.		500	21	1.61	2.5	51,200
	3.		200	16	0.72	2.8	82,000
2	4.	600/4	1000	22	1.71	2.5	78,600
	5.		500	20	1.42	2.5	97,600
	6.		200	4	0.46	2.5	112,300
3	7.	400/8	1000	21	1.68	2.4	115,400
	8.		500	15	1.35	2.5	112,500
	9.		200	3.5	0.31	3.3	73,300
4	10.	400/4	1000	22	1.72	2.6	84,900
	11.		500	11	0.59	2.9	88,900
	12.		200	4	0.21	3.7	90,100
5	13.	200/4	1000	17.5	1.61	2.3	58,900
	14.		500	15	1.02	2.4	78,300
	15.		200	11	1.14	2.6	52,000
6	16.	400/4	1000	13.5	0.65	2.6	110,100
	17.		500	12	0.52	2.6	140,000
	18.		200	5	0.26	2.5	140,200

[1]Condition: Temp. 70°C, P = 1 atmosphere, t = 30 min.

[2]KgPE/gZr/h.

[3]Initial Rp in $M.sec^{-1}$

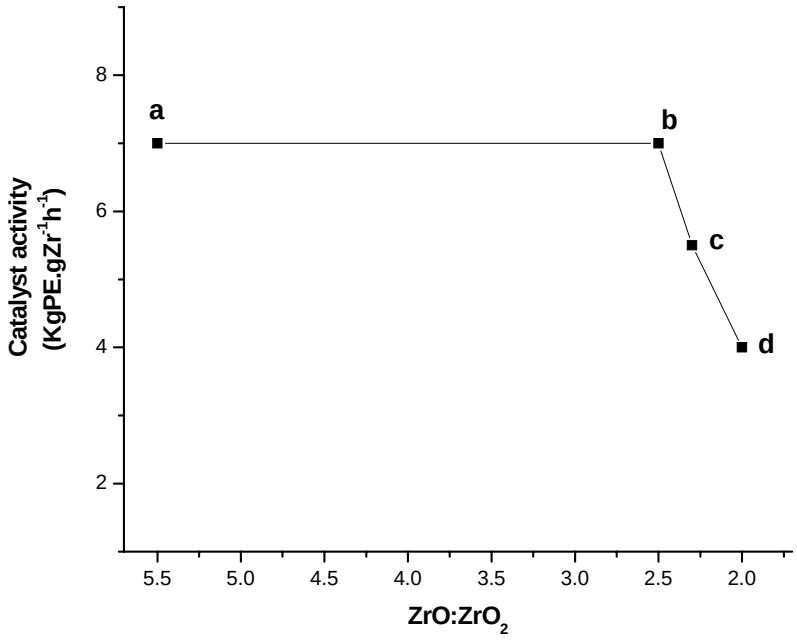

Fig 4.6: Activity of ethylene polymerization as function of $ZrO:ZrO_2$ ratio: a-d: catalysts **2c** to **5c,** Table **4.5**, (conditions of polymerization: [Zr] =4.0-4.8×10^{-6} mol, temp. = 50°C, pressure = 1 atm., AL/Zr = 500, time = 30 min).

4.3.4. Molecular weights and molecular weight distributions

The GPC chromatograms of the polymers obtained show the most probable distribution of molecular weights (Fig **4.7**). As expected the $\overline{M_W}$ of the polymers increased with the decrease in the polymerization temperature and the Al/Zr ratio. The molecular weight is also dependant on temperature of calcinations of silica (Fig **4.8**).

It is observed that with the reduction in the calcination temperature of silica $\overline{M_W}$ decreases along with the catalyst activity. Similar kind of observation was reported by dos Santos et al (28). This observation was attributed to a chain transfer process which was more dominant when silica is calcined at lower temperature. However, the authors did not elaborate on this observation.

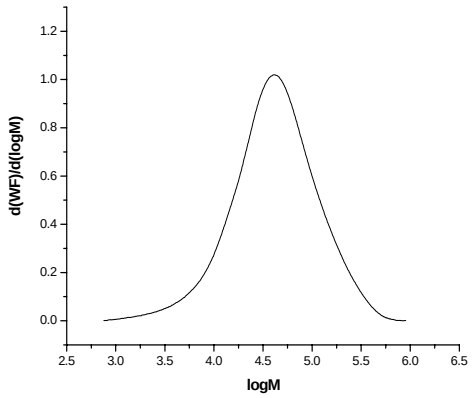

(a) entry 1, Table **4.5**

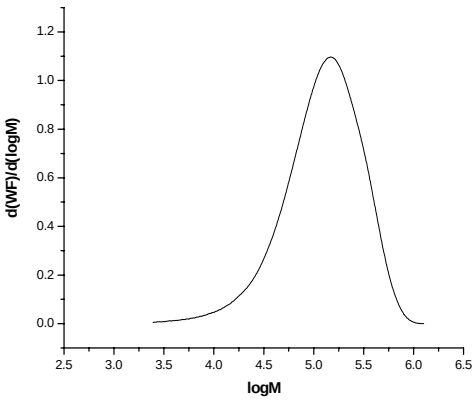

(b) entry 4, Table **4.5**

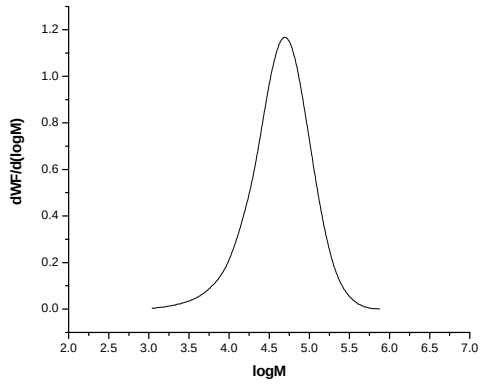

(c) entry 7, Table **4.5**

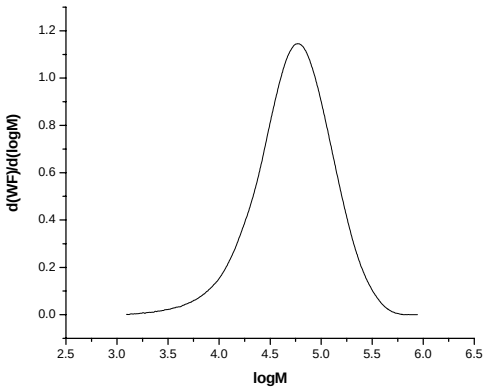

(d) entry 10, Table **4.5**

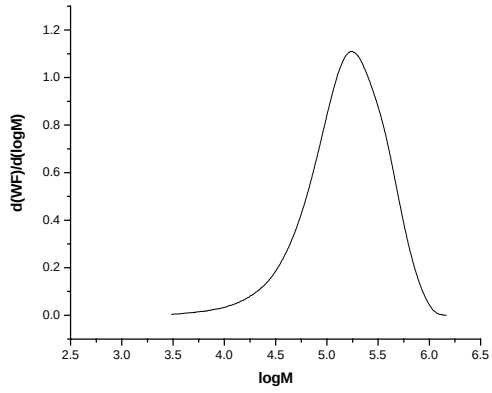

(e) entry 13, Table **4.5**

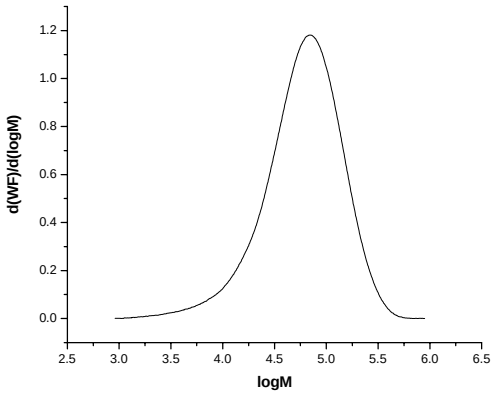

(f) entry 16, Table **4.5**

Fig 4.7: Representative example of GPC of the polymers, a to f catalysts **1** to **6**

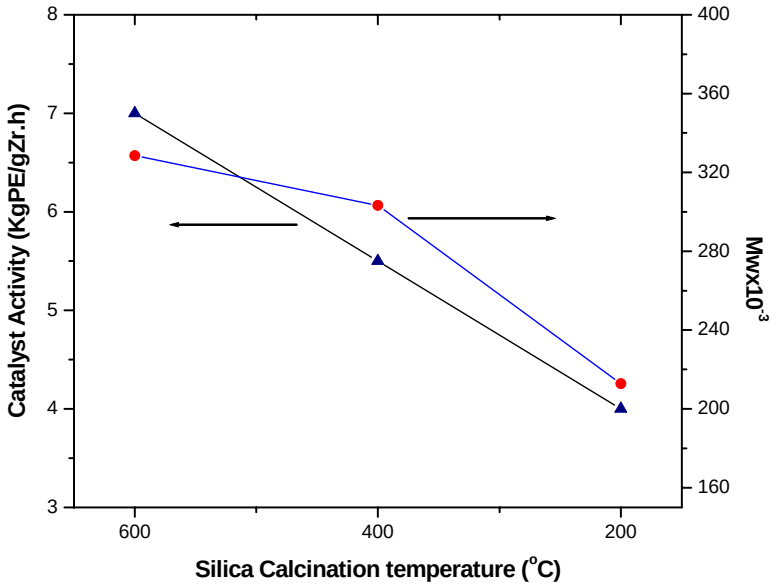

Fig 4.8: Effect of calcination temperature of silica upon the catalyst activity and the average molecular weight, entry no. **6** (600°C) **12** (400°C) and **15** (200°C) of Table **4.5**, (Conditions of Polymerization: [Zr] = 4.0-4.8×10^{-6} mole, temperature = 70°C, pressure = 1 atm., AL/Zr = 500, time = 30 min)

One probable explanation is the change in the structure of methylaluminoxane due to a presence of a higher quantity of free hydroxyls in the catalyst, which could be responsible for the higher proportion of chain transfer to aluminum and subsequent reduction in the $\overline{M_W}$ of the polymer.

4.3.5. Kinetics of polymerizations

The kinetics of ethylene polymerization was studied with silica supported Cp_2ZrMe_2 catalysts. The kinetic profiles of catalysts **1** and **2** are shown in Fig **4.9** and are representative of the effect of calcination time of silica. No major difference in kinetics is discernible. However, the initial rate of the catalyst **1** is higher than that of the catalyst **2.** The effect of calcination temperature of silica on the kinetic profile using catalysts **2**, **4** and **5** are shown in Fig **4.10**. Catalyst **2** showed the highest activity followed by the activity of catalyst **5** and catalyst **4.**

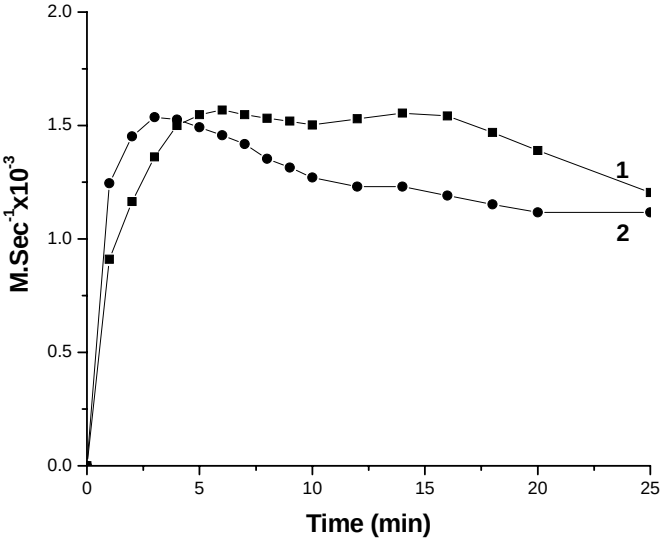

Fig. 4.9: Kinetic profiles of catalysts **1**and **2,** entry no. 1 and 4 of Table **4.5**: Effect of calcination time

The initial rate of polymerization of the three catalysts also follows the same order. This shows that the initial rate is higher in those catalysts where the silica is calcined at higher temperature. This implies larger number of active sites in the catalysts wherein silica is calcined at higher temperature.

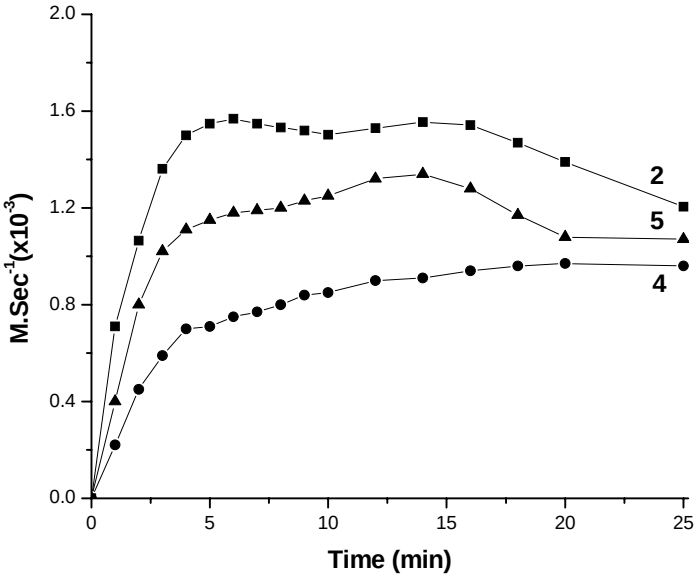

Fig. 4.10: Kinetic profiles of catalysts **2, 4** and **5,** entry no. 4, 10 and 13 of Table **4.5:** Effect of calcination temperature

The initial rate of polymerization of catalyst **5** is higher then that of catalyst **4** in spite of the fact that the calcination temperature in case of catalyst **4** is higher than that of catalyst **5**. This is probably due to the increase in the real concentration of MAO during the polymerization, because of partial hydrolysis of the associated TMA by the free hydroxyls of silica **(**as discussed in Section **4.3.3).**

4.3.6. Effect of pretreatment of silica with MAO on properties of supported catalysts

The predominant mode of preparation of silica-supported metallocene reported in the literature involves pretreatment of silica with MAO. In this method the surface hydroxyls on silica react with Al-CH_3 bonds, resulting in an anchoring of organoaluminum compound on silica. The zirconocene present in the homogeneous phase is activated by a heterogeneous silica supported organoaluminum cocatalyst. Conceptually, such a catalyst is different from one, wherein, the zirconocene is heterogenized on a silica support and the cocatalyst is present in a homogeneous phase. It was, therefore of interest to compare the behavior of the above two type of cocatalysts under identical conditions. The results are summarized in Table **4.7**. The kinetics of ethylene polymerization using catalysts **4** and **6** are shown in Fig. **4.11**

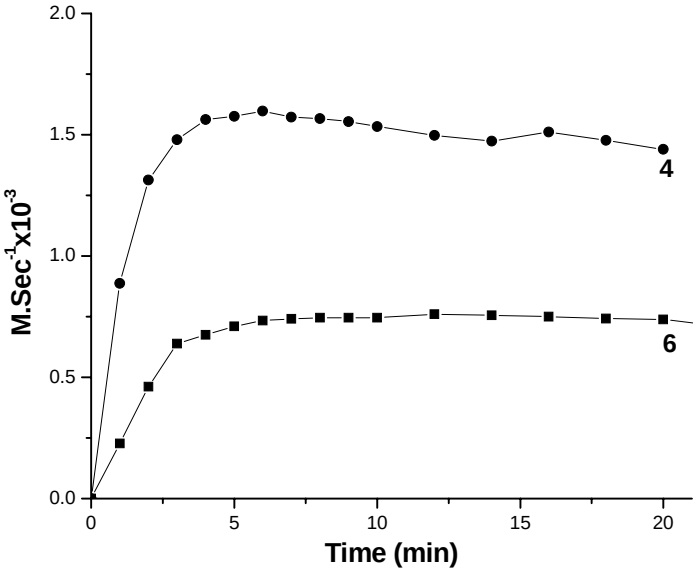

Fig. 4.11: Kinetic profiles of catalyst **4** and catalyst **6,** entry no. 10 and 13 of Table **4.5:** Effect of MAO pretreatment

Table 4.7: Features of ethylene polymerization

Catalyst	Silica calcinations condition °C/time h	MAO used for pre-treatment, mmol of Al	$\frac{[Al]_{total}}{[Zr]}$	Temp °C	Catalyst activity kgPE./gZr-/h	Rp ($\times 10^3$)[1] [M/sec]	$\overline{M_w}$	PDI
4	400/4	--	500	50	5.5	0.32	303,200	3.5
6	400/4	4.2	512	50	1.5	0.16	278,800	3.1

[1]Initial Rp ($M.sec^{-1}$)

Catalyst **6** shows a lower catalyst activity as well as initial rate of polymerization. The kinetic behavior of the two catalysts is similar. No significant differences in $\overline{M_W}$ or molecular weight distribution is observed.

The enhanced catalytic activity and higher R_P of catalyst **4c**, wherein the zirconocene is directly anchored on silica implies enhanced stability of the active site on catalyst **4c** relative to catalyst **6c**. This is reasonable, since in catalyst **6c** the active site is expected to have higher mobility as it is only weakly held onto the support by ionic forces. Consequently, similar to active sites in homogeneous catalyst several deactivation processes can be anticipated. Covalent anchoring of the zirconocene on silica through Si-O-Zr bonds leads to more stable active sites, resulting in superior activity and improves kinetics.

4.3.7. Nature of catalytically active sites in silica supported metallocenes

Based on the results obtained the nature of active sites on silica supported zirconocene can be represented as shown in Fig **4.12 a**. The cationic site is generated by the loss of Cp from the zirconocene upon reaction with silica. The Si-O-Zr covalent bond provides the active site with additional stability. The Zr in its higher valence state is also stabilized by such covalent anchoring onto the solid support.

In contrast, when silica is pretreated with MAO, the cocatalyst is covalently anchored on silica (Fig **4.12 b**). The active site is associated with the silica-supported methylaluminoxane through weak electrostatic forces.

The subtle difference in the nature of active sites is reflected on the kinetics of ethylene polymerization (Table **4.7**).

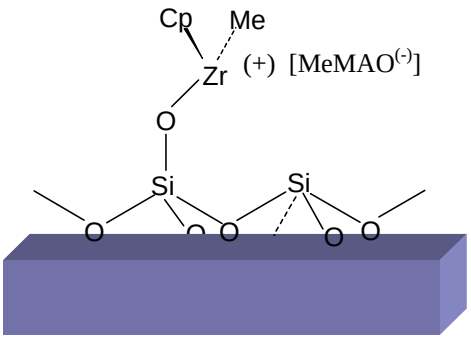

(a)

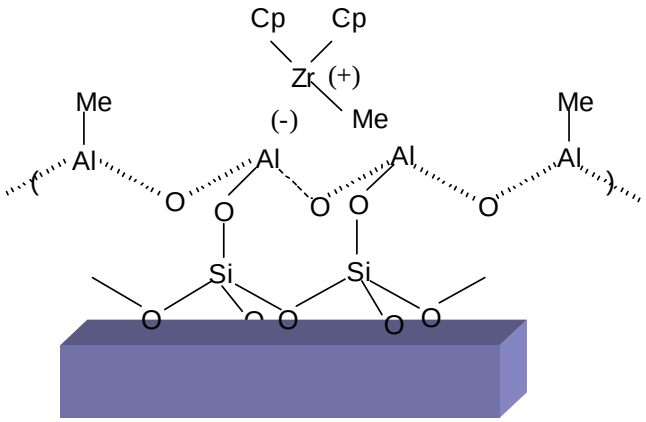

(b)

Fig. 4.12: (a) Catalytically active site on silica supported Cp_2ZrMe_2 (b) silica pretreated with MAO followed by reaction with Cp_2ZrMe_2

4.4. Conclusions

a. Cp_2ZrMe_2 can be directly supported on calcined silica. A chemical reaction resulting in a covalent Si-O-Zr bond is implicated during such a process.

b. The catalytically active sites are generated by loss of Cp group from Cp_2ZrMe_2.

c. Two types of Zr-O species can be detected on the surface of silica. The relative concentration of these species on the surface of silica influence both the catalyst activity as well as $\overline{M_w}$ of the resulting polyethylene (Table **4.8**)

Table 4.8: Effect of the nature of Zr on the silica support on polymerization of ethylene[1]

	Catalyst designation			
	Catalyst **1**	Catalyst **2**	Catalyst **3**	Catalyst **5**
ZrO/ZrO_2 (XPS)	--	5.5	2.5	2.0
Catalyst activity ($KgPE.gZr^{-1}h^{-1}$)	11	7	7	4
R_p ($M.sec^{-1}$) $\times 10^4$	8.7	6.1	5.8	5.4
$\overline{M_w}$	325,700	328,600	335,200	212,800
PDI	3.3	3.2	2.9	3.3

[1]Conditions: Temperature = 50°C, [Al]/[Zr] = 500, P = 1 atmosphere

d. The nature and amount of surface hydroxyl group influence the kinetics of polymerization. It is observed that with the increase of calcination temperature of silica and time of calcinations, the rate of polymerization (Rp) at the initial stage is higher (Table **4.8**). This shows that the number of active species is higher when the silica is calcined at higher temperature and time.

e. When silica is pretreated with MAO and then reacted with Cp_2ZrMe_2 a conceptually different active site is formed, wherein, the aluminum is supported on silica and the active site is loosely held onto the support by electrostatic forces. Such catalysts show lower catalytic activity and rate of polymerization compared to a catalyst, wherein, the zirconium is covalently bonded to the silica and the aluminum is loosely held onto the support by electrostatic forces.

4.5. References

1. Ribeiro, M. R.; Deffieux, A.; Portela, M. F. *Ind.Eng.Chem.Res.* **1997,** *36*(4), 1224-1237.
2. Ciardelli, F.; Altomare, A.; Michelotti, M. *Catal.Today,* **1998,** *41*(1-3), 149-157.
3. Alt, H. G. *J.Chem.Soc., Dalton Trans.* **1999,**(11), 1703-1710.
4. Hlatky, G. G. *Chem.Rev.(Washington, D.C.)* **2000,** *100*(4), 1347-1376.
5. Carnahan, E. M.; Jacobsen, G. B. *CATTECH* **2000,** *4*(1), 74-88.
6. Kaminsky, W.; Renner, F. *Makromol.Chem.* **1993,** *Rapid Commun., 14*(4), 239-243.
7. Chen, Y.-X.; Rausch, M. D.; Chien, J. C. W. *J.Polym.Sci., Part A: Polym.Chem.* **1995,** *33*(13), 2093-2103.
8. Soga, K.; Kaminaka, M. *Makromol.Chem., Rapid Commun.* **1992,** *13*(4), 221-224.
9. Sacchi, M. C.; Zucchi, D.; Tritto, I.; Locatelli, P.; Dall'Occo, T. *Macromol.Rapid Commun.* **1995,** *16* (8), 581-590.

10. Kaminaka, M.; Soga, K. *Makromol.Chem., Rapid Commun.* **1991,** *12*(6), 367-372.

11. Soga, K.; Kaminaka, M. *Makromol.Chem.* **1993,** *194*(6), 1745-1755.

12. dos Santos, J. H. Z.; da Rosa, M. B.; Krug, C.; Stedile, F. C.; Haag, M.; Dupont, J.; Forte, M. d. C. *J.Polym.Sci., Part A: Polym.Chem.* **1999,** *37*(13), 1987-1996.

13. Quijada, R.; Rojas, R.; Alzamora, L.; Retuert, J.; Rabagliati, F. M. *Catal.Lett.* **1997,** *46*(1,2), 107-112.

14. Galland, G. B.; Seferin, M.; Mauler, R. S.; Dos Santos, J. H. Z. *Polym.Int.* **1999,** *48*(8), 660-664.

15. Legrand, A. P. *The Surface Properties of Silicas;* Wiley: Chichester, 1998.

16. Yermakov, Yu. I.; Kuznetsov, B. N.; Zakharov, V. A. 8 ed.; 1981; Chapter 2, pp. 59-120.

17. Collins, S.; Kelly, W. M.; Holden, D. A. *Macromolecules* **1992,** *25*(6), 1780-1785.

18. dos Santos, J. H. Z.; Krug, C.; da Rosa, M. B.; Stedile, F. C.; Dupont, J.; Camargo Forte, M. *J.Mol.Catal.A: Chem.* **1999,** *139*(2-3), 199-207.

19. Jezequel, M.; Dufaud, V.; Ruiz-Garcia, M. J.; Carrillo-Hermosilla, F.; Neugebauer, U.; Niccolai, G. P.; Lefebvre, F.; Bayard, F.; Corker, J.; Fiddy, S.; Evans, J.; Broyer, J. P.; Malinge, J.; Basset, J. M. *Journal of the American Chemical Society* **2001,** *123*(15), 3520-3540.

20. Spoto, G.; Zecchina, A.; Bordiga, S.; Dante, R. *Mater.Chem.Phys.* **1991,** *29*(1-4), 261-269.

21. Camargo Forte, M.; de cunha, F. V.; dos Santos, J. H. Z. *J.Mol.Catal.A: Chem.* **2001,** *175* 91-103.

22. Atiqullah, M.; Faiz, M.; Akhtar, M. N.; Salim, M. A.; Ahmed, S.; Khan, J. H. *Surf.Interface Anal.* **1999,** *27*(8), 728-734.

23. Rausch, M. D. *J.Am.Chem.Soc.* **1973,** *95* 6263.

24. Ward, D. G. US 5,583,085, **1996**.

25. Richter, K.; Peplinski, B. *J.Electron Spectrosc.Relat.Phenom.* **1978,** *13*(1), 69-71.

26. Kaminsky, W.; Strubel, C. *J.Mol.Catal.A: Chem.* **1998,** *128*(1-3), 191-200.

27. dos Santos J. H. Z., Krug, C., da Rosa M. B., Stedile F. C., Dupont J., Forte M. C. *J.Mol.Catal.A: Chem.* **1999,** *128*(2-3), 199-207.

28. dos Santos, J. H. Z.; Larentis, A.; de Rosa, M. B.; Krug, C.; Baumvel, I . J. R.; Dupont, J.; Stedile, F. C.; Forte, M. d. C. *Macromol. Chem. Phys.* **1999**, *200(4)*, 751-757.

5. Silica supported 2,6-bis[1-(2,6-diisopropylphenylimino) ethyl] pyridine iron (II) dichloride catalyst. Nature of metal-support interaction

5.1 Introduction

Late transition metal catalysts are now well established as a class of high activity catalysts for olefin polymerization capable of providing a range of polyolefin structures (1-3). They are activated by both alkylaluminums and other Lewis acids. Late transition metal catalysts are less oxophilic and, hence, are more tolerant to heteroatoms. Therefore, they have been considered as potential catalysts for copolymerizing olefins with polar comonomers. However, to date, these are no clear example of such copolymerization in the literature. Just as for metallocenes, there has been substantial interest in exploring supported late transition metal catalyst for olefin polymerization. The most important reason is to adopt such catalysts for industrially relevant polyolefin processes, namely, gas and slurry phase processes.

The general methods used in the literature for supporting late transition metal catalysts are,

a. supporting the catalysts on silica previously pretreated with MAO, in a slurry of toluene (4,5).
b. reaction of catalysts with MAO in toluene followed by supporting the resulting complex onto silica (6-9).
c. chemically tethering the ligands of a late transition metal catalyst onto the surface of silica (10,11).

2,6-diacetylpyridine-bis-(2,6-diisopropylphenylamine) iron (II) dichloride in conjunction with MAO is known to produce linear polyethylene with high molecular weights (12,13). In this chapter the Fe(II) bispyridyl imine catalyst was supported on silica which had been previously calcined at 200, 400 and 600 ^{o}C. The key objective of this study was to investigate the nature of interaction between the catalyst complex and the silica surface and to explore the effect of hydroxyl concentration and the relative ratio of the paired and isolated hydroxyls on the activity of the catalyst. The

catalyst was supported onto silica using two methods, namely,
a. pretreating silica with MAO followed by supporting the catalyst onto silica and
b. pretreating the catalyst with MAO followed by supporting the complex onto silica.

In a separate study, an attempt was made to modify the ligand used for the preparation of the catalyst complex with a suitable functional group to enable its reaction with the free hydroxyls of silica surface, as an approach to chemically tether the catalyst on silica surface.

5.2. Experimental part

5.2.1. Reagents and materials

The ligand precursors, 2,6-diacetylpyridine and 2,6-diisopropylaniline were procured from Aldrich, USA and used without purification. Ferrous chloride was procured from Sigma USA. 4-Hydroxypyridine-2, 6-dicarboxylic acid (chelidamic acid) were purchased from Aldrich USA and used as such.

5.2.2. Synthesis and characterization of the 2,6-bis[1-(2,6-diisopropylphenylimino) ethyl] pyridine iron (II) dichloride

5.2.2.1. Preparation of 2,6-diacetylpyridinebis (2,6-diisopropylaniline)

To a solution of 2,6-diacetylpyridine (1 g, 6.1 mmol) in dry toluene (10 mL) was added 2,6-diisopropylaniline (2.3 mL, 12.3 mmol). 10 mg of p-toluenesulphonic acid was added to the mixture and the mixture was refluxed under nitrogen. A Dean-Stark apparatus was used to remove the water produced during the reaction. The precipitated yellow solid was filtered after cooling and recrystallized in dichloromethane/hexane and finally yellow solid dried under vacuum. Yield 2.35 g (79%). ^{1}H NMR ($CDCl_3$): δ 8.5 (d, 2H, Py-H_m), 7.9 (t 1H, Py-H_p), 7.1 (m, 6H, Ar-H), 2.79 (m, 4H $CHMe_2$), 2.28 (s, 6H, N=CMe), 1.18 (d, 24H, $CHMe_2$). Anal. ($C_{33}H_{43}N_3$) calc: C, 82.32; H, 8.94; N, 8.73. Found: C 82.10; H, 8.72; N, 8.70.

5.2.2.2. Preparation of 2,6-bis[1-(2,6-diisopropylphenylimino) ethyl] pyridine iron (II) dichloride (catalyst 1)

The synthesis of the catalyst was performed according to reported method (14). A suspension of 1 (1.0 g, 2.05 mmol) in n-butanol was added to a solution of anhydrous ferrous chloride (0.26 g, 2.05 mmol) in n-butanol. The mixture was stirred at 80°C for 15 min, following which a blue colored solution appeared. The reaction was then allowed to cool at room temperature. The reaction mixture was concentrated and diethyl ether was added to the solution to precipitate the product as a blue powder. The product was washed with diethyl ether, filtered and dried under vacuum. Yield 1.01 g (81%). Anal. ($C_{33}H_{43}N_3FeCl_2$): C, 65.14; H, 7.12; N, 6.91. Found: C, 64.95; H, 7.25; N, 6.68.

5.2.3. Preparation of silica supported 2,6-bis[1-(2,6-diisopropylphenylimino) ethyl] pyridine iron (II) dichloride catalyst

5.2.3.1. Silica supported 2,6-bis[1-(2,6-diisopropylphenylimino) ethyl] pyridine iron (II) dichloride (catalyst 2)

1 g of calcined silica was taken in a round bottom flask containing a magnetic needle and fitted with a septum adapter. 10 mL of toluene was added to the flask under nitrogen atmosphere. In a separate round bottom flask 105 mg of the catalyst **1** (0.17 mmol) was taken and 20 mL of toluene added to it. The catalyst **1** solution was slowly added to silica, and the mixture was stirred at 50°C for 2 h. The mixture was then cooled, washed and then filtered thrice with 10 mL of toluene. Finally the deep blue colored solid obtained was dried under vacuum.

5.2.3.2. 2,6-bis[1-(2,6-diisopropylphenylimino) ethyl] pyridine iron (II) dichloride on silica, pretreated with MAO (catalyst 3)

1.3 g of calcined silica was taken in a round bottom flask fitted with a septum adapter and containing a magnetic needle. To this was added 15 mL of dry toluene followed

by 0.7 mL of MAO, containing 4.2 mmol of aluminum, while stirring. The mixture was stirred for 2 h at 50°C. The mixture was then cooled, filtered and the solid was washed with 10 mL of toluene thrice. Finally the solid was dried under vacuum.
0.8 g of the above solid was taken in a round bottom flask fitted with septum adapter and 10 mL of toluene was added. 80 mg of the catalyst **1** (0.13 mmol) was taken in a separate round bottom flask and dissolved in 20 mL of toluene. The catalyst **1** solution was slowly added to the silica and the mixture was stirred at 50°C for 2 h. The mixture was then cooled, washed thrice with 10 mL of toluene and filtered. The pale blue colored solid obtained was dried under vacuum.

5.2.3.3. 2,6-bis[1-(2,6-diisopropylphenylimino) ethyl] pyridine iron (II) dichloride, pretreated with MAO and supported on silica (Catalyst 4)

100 mg of the catalyst **1** (0.16 mmol) was taken in a round bottom flask fitted with a septum adaptor. 10 mL of toluene was added to the flask. This was followed by slow addition of 0.3 mL of MAO solution, containing 1.8 mmol of aluminum. The mixture was stirred for 1 h. In a separate flask 1 g of silica was taken and slurried with 10 mL of toluene. A mixture of catalyst **1**/MAO was added slowly under stirring to the slurry of silica. The mixture was stirred for 3 h at 50°C. The mixture was then cooled, washed thrice with 10 mL of toluene and filtered. The pale blue colored solid obtained was dried under vacuum.

5.2.4. Synthesis of chemically modified 2,6-bis[1-(2,6-diisopropylphenylimino) ethyl] pyridine iron (II) dichloride catalyst

5.2.4.1. Diethyl 4-hydroxypyridine –2, 6-dicarboxylate (2)

The diester was synthesized following a reported method (15). Chelidamic acid (**1**) (2 g, 11 mmol) was taken in a round bottom flask and connected to a septum adaptor and a nitrogen inlet. 50 mL of dry ethanol is added to the flask followed by 0.2 mL of sulfuric acid. The content was refluxed under nitrogen during which time the previously insoluble acid dissolved in ethanol. The reflux was continued for 8 h and

then cooled. The solvent was removed under vacuum and the remaining viscous residue was poured into water. The white precipitate obtained was collected by filtration. The crude product was recrystallized from dilute ethanol. Yield: 2.2 g (85%)

^{1}H NMR ($CDCl_3$): δ 1.45 (t, 6H, CH_3), 4.45 (q, 4H, CH_2), 7.78 (s, 2H, Hpy) (Fig **5.1**)

Analysis: $C_{11}H_{13}NO_5$, Calculated: C, 55.2; H, 5.4; N, 5.9. Found: C, 54.5; H 5.1; N, 5.3.

5.2.4.2. Diethyl 4-(sodiumoxy)pyridine-2,6-dicarboxylate (3)

The sodium salt was synthesized following a reported method (16). 2 g (8.4 mmol) of **2** was dissolved 20 mL of dry ethanoland mixed with an absolute ethanolic solution of 1 equivalent of sodium. The mixture was refluxed for 15 min and cooled. Part of the ethanol was removed under vacuum. Ether was added to the turbid solution when the sodium salt started precipitating out of the solution. The addition of ether was continued till the precipitation of the sodium salt was complete. The solid was filtered and dried under vacuum. Yield: 1.8 g (82.%)

5.2.4.3. Diethyl 4-(3-bromopropoxy) pyridine-2,6-dicarboxylate (4)

A mixture of 1.7 g (6.5 mmol) of **3** and 14.1g of 1,3-dibromopropane (70 mmol) were taken in 10 mL of dry DMF and to it 2.0 mL of tris(3,6-dioxaheptyl)amine (TDA-1) was added. The mixture was heated at 70°C for 16 h. The mixture was then cooled and the solvent evaporated under vacuum. The oily liquid thus obtained was washed with 50 mL water followed by 20 mL hexane. The oil was then dissolved in dichloromethane and dried using anhydrous sodium sulfate. The solution was filtered and the solvent evaporated to obtain a reddish oil. Yield =1.8 g (77%)

^{1}H NMR ($CDCl_3$): δ 1.45 (t, 6H, CH_2CH_3), 2.40 (m, 2H, $BrCH_2CH_2$), 3.62 (t, 2H, $BrCH_2$), 4.32 (t, 2H, OCH_2), 4.45 (q, 4H, CH_3CH_2), 7.80 (s, 2H Hpy) (Fig. **5.2**).

Analysis: $C_{14}H_{18}NO_5Br$, Calculated: C, 46.7; H, 5.0; N 3.9. Found: C, 46.2; H, 4.1; N, 4.1.

5.2.4.4. 4-(3-bromopropoxy) pyridine-2,6-dicarboxylic acid (5)

1.6 g (4.5 mmol) of **4** was taken in 50 mL of 10% sodium hydroxide and stirred for 30 min. The solution was then acidified with dilute hydrochloric acid. A white precipitate was formed which was filtered and dried under vacuum. Yield = 0.96 g (71%).
^{1}H NMR ($CDCl_3$): 2.40 (m, 2H, $BrCH_2CH_2$), 3.62 (t, 2H, $BrCH_2$), 4.32 (t, 2H, OCH_2), 7.80 (s, 2H Hpy).

5.2.4.5. 4-(3-bromopropoxy)pyridine-2,6-dicarbonyl dichloride (6)

0.9 g (3.0 mmol) of **5** was taken in dry dichloromethane and to it 0.5 mL of oxalyl chloride was added. The mixture was stirred for 1 h till the white solid dissolved in the organic solvent. The solvent and the excess oxalyl chloride were removed under vacuum. The yellowish paste was extracted thrice with 10 mL of dry ether and finally the ether was removed under vacuum. No further purification of the product was attempted and was used as such for the next step. Yield = 0.81g (81%).
^{1}H NMR ($CDCl_3$): 2.40 (m, 2H, $BrCH_2CH_2$), 3.62 (t, 2H, $BrCH_2$), 4.32 (t, 2H, OCH_2), 7.80 (s, 2H Hpy) (Fig **5.3**).

5.2.4.6. 2,6-di-(azoacetyl)-4-(3-bromopropoxy)pyridine (7)

This reaction was performed following a reported method (17). In an atmosphere of nitrogen 40 mL of dry diethyl ether containing approximately 0.75 g (18 mmol) of diazomethane (prepared by reacting N-nitroso-N-methyl urea with sodium hydroxide in diethyl ether) were cooled to 0°C. A solution of **6** (0.75 g, 2.2 mmol) in 20 mL of dry diethyl ether was added dropwise. The reaction flask was agitated manually to disperse the yellow precipitate formed. The flask was further agitated for 1 h after completion of the addition. The precipitate was collected by filtration and washed with 20 mL of diethyl ether. The yellow solid obtained was dried under vacuum and stored in absence of light. Yield: 0.45 g (62%).
^{1}H NMR ($CDCl_3$): 2.40 (m, 2H, $BrCH_2CH_2$), 3.62 (t, 2H, $BrCH_2$), 4.32 (t, 2H, OCH_2), 6.6 (s, 2H, CHN_2) 7.80 (s, 2H Hpy) (Fig **5.4**).

5.2.4.7. 2,6-diacetyl-4-(3-bromopropoxy)pyridine (8)

This step is performed following a reported method (17). A solution of **7** (0.4 g, 1.2 mmol) in 30 mL of dichloromethane was added drop wise to a briskly stirred mixture of 10 mL of dichloromethane and 3 g of 45% aquous solution of hydrogen iodide. Stirring was continued for 48 h. At the end of the stirring 20 mL of water was added and the dichloromethane layer was separated. The water layer was extracted four times with dichloromethane (10 mL). The combined organic layer was washed first with 10% sodium thiosulfate solution, then with water, dried over sodium sulfate and finally the solvent removed. Yield: 0.32 g,(95%)

^{1}H NMR ($CDCl_3$): 2.40 (m, 2H, $BrCH_2CH_2$), 3.62 (t, 2H, $BrCH_2$), 4.32 (t, 2H, OCH_2), (s, 2.75 (s, 6H, $COCH_3$) 7.80 (s, 2H Hpy) (Fig **5.5**).

Analysis: $C_{12}H_{14}NO_3Br$: Calculated: C, 51.4, H 5.0, N, 5.0. Found: C, 50.1, H 3.9; N, 6.5.

5.2.4.8. 2,6-bis[1-(2,6-diisopropylphenylimino) ethyl]-4-(3-bromopropxy) pyridine (9)

To a solution of **8** (0.28 g, 1 mmol) in dry toluene (10 mL) was added 2,6-diisopropylaniline (2.1 mmol) and the mixture was refluxed under nitrogen. A Dean-Stark apparatus was used to remove the water produced during the reaction. The precipitated yellow solid was filtered after cooling and washed with chilled methanol. Yield: 0.51 g (82%).

^{1}H NMR ($CDCl_3$): δ 1.14 (m, 24H, $iPrCH_3$), 2.26 (s, 6H, $N=CCH_3$), 2.42 (m, 2H, $BrCH_2CH_2$), 2.77 (m, 4H, iPrCH), 3.65 (t, 2H, $BrCH_2$), 4.34 (t, 2H, OCH_2), 7.14 (m, 6H, HBz), 8.03 (s, 2H, Hpy) (Fig **5.6**).

Analysis: $C_{36}H_{48}N_3OBr$. Calculated C 69.9, H 7.7, N 6.2. Found C 68.8, H 7.1, N 6.4.

5.2.4.9. 2,6-bis[1-(2,6-diisopropylphenylimino)ethyl] – 4 - (3-bromopropxy) pyridine iron(II) dichloride (10)

The synthesis of the catalyst was performed according to the method reported in section **5.2.2.2.** Yield: 0.55 g (90%)

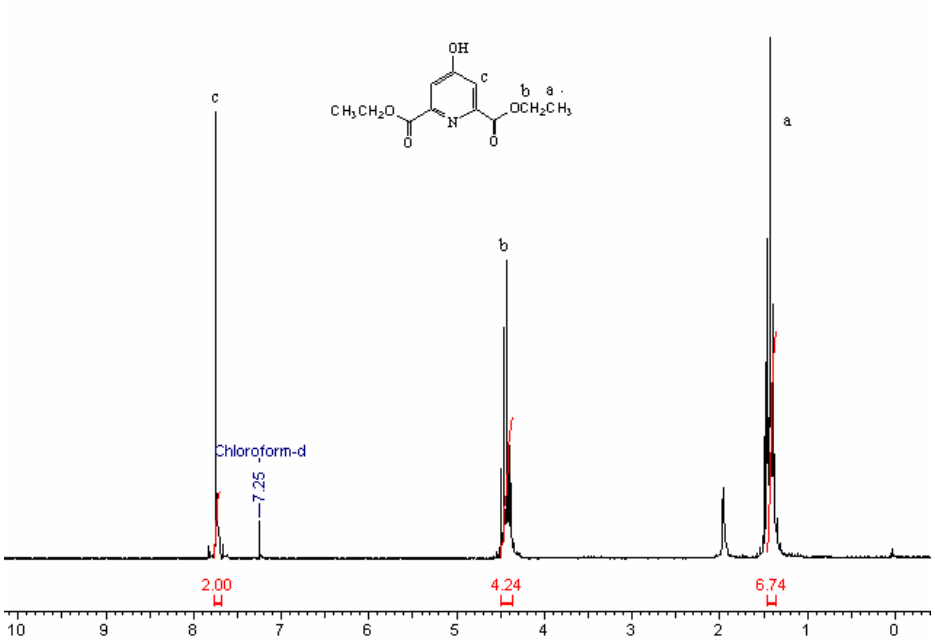

Fig **5.1**: ^{1}H NMR spectrum of **2**

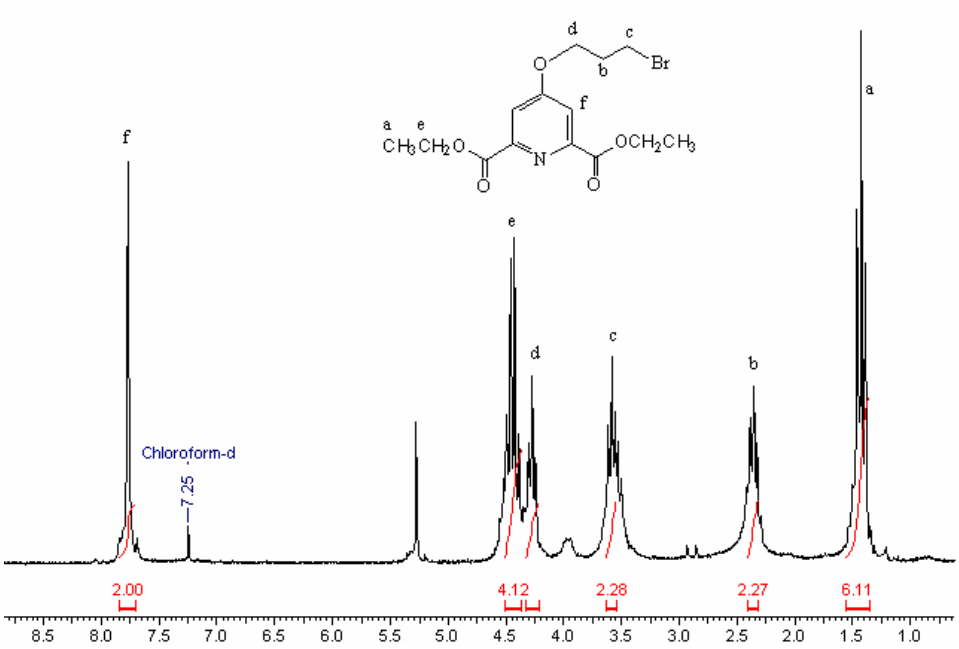

Fig **5.2**: ^{1}H NMR spectrum of **4**

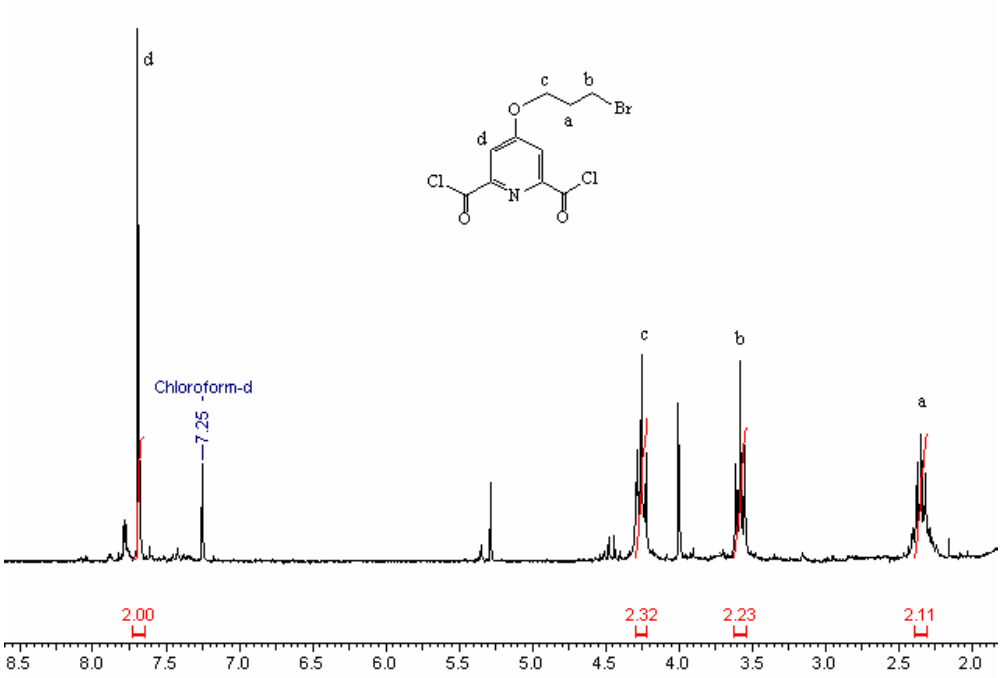

Fig **5.3**: ^{1}H NMR spectrum of **6**

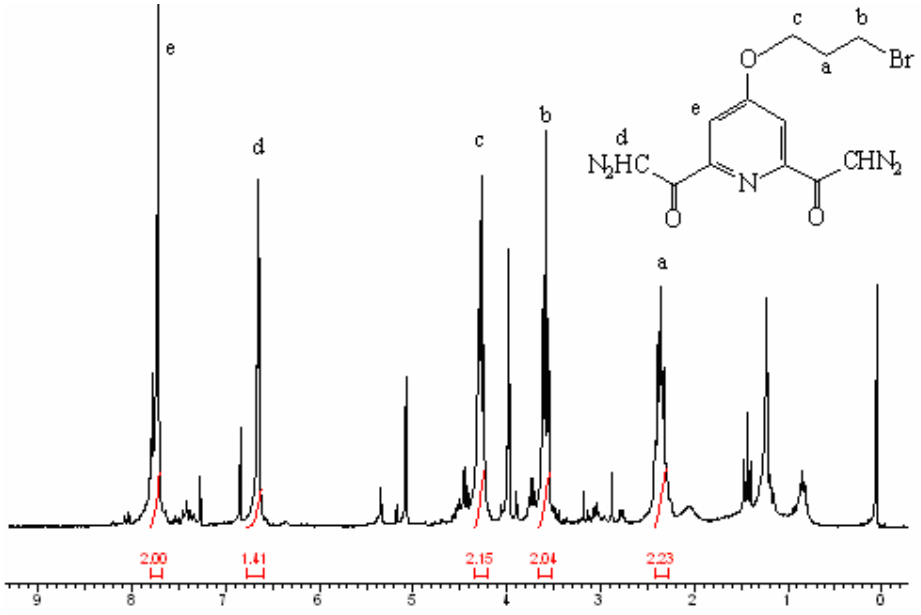

Fig **5.4**: ^{1}H NMR spectrum of **7**

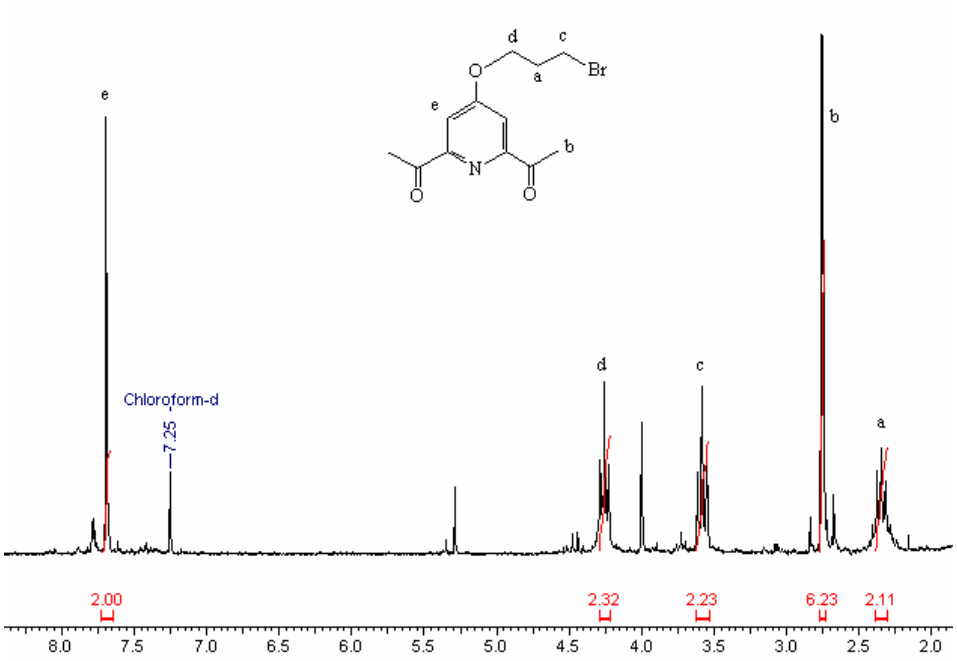

Fig **5.5**: ^{1}H NMR spectrum of **8**

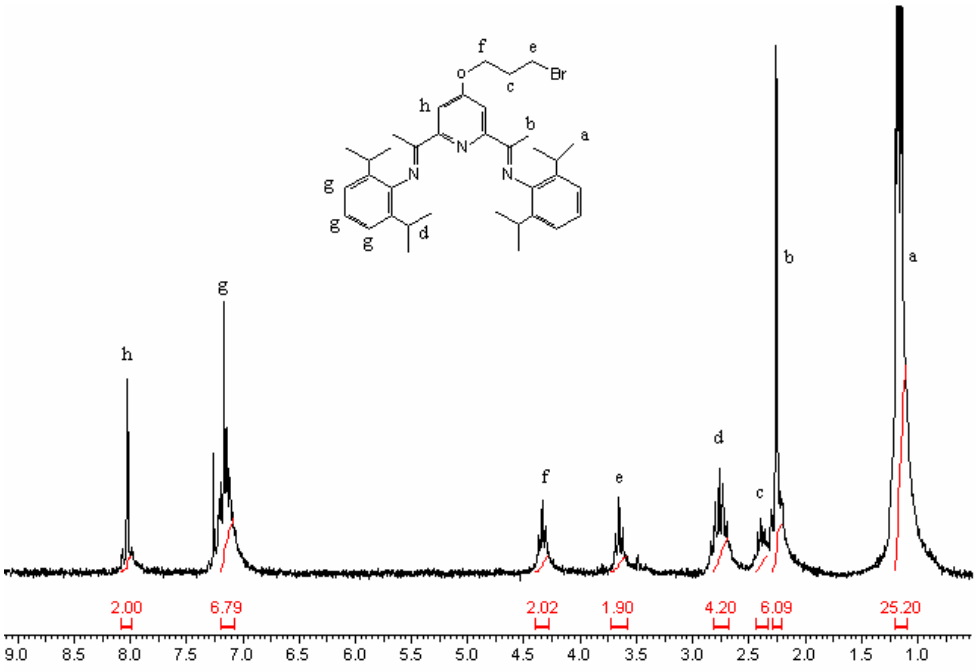

Fig **5.6**: ^{1}H NMR spectrum of **9**

5.2.4.10. Preparation of the silica supported catalyst

The preparation of silica-supported catalyst was performed according to the method reported in section **5.2.3.1.** 1 g of calcined silica was taken in a round bottom flask containing a magnetic needle and fitted with a septum adapter. 10 mL of toluene was added to the flask under nitrogen atmosphere. In a separate round bottom flask 120 mg of **14** was taken and 20 mL of toluene added to it. The catalyst **1** solution slowly added to the silica, and the mixture stirred at 50°C for 2 h. The mixture was then cooled and washed five times with 10 mL of toluene. The white colored solid obtained was dried under vacuum. Yield: 0.92 g.

5.2.5. Characterization of the catalysts

Elemental analyses were performed by the microanalytical services of the National Chemical Laboratory. ^{1}H NMR spectra were recorded on a Bruker spectrometer at 200 MHz.The Fe content of the supported catalyst was estimated ICP analysis following the method described in chapter 3. The free hydroxyl contents of the silica, before and after the catalyst supporting, were estimated by the method described in Chapter 4, section **4.2.6.1**.

5.2.5.1. Extraction of the metal from supported catalysts

100 mg of the supported catalyst were taken in a round-bottomed flask and stirred in 10 mL of toluene at 50°C for 4 h. The solvent was filtered. This experiment was repeated in presence of MAO. The toluene filtrate obtained was evaporated to dryness, the residue dissolved in 2(N) sulfuric acid and used for the measurement of the iron content by ICP.

5.2.5.2. X-ray photoelectron spectroscopy of the catalysts

The X-ray photoelectron spectroscopy of the catalysts was performed according to the method described in Chapter 4, section **4.2.8.2**. Pellets of 10 mm x 1 mm dimension

were made from solid catalysts with the help of a die and subjected to hydraulic press under nitrogen flow. The pellets thus obtained were then introduced into the fast entry air-lock chamber of the instrument while retaining the base pressure of the analysis chamber at a base pressure of 10^{-10} mbar. From the air-lock chamber the samples were transferred to the analysis chamber. The samples were degassed for approximately 15-16 h for before the analyses were done.

The data analysis of the spectra were done using the standard methods like background subtraction, smoothening and non-linear (Gaussian) least square curve fitting. The peak position and the intensity were roughly assigned on the spectra, and were used as the crude value for the curve-fitting program.

The XPS peaks corresponding to the C(1s) and Fe(2p) were recorded.

The XPS peaks obtained are represented as such, after a standard smoothening. In case of multiple peaks they are deconvoluted. In case of the carbon the deconvolutions of the spectra is done by nonlinear curve fitting, using a Gaussian equation.

$$Y = P1*\exp(-0.5*((x-P2)/P3)^2)+P4*\exp(-0.5*((x-P5)/P3)^2)$$

where P1 and P4 are the intensities, P3 is the half line width, P2 and P5 are the binding energy values. This is done with an anticipation that each of the spectra contain two peaks.

5.3 Results and discussion

Five catalysts were taken up for the study. Catalyst **2a**. **2b** and **2c** were prepared by supporting catalyst **1** on calcined silica at three temperatures, namely, 600 °C for 8 h (catalyst **2a**), 400°C for 8 h (catalyst **2b**) and 200°C for 8 h (catalyst **2c**). Catalyst **3** was prepared by supporting catalyst **1** on to silica (calcined at 400°C for 8 h) which had been previously pretreated with MAO. Catalyst **4** was prepared by treating catalyst **1** with MAO first followed by supporting on silica calcined at 400°C for 8 h.

5.3.1. Metal content in the catalysts

Table **5.1** shows the metal content in the five catalysts as determined by ICP analysis. No significant change in metal content is observed with silica calcined at different temperatures. In comparison, when a Cp_2ZrMe_2 is supported on silica calcined at identical temperatures a monotonic decrease in Zr loading with increasing calcining temperature is observed due to decreasing concentration of OH groups (Chapter **4**).

5.3.2. Nature of metal support interactions

The nature of the interaction between the catalysts and the silica surface was examined by two methods, namely, by measuring the free hydroxyls present on the surface of the silica before and after supporting of the catalysts and by the use of X-ray photoelectron spectroscopy. Table **5.1** shows the free hydroxyl content of the catalysts **2a-c**. It is seen that there is no depletion of free hydroxyls due to the reaction of catalyst **1** onto silica. In catalyst **3** there was a depletion of free hydroxyls, presumably, on account of the reaction of MAO with the hydroxyl groups of silica. The free hydroxyl content of catalyst **4**, prior to supporting, is basically equivalent to the free hydroxyl found on silica, calcined at 400°C for 8 h. Upon supporting the catalyst only a small reduction in the free hydroxyl group is observed.

The X-ray photoelectron spectra of the supported catalysts were recorded. The binding energies of Fe centers are given in Table **5.2**. It can be seen that the binding energy value of Fe in the homogeneous catalyst is lower than that of the supported catalyst (Fig **5.7**). The increase in the binding energy from the homogeneous catalyst to the heterogeneous catalysts is indicative of the presence of some weak secondary interactions, between Si-OH and Fe-Cl (Fig **5.11**). However there is no change in the binding energy of the Fe as a function of temperature of calcination of silica (catalyst **2a-2c**, Fig **5.8**).

It is, thus, inferred that the electronic environment of the metal centers are not affected by either the quantity or the nature of the hydroxyl groups present on the silica surface. This implies that the catalyst has no strong interaction with the surface of silica. This observation is contrary to that of Semikolenova et al (18) who reported that the supporting of iron complex on the silica surface occurs by multiple bonding of the catalyst with silica surface via interaction of pyridyl and phenyl groups of the ligand with the OH group of silica. However, this conclusion was not substantiated

by any experimental evidence. XPS, however, provides no evidence of any significant bonding between the catalyst and the surface hydroxyls.

Table 5.1: Depletion of free hydroxyls and % Fe of various silica supported 2,6-diacetylpyridine-bis-(2,6-diisopropylphenylanil) iron(II) dichloride catalyst

Catalyst No.	Silica Calcination temp. (°C)/time (h)	Free hydroxyls of silica[1]		% Fe
		Before supporting	After supporting	
2a	600/8 h	1.81	1.79	0.56
2b	400/8 h	2.29	2.29	0.61
2c	200/8 h	2.47	2.50	0.63
3	400/ 8 h	2.21	0.24	0.75
4	400/8 h	2.10	1.91	0.20

[1]mmol of OH/g of silica.

Table 5.2: The XPS binding energy of silica supported Fe (II) catalyst

Catalyst No.	Fe $(2p)_{3/2}$ binding energy (eV)
1	710.8
2a	711.8
2b	711.7
2c	711.8
3	712.8
4	712.8

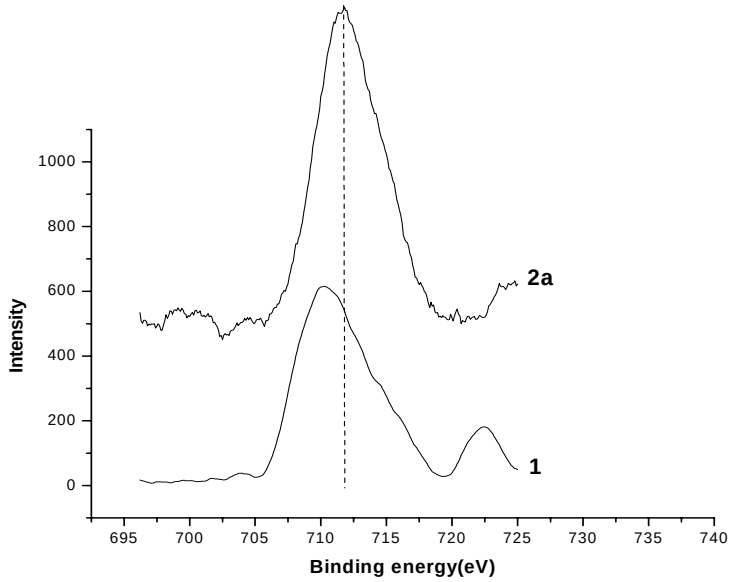

Fig 5.7: Binding energy of Fe ($2p_{3/2}$) center in catalyst **1** and **2a**

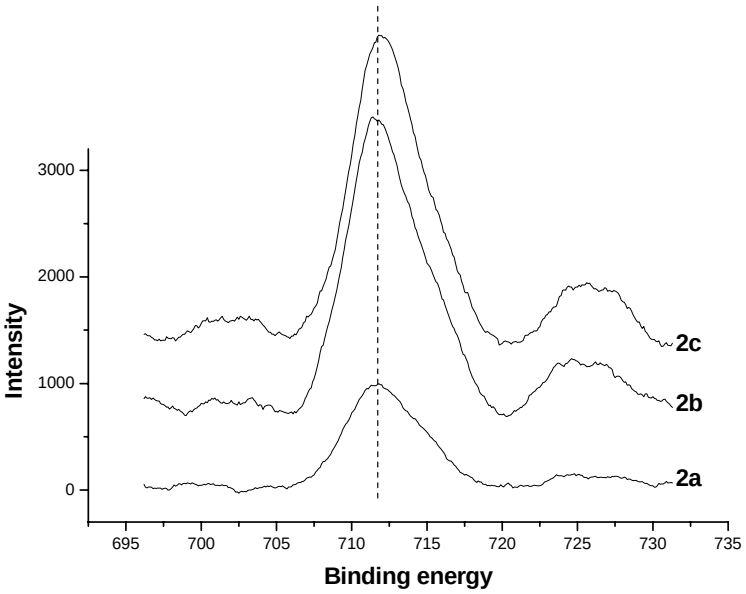

Fig 5.8: Binding energy of Fe ($2p_{3/2}$) center of catalysts **2a-c**: effect of silica calcination temperature

The binding energy value of the Fe centers of catalyst **3** and **4** are higher than catalysts **2a-c** as well as the homogeneous catalyst. This is presumably due to a cationic charge on iron, which renders the loss of electron from the metal center more difficult. Ma et al (19) reported similar increase in the binding energy of the Fe ($2p_{3/2}$) center from 710.5 eV to 711. 8 eV when the iron catalyst was supported onto silica pretreated with MAO.

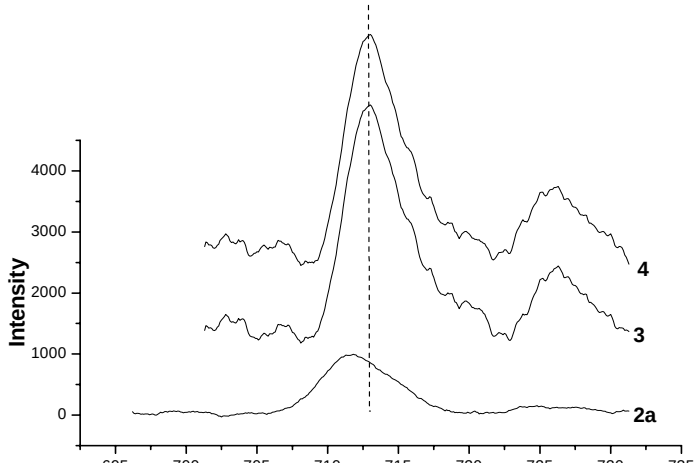

Fig 5.9: Binding energy of Fe ($2p_{3/2}$) center of catalysts **2a**, **3** and **4**: Effect of pretreatment of the silica (catalyst **3)** and pretreatment of catalyst (catalyst **4**)

5.3.3. Polymerization of ethylene using supported 2,6-bis[1-(2,6-diisopropylphenylimino) ethyl] pyridine iron (II) dichloride catalysts

Polymerization of ethylene was performed using all the five catalysts using MAO as the cocatalyst. The polymerizations were preformed at 1 bar ethylene pressure and for 30 min. The results are given in tables **5.3** and **5.4**. The polymerization activity is reported after 10 min and 30 min of polymerization. It is seen that the polymerization activity decreases with an increase in temperature in all the supported catalysts. The activities of catalysts **3** and **4** are lower than the catalysts **2a-2c**. It is observed that the catalyst prepared using silica support with lower hydroxyl content exhibits a higher catalytic activity.

Table 5.3: Ethylene polymerization using Catalyst **1**, **2a, 2b and 2c**[a]

Entry No.	Polym Temp (°C)	Al/Fe Ratio	Activity (KgPE/molFe/h)		Mp_1[b]	Mp_2[c]	R_p[d] × 10^3
			After 10 min	After 30 min			
Catalyst **1**							
1	30	1000	4670	1510	600	91,700	2.60
Catalyst **2a**							
2	30	1000	4318	1628	2480	98,500	2.09
3	40	1000	4126	1400	2100	78,500	1.79
4	50	1000	3355	1380	1850	71,300	1.78
5	50	500	660	-	1400	22,800	1.46
6	50	1500	3811	1389	1700	41,200	1.90
Catalyst **2b**							
7	30	1000	4065	1529	2300	92,500	1.86
8	40	1000	3156	1087	2000	80,000	1.75
9	50	1000	3108	1150	1600	42,600	1.72
10	50	500	2221	-	1100	23,800	1.64
11	50	1500	3463	1241	2100	36,400	1.70
Catalyst **2c**							
12	30	1000	3042	1468	540	91,600	1.71
13	40	1000	2982	1431	1150	65,000	1.28
14	50	1000	2335	887	3750	46,500	1.21
15	50	500	2315	832	1150	22,700	1.02
16	50	1500	2395	983	650	32,510	1.23

[a] Pressure: 1 atm.; time: 30 min; [Fe] = 1-1.5×10^{-6} mol.; Toluene =50 mL

[b] Peak molecular weight of lower molecular weight fraction

[c] Peak molecular weight of higher molecular weight fraction

[d] $M.sec^{-1}$

Table 5.4: Ethylene polymerization using Catalysts **3** and **4**[a]

Entry No.	Polym Temp (°C)	Al/Fe Ratio	Activity (KgPE/molFe/h)		Mp_1[b]	Mp_2[c]	R_p[d]× 10^3
			After 10 min	After 30 min			
Catalyst **3**							
1	30	1000	1500	830	1400	140,000	0.66
2	40	1000	1607	857	1400	72,400	0.73
3	50	1000	911	386	1250	92,500	0.42
4	50	500	916	382	1450	111,300	0.51
5	50	1500	828	427	1320	64,300	0.50
Catalyst **4**							
6	30	1000	1856	980	3200	191,300	1.12
7	40	1000	916	498	3100	177,500	0.66
8	50	1000	1055	520	2800	172,000	0.65
9	50	500	644	389	2900	273,400	0.47
10	50	1500	997	499	2900	145,200	0.48

[a] Pressure: 1 atm.; time: 30 min; [Fe] = 2-2.6×10^{-6} mol.; Toluene = 50 mL

[b] Peak molecular weight of lower molecular weight fraction

[c] Peak molecular weight of higher molecular weight fraction

[d] M.sec^{-1}

5.3.4. Kinetics of polymerization

The kinetics of polymerization of ethylene with all the five catalysts were studied. The results are shown in Fig **5.10-5.12**. The initial R_p values were calculated from linear extrapolation of the initial rate values in the ascending part of the kinetic curves. Fig **5.10** shows the kinetics of polymerization of catalyst **1** and **2a**. It is seen

that catalyst **1** exhibits an initial surge in the catalytic activity followed by a rapid decay. This is typical of homogeneous catalysts. The rate of decay in case of supported catalyst is much slower. This demonstrates the beneficial effect of the silica support on the kinetics of polymerization. The initial Rp values for the two catalysts are however similar. Fig **5.5** shows the kinetic profiles of catalysts **2a-c.** It is observed that initial R_P increase in the order **2a**>**2b**>**2c**. Thus, the catalyst prepared from a support calcined at higher temperature shows the highest peak rate.

The initial rate of polymerization of catalyst **2b**, **3** and **4** are shown in Fig **5.12**. In all these cases, the silica used for catalyst preparation was calcined at 400°C for 8 h. The initial rate of **2b** is higher than either **3** and **4.** Thus, prereacting the surface hydroxyl groups of silica with MAO has a deleterious effect on catalyst activity.

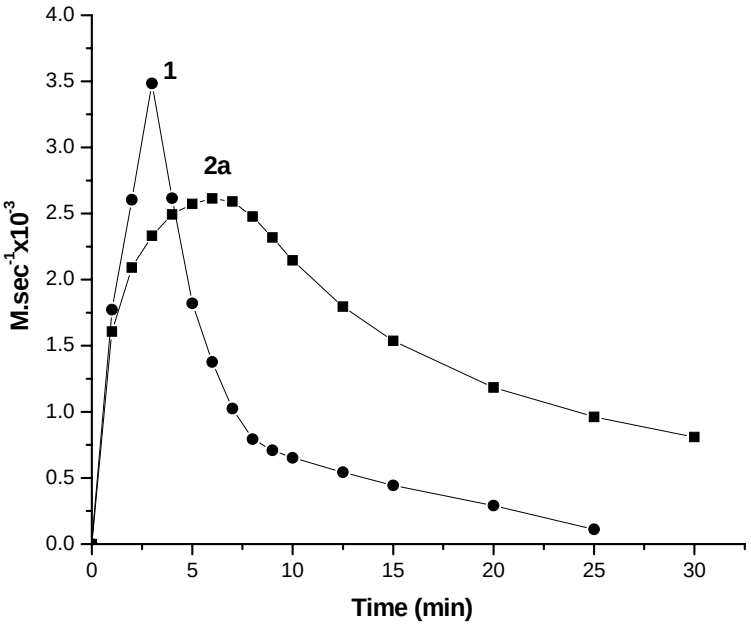

Fig 5.10: Kinetics of Polymerization of catalysts **1** (entry 1, Table **5.3**) and **2a** (entry 2, Table **5.**3): Effect of heterogenization of the catalyst

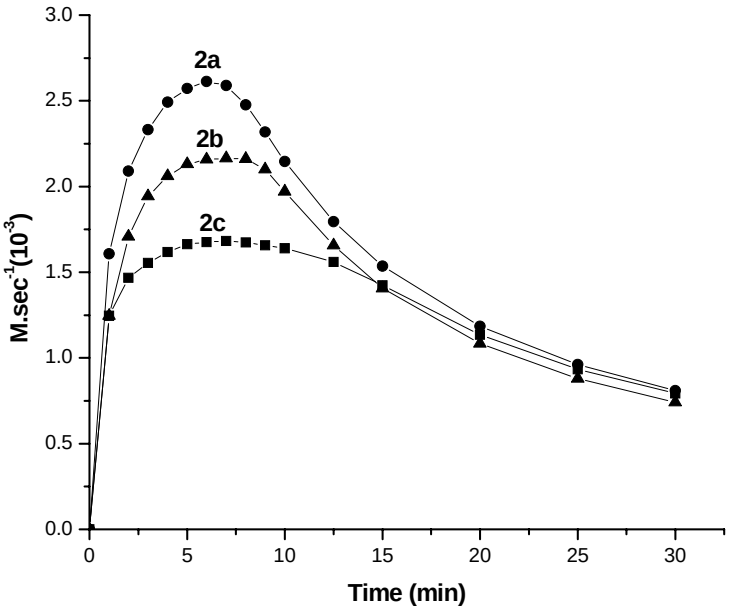

Fig 5.11: Kinetics of polymerization of catalysts **2a**, **2b** and **2c**: Effect of silica calcination temperature (entry 2, 7 and 12, Table **5.3**)

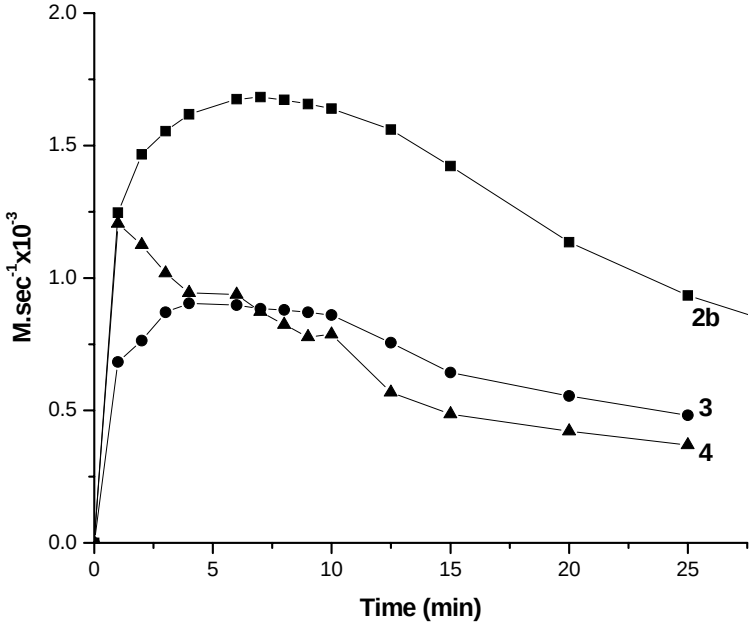

Fig 5.12: Kinetics of polymerization of catalysts **2b** (entry 7, Table **5.3**), **3**, and **4** (entry 1 and 6, Table **5.4**): Effect of pretreatment of the silica (**3**) and catalyst (**4**) with MAO

5.3.5. Molecular weight and molecular weight distributions

All polymers exhibit two distinct peaks in GPC (bimodal peaks). This observation is similar to what has been observed for homogeneous catalyst. Fig **5.13** shows the effect of heterogenization and calcination temperature of silica on the nature of molecular weight distributions. Use of silica calcined at lower temperatures as a catalyst support leads to marginal decrease in peak molecular weights. Apparently, residual hydroxyl groups have an adverse effect on molecular weights. This observation is further substantiated by the fact that when silica is pretreated with MAO, there is a significant increase in peak molecular weights (Fig **5.14**). Higher molecular weight polymers are obtained when a catalyst complex is preformed and then supported onto silica.

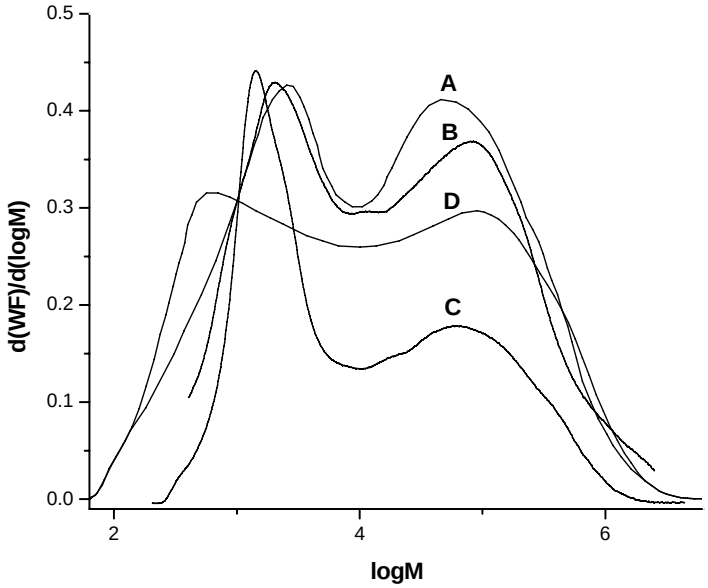

Fig 5.13: GPC of polymers obtained from catalysts **2a** (**A** entry 2, Table **5.3**), **2b** (**B** entry 2**,** Table **5.4**), **2c**(**C** entry 2, Table **5.5**) and catalyst **1** (**D**)

Fig **5.14** shows the effect of polymerization temperature on the nature of molecular weight distributions. It is observed that both Mp_1 and Mp_2 shift towards lower molecular weight with increasing temperature.

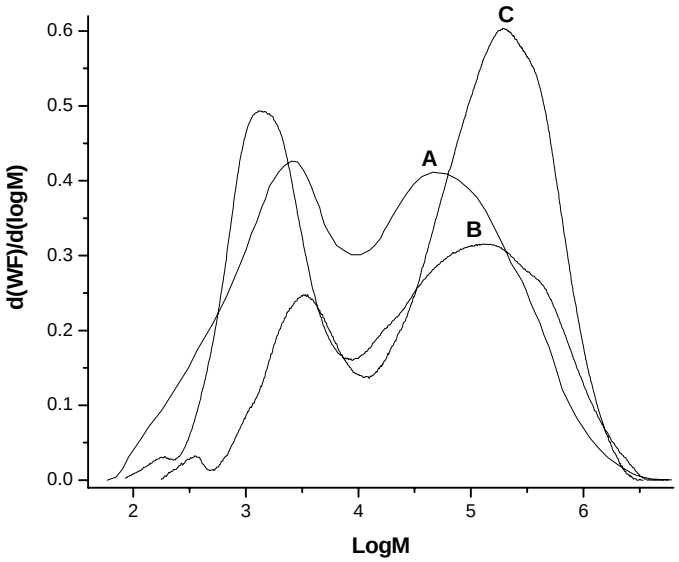

Fig **5.14**: GPC of polymers obtained from catalyst **2b**, (**A** entry 1, Table **5.4**), catalyst **3** (**B** entry 1, Table **5.6**) and catalyst **4** (**C** entry 1, Table **5.7**)

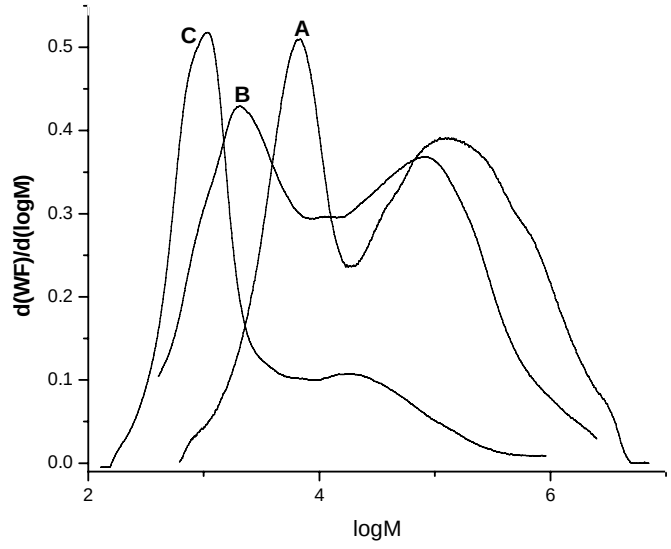

Fig 5.15: GPC of polymers obtained from catalyst **2b,** at 30°C (**A** entry 1, Table **5.4**), 40°C (**B** entry 2, Table **5.4**) and 50°C (**C** entry 3, Table **5.4**)

5.3.6. Nature of active sites and mechanism of polymerization

A summary of salient results obtained with various silica supported Fe(II) pyridylimine catalysts are given in Table **5.5**.

Table 5.5: Polymerization of ethylene using silica supported Fe (II) pyridylimine catalyst: summary of results[a]

	Catalyst designation					
	Catalyst **1**	Catalyst **2a**	Catalyst **2b**	Catalyst **2c**	Catalyst **3**	Catalyst **4**
Catalyst activity (KgPE.molFe^{-1}.h^{-1})	1510	1628	1529	1468	830	980
Initial $R_p \times 10^4$ M.sec^{-1}	26.0	20.9	18.6	17.1	6.6	10.2
Mp_2	91,700	98,500	92,500	91,600	140,000	191,300

[a]Conditions: Temperature = 30°C, [Al]/[Zr] = 1000, P = 1 atmosphere

Any discussion on the nature of active sites and mechanism must take into consideration the following experimental observations

a. Supporting the catalyst on suitably activated silica increases the catalyst activity.
b. The catalyst activity as well as initial R_p decreases with increasing hydroxyl content on silica (**2a** >**2b**>**2c**). However it is pertinent to recognize that under polymerizing conditions, these residual hydroxyl contents will react with the organoaluminium compounds used as cocatalysts.
c. Complete removal of all hydroxyl groups by pretreating silica with MAO, leads to a significant drop in catalyst activity as well as initial R_p.

d. Supporting the catalyst on suitably activated silica leads to a small increase in molecular weight compared to soluble catalyst.

e. However, peak molecular weight decreases with decreasing calcination temperature of the support.

f. Pretreatment of silica with MAO followed by treatment with the Fe (II) catalyst led to significant increase in peak molecular weights.

g. Preforming the Fe (II) – MAO complex followed by treatment with silica led to even higher peak molecular weights.

Silica support with low hydroxyl content may offer just enough weak interactions between the catalyst and isolated hydroxyl groups on the surface of the support as shown in Fig **5.16**.

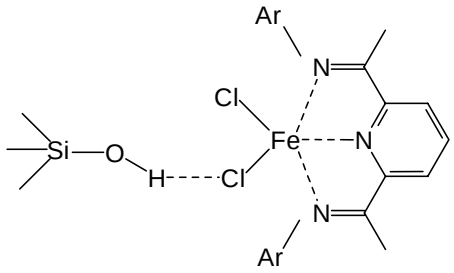

Fig 5.16: Schematic representation of H----Cl hydrogen bonded supported Fe (II) pyridylimine catalyst

Such Cl–H weak hydrogen bonds are ubiquitous in the literature. These weak interactions can stabilize the active site and thus alter the nature of polymerization kinetics (Fig **5.10**). The small decrease in initial R_p, catalyst activity and peak molecular weight upon using silica bearing higher hydroxyl group can be attributed to the partial loss of MAO by the reaction with the hydroxyl groups on silica and the consequent decrease in Al/Fe ratio.

Complete elimination of hydroxyl groups in silica has an adverse effect on catalyst activity and initial R_p. Under these conditions the catalyst is most probably held on to the surface of silica through weak physical adsorption. Under these circumstances silica support does not exert any stabilizing influence on the active site.

The most significant observation is that the catalyst prepared using silica pretreated with MAO produces polymers with substantially higher peak molecular weights than

silica which has not been pretreated with MAO. Taken together with the observation that catalysts **3** and **4** show reduced rate of polymerization, this is indicative of much lower active site concentration under these conditions. There is considerable ambiguity in the literature on the nature of active sites in the case of Fe (II) iminopyridyl catalyst system (20) Fe (III) species are implicated as active sites although their precise nature remains to be determined. For some reasons, either less active sites are formed when a MAO pretreated silica is used (catalyst **3**) or the active sites generated are partially destroyed when they are brought in contact with silica calcined at 400^{o} C for 8h (catalyst **4**)

5.3.7. Chemical tethering of the modified iron catalyst onto the surface of silica

With an objective to chemically tether the catalyst onto the surface of silica, synthesis of a new ligand, namely, 2,6-bis[1-(2,6-diisopropylphenylimino)ethyl]-4-(3-bromopropoxy) pyridine (**9**) was attempted. The reaction scheme is shown in Scheme **5.1**. The ligand was synthesized using eight steps starting from commercially available chelidamic acid (**1**). The overall yield of **9** was 40%. The NMR spectrum of **9** is shown in Fig **5.6**. The Fe(II) catalyst was made using the ligand **9** and then reacted with silica calcined at 600°C for 8 h. It was anticipated that the residual hydroxyl group on silica will react with the bromoalkyl group of the ligand associated with the catalyst. A similar strategy was earlier reported by Lee et al for chemically linking a zirconocene catalyst onto the surface of silica (21). However attempts to chemically link the Fe (II) catalyst bearing the ligand **9** to silica failed. The reason for this is not clear at the present time. It is, however, pertinent to note that Lee et al (21) used a five carbon spacer as against a three carbon spacer used in the present example.

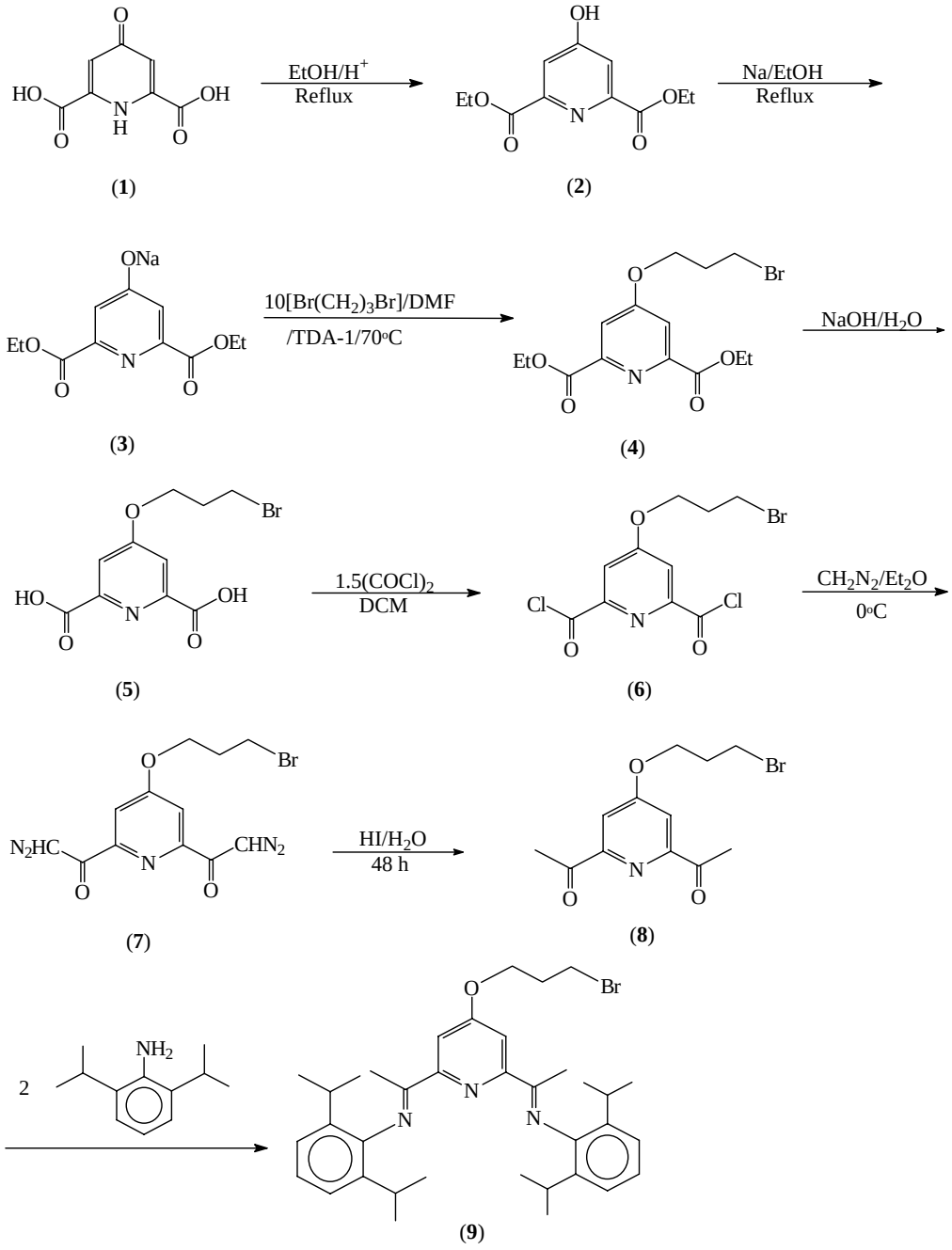

Scheme 5.1: Reaction scheme used for the synthesis of the functional ligand

5.4. Conclusions

a. 2,6-Diacetylpyridine-bis- (2,6 diisopropylphenylanil) iron(II) dichloride catalyst does not exhibit any chemical bonding to the silica support, as evident by the fact that the concentration of the free hydroxyl groups on silica remain unchanged before and after the supporting the complex.

b. The electronic environment of iron in the complex also remains unchanged with varying calcination temperature of silica.

c. The catalytic activity for polymerization of ethylene is higher at higher silica calcinations temperature. The residual hydroxyl groups of silica at lower calcinations temperature adversely affect catalyst activity.

d. All the polymers exhibit bimodal molecular weight distributions. This is similar to the behavior of homogeneous catalyst. The free hydroxyl concentration of the silica has an adverse effect on the molecular weight.

e. The calcinations temperature and, hence, concentration of free hydroxyl groups influences the kinetics of polymerization. The initial R_p decreases with increasing free hydroxyl content of silica probably due to the partial loss of MAO by the reaction with the hydroxyl groups on silica and the consequent decrease in Al/Fe ratio.

f. The activity of the catalyst with MAO pretreated silica is lower, due to the lower stabilization of the active sites by the support.

g. The peak molecular weights of the polymers obtained from the catalyst prepared using silica pretreated with MAO is higher than the catalysts in which silica is not pretreated with MAO. It is even higher when the cationic active site is preformed and then treated with silica. This is indicative of much lower active site concentration. A part of the active site is probably destroyed during the supporting of the catalysts in these two cases.

5.5. References

1. Mecking, S. *Angew. Chem. Int. Ed.* **2001,** *40*(3), 534-540.
2. Gibson, V. C.; Spitzmesser, S.K. *Chem. Rev.* **2003**, *103*(1), 283-315.
3. Ittel, S. D.; Johnson, L. K.; Brookhart, M. *Chem. Rev.* **2000,** *100*(4), 1169-1203.
4. Berardi, A.; Speakman, J. G. France PCT Int. Appl. WO 0024788, **2000**.
5. Gibson, V. C.; Kimberley, B. S.; Maddox, P. J.; Mastroianni, S. United Kingdom PCT Int. Appl. WO 0015646, **2000**.
6. Kimberley, B. S.; Pratt, D. United Kingdom PCT Int. Appl. WO 9946304, **1999**.
7. Kimberley, B. S.; Samson, J. N. R. United Kingdom PCT Int. Appl. WO 9946303, **1999**.
8. Canich, J. A. M.; Vaughan, G. A.; Matsunaga, P. T.; Gindelberger, D. E.; Shaffer, T. D.; Squire, K. R. US 6492473, **2002**.
9. Mackenzie, P. B.; Moody, L. S.; Killian, C. M.; Ponasik, Jr. J. A.; McDevitt, J. P.; Lavoie, G. G. US 6303720, **2001**.
10. Preishuber-Pflugl, P.; Brookhart, M. *Macromolecules* **2002,** *35*(16), 6074-6076.
11. Kaul, F. A. R.; Puchta, G. T.; Schneider, H.; Bielert, F.; Mihalios, D.; Herrmann, W. A. *Organometallics* **2002,** *21*(1), 74-82.
12. Birtovsek, G. J. P.; Gibson, V.; Kimberley, B. S.; Maddox, P. J.; McTavish, S. J.; Solan, G. A.; White, A. J. P.; Williams, D. J. *Chem.Commun.(Cambridge)* **1998,** *7* 849-850.
13. Bennett, A.; Anne, M. WO 9827124 A1, **1998**.
14. Britovsek, G. J. P.; Bruce, M.; Gibson, V. C.; Kimberley, B. S.; Maddox, P. J.; Mastroianni, S.; McTavish, S. J.; Redshaw, C.; Solan, G. A.; Stroemberg, S.; White, A. J. P.; Williams, D. J. *J.Am.Chem.Soc.* **1999,** *121*(38), 8728-8740.

15. Markees, D. G. *J. Org. Chem*. **1964,** *29* 3120-3121.

16. Markees, D. G.; Dewey, V. C.; Kidder, G. W. *J. Med. Chem.***1968,** *11* 126-129.

17. Dumont, A.; Jacques, V.; Desreux, J. F. *Tetrahedron* **2000,** *56* 2043-2053.

18. Semikolenova, N. V.; Zakharov, V. A.; Talsi, E. P.; Babushkin, D. E.; Sobolev, A. P.; Echevskaya, L. G.; Khysniyarov, M. M. *Journal of Molecular Catalysis A: Chemical* **2002,** *182-183* 283-294.

19. Ma, Z.; Sun, W. H.; Zhu, N.; Li, Z.; Shao, C.; Hu, Y. *Polym. Int.* **2002,** *51*(4), 349-352.

20.Britvosek, G. J. P.; Clentsmith, G. K. B.; Gibson, V. C.; Goodgame, D. M. L.; Mctavish, S. J.; Pankhurst, Q. A. *Catal. Commun.* **2002,** *3*, 207-211.

21. Lee, D. H.; Lee H. B.; Noh, S. K.; Song, B. K.; Hong, S. M. *J. Appl. Polym. Sci.* **1999,** *71* 1071-1080

6. In-situ polymerization of ethylene using late transition metal catalysts supported on clay

6.1 Introduction

There has been a recent upsurge in studies related to preparation and properties of polymer layered silicate (clay) nanocomposites (1-5). The basic motivation for this interest is the possibility that new materials with enhanced chemical, physical, mechanical and functional properties can be discovered. Polymer-layered silicate nanocomposite generally exhibit improved mechanical properties because reinforcement in the composites occurs in two dimensions rather than one dimension. The nanocomposites further exhibit remarkable increase in thermal stability as well as show self-extinguishing characteristics. They also show several fold reduction in the permeability of small gases, e.g., O_2, H_2O, He, CO_2 because of the introduction of "tortuosity" in the diffusion path of the permeate gases (6-12). In a polymer-clay nanocomposite the clays are dispersed in the polymer matrix in the nanoscale, that is, at least one dimension of the clay particles is in the nanometer scale. Such delaminated nanocomposites exhibit improved physical properties compared to conventional filled polymer composites at much lower silicate content (≤ 5wt%). Consequently, they are far lighter in weight than conventional filled polymers and make them competitive for specific application.

The structure of nanocomposite can be defined schematically as shown in fig **6.1**. In case of **6.1a** the host silicate retains its well-ordered, multilayered structure and the polymer intercalates within the galleries of the silicate layers. In case of **6.1b** the silicate looses its structural identity and disperses randomly in the polymer matrix (13).

The silicates used in the nanocomposites belong to a group called phylosilicates. Their crystal lattice is made up of a layer of two layers of silica fused to an edge shaped octahedral sheet of alumina or magnesia (Fig **6.2a**). The entire layer is around 1 nm in thickness and 300 Å to several microns in the lateral dimension (Fig **6.2b**). When these layers are stacked upon each other a regular van der Waals gap called a gallery or interlayer is formed. Isomorphic substitution inside the layers generates negative charges, which are counterbalanced by alkali or alkaline earth cations.

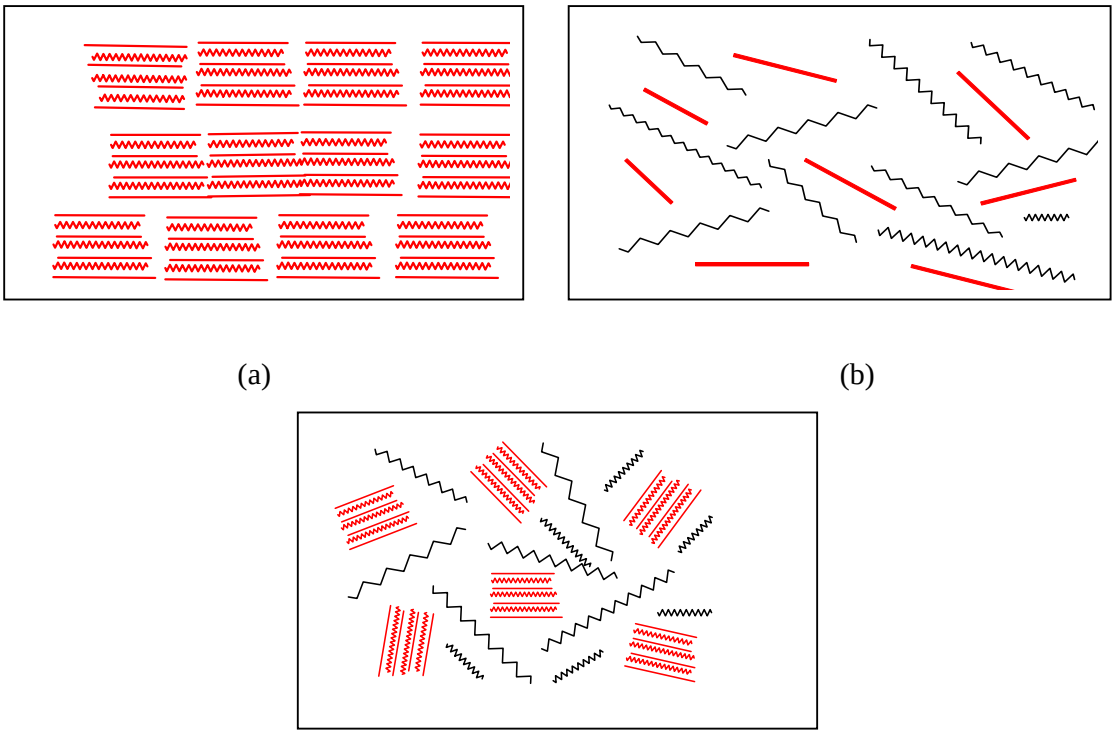

Fig 6.1: Polymer clay hybrid structure: (a) well-ordered silicate layers and intercalated polymer chains, (b) randomly exfoliated clay platelets dispersed within the polymer matrix, (c) semi-exfoliated composite, with small stacks of intercalated clay layers embedded within the polymer matrix

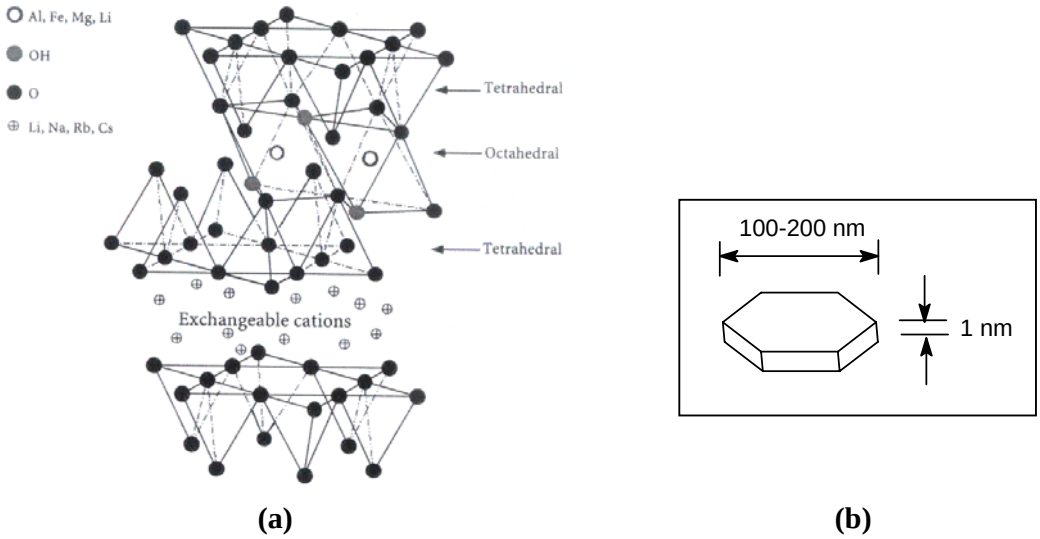

Fig 6.2: Structure of 2:1 layered silicates (a) and clay platelets (b)

The silicates commonly used for the purpose of nanocomposite formation are montmorillonite, hectorite, saponite, naturally occurring perovskite etc. They generally have a large surface area. The surface also contains some amount of negative charge (known as cation exchange capacity) expressed as milli-equivalent/g. This is because of the fact that the majority of the charge balancing cations are present in the interlayer space and very few on the external surface. The cations present inside the gallery can be replaced by other organic cations like alkylammonium cations. Thus, the Na^+ cations present in the clay are replaced by long chain alkylammonium cations. Since the surfaces of the silicate layers are negatively charged the cationic head group prefers to stay on the surface and the aliphatic chain stays away from the surface. By doing so the mainly hydrophilic galleries of the silicates can be made more hydrophobic. Also the inter-gallery distances are enlarged by such exchange. Due to the enhanced organophilicity and expanded inter-gallery spacing of the silicates layers it becomes possible to intercalate polymers inside the galleries.

Synthesis of polymer clay nanocomposites can be performed by several methods, the most important of which is the in situ polymerization, where the monomers are first introduced into the clay galleries, expanded by a suitable modifier, followed by polymerization of the monomers inside the gallery. Several polymer clay nanocomposites have been synthesized using this technique. Example are nanocomposites of nylon (14), poly(ether)s, poly(urethane)s (15), poly(acrylamides)s (16), poly(imide)s and poly(styrene)s (17,18). Generally, this method results in exfoliated polymer-clay nanocomposites.

The second approach is melt intercalation of the polymers using conventional melt processing techniques. The polymer and the modified clay are heated above the glass transition or the melting temperature of the polymer and subjected to shear in suitable processing equipment such as an extruder. A compatibilizing agent is also often found necessary. Several polymers nanocomposites are prepared using this process, namely poly(styrene)s (19), poly(propylene)s (20,21), poly(styrene-co-butadiene)s (22) and nylon-6 (23). Generally only intercalated nanocomposites are obtained by this method.

The third approach is solution intercalation where the polymer solutions are added to dispersions of delaminated sodium layered silicates. This method is mainly applicable

for water-soluble polymers, for example poly(vinyl alcohol)s (24), poly(ethylene oxide)s (24,25) and poly(acrylic acid)s .

The formation of a polymer clay nanocomposite depends mainly on the polymer/silicate compatibility, that is the nature of the polymer (polar/nonpolar), the surface energy of the silicate surface and the structures of the modifiers. As the polymer intercalates into the silicate layers, it gets confined inside the layers resulting in a decrease in the overall entropy of the polymer chain. This has to be compensated by a favorable enthalpy change, arising due to a favorable polymer-clay interaction. This is readily achieved with high surface energy polymers such as polyamides, where polarity and hydrogen bonding abilities generate the required amount of energy necessary for the hybrid formation. In such cases melt intercalation of the polymers into the silicate layers can be easily achieved. In case of low surface energy polymers like polypropylene and polyethylene such intercalation may not be possible. However, use of a suitable modifier (compatabilizing agent) can make incompatible polymer to intercalate into the silicate galleries. The best example can be found in case of polypropylene-clay system. In initial attempts polar functional groups were introduced onto the polypropylene chain in order to enhance the interaction between the polymer and the silicate surface. However, in order to facilitate the formation of an intercalate, an organic solvent was needed, in which the silicate was difficult to disperse, and a poor nanolayer dispersion of the clay was observed. In an alternate method a mixture of stearylammonium-exchanged montmorillonite, maleic anhydride modified propylene oligomers and homopolypropylene was melt processed to obtain a intercalated polypropylene-clay nanocomposite (20,21).

In a recent publication Gopakumar et al compared the exfoliation of the composites obtained by melt compounding of a surface modified montmorillonite (ion exchanged with a dimethyl dialkyl-ammonium salt) with polyethylene and a maleic anhydride grafted polyethylene (26). They observed that the highest exfoliation could be obtained when both the polymer and the clay were modified. It was also observed that the composite obtained from the unmodified polyethylene and modified clay (5%) increases the Young's modulus by 9% over pure polyethylene, whereas, in case of the composite obtained from the grafted polyethylene and modified clay (5%) increases the Young's modulus by 30%. The effect was also observed in the crystallinity of the

composites, where the completely exfoliated system exhibited an enhanced polymer crystallization rate, increased crystallization temperature and reduced degree of crystallization.

A simpler approach is the intra-gallery polymerization. This method is very useful for polymers, which encounter substantial thermodynamic barrier to intercalation. Polyolefin nanocomposites, in particular, have been prepared by such polymerization processes. Tudor et al. were first to employ this technique to generate polypropylene-clay nanocomposites (27). In this method a synthetic hectorite was treated with methylaluminoxane followed by the metallocene $Cp_2Zr(Me)(THF)^+$. After MAO incorporation no noticeable increase in the layer spacing was observed, but incorporation of the metallocene into the catalyst resulted in an increase of 0.47 nm (from 0.96 nm to 1.43 nm) in the gallery spacing. In another method the catalyst was directly incorporated into a fluorinated mica type silicate, which was devoid of any surface OH group without pretreatment by MAO. The two supported catalysts were used to polymerize propylene, using MAO as the cocatalyst. The catalysts exhibited high polymerization activity and resulted in PP oligomers. However no structural information was provided to understand the extent of intercalation or exfoliation. Recently Jin et al have reported heterogenizing $TiCl_4$ into the galleries of montmorillonite modified with methyl tallow bis(2-hydroxyethyl) quarternary ammonium moiety (28). The polymerization activity was found to be low (co-catalyst: Et_3Al). This was attributed to the free hydroxyl groups of the modifier, present at the surface of the clay and responsible for destroying the active sites. Exfoliation of the clay was observed in case of the hydroxy-modified silicate, whereas in case of simple sodium montmorillonite a slight shift in the scattering angle of the clay was observed. The extent of disappearance of XRD peaks could not be improved with increase in the $TiCl_4$ concentration. This indicated that in case of unmodified montmorillonite the polymerization was taking place outside the layers of the silicate.

Alexandre et al. synthesized polyethylene silicate nanocomposites by the in-situ polymerization of ethylene using a CGC (*tert*-butylamido) dimethyl (tetramethyl-η^5-cyclopentadienyl) silane titanium (IV) dimethyl (29). Three different clays were used, namely, montmorillonite, hectorite and kaolin for comparative studies. The clay samples were treated with MAO (free of TMA) and used during polymerization along

with the CGC. It was concluded from their studies that the nanocomposites consisting of polyethylene and non-modified layered silicates (hectorites, and montmorillonite) can be prepared provided that the silicate is pretreated with sufficient amount of MAO. It was also observed that these nanocomposites are thermo-dynamically unstable, since it was observed that the exfoliated structures collapse in the melt into non-regular intercalated structures.

Heinemann et al. reported the in situ polymerization of ethylene to produce PE nanocomposites (30). Layered silicates like bentonite, modified with dimethyldistearylammonium or dimethylbenzylstearylammonium cations, were used for the composite formation. For a comparison unmodified hectorite and fluoromica were also used. Ethylene homo and copolymerization were performed using the following method. The silicate was first taken in toluene and dispersed followed by addition of 1-octene. The reactor was then saturated with ethylene and then the catalyst was added to initiate the polymerization. Three catalysts were used for polymerization, one metallocene $Me_2Si(2\text{-methylbenz[e]Indenyl})_2ZrCl_2$ (MBI), one nickel catalyst *N, N'*-bis(2, 6-diisopropylphenyl)-1, 4-diaza-2, 3-dimethyl-1 ,3-butadienenickel (DMN) and one palladium catalyst [$(ArN{=}C(Me)\text{-}C(Me){=}NAr)Pd(CH_3)(NC\text{-}CH_3)]^+$ BAr_4' (DMPN/borate). Nanocomposites were formed when the polymerization was carried out using the modified clay. However in the case of unmodified clay and by melt blending of a preformed HDPE and modified bentonite only microcomposites were formed. Incorporation of the C-6 branch in the polymer chain increases the compatibility of the modified silica and the polymer giving rise to a better nanocomposite.

Bergman et al. intercalated a Brookhart type palladium catalyst [{2, 6-$Pr^i_2C_6H_3N$ = $C(Me)C(Me)$ = $NC_6H_3Pr^i_2$-2, 6}$Pd(CH_2)_3CO_2Me][B(C_6H_3(CF_3)_2)_4]$into synthetic fluorohectorite (31). Initial attempt to intercalate the catalyst into the gallery of clay failed. However, upon using an organically modified silicate with 1-tetradecylammonium cation, the catalyst was found to be intercalated. WAXD analysis revealed a structural change with an increase in the basal spacing from 1.99 to 2.76 nm. Polymerization of ethylene was performed using the solid catalyst. Complete exfoliation of clay occurred after 12 h. The polymers obtained were highly branched and possessed high molecular weight (Mn = 159,000).

In this chapter, we describe studies aimed towards preparation of polyethylene nanocomposites using late transition metal catalysts by in-situ polymerization. For this purpose two catalysts were chosen, namely, [(N, N'-diisopropylbenzene)-2,3-(1,8-naphthyl)-1,4-diazabutadiene) nickel(II) dibromide and 2,6-bis[1-(2,6-diiso propylphenylimino) ethyl] pyridine iron(II) dichloride. A modified montmorillonite C-20A was used. The objective of the present study was to evaluate the efficiency of these two types of catalysts to generate intercalated/exfoliated clay-polyethylene nanocomposites via an in-situ polymerization technique.

6.2. Experimental part

6.2.1. Reagents and materials

All operations were performed under argon atmosphere using standard Schlenk techniques. The solvents were dried using standard procedures. The catalysts were stored and transferred inside a Labmaster 100 m Braun inert atmosphere glove box. Ethylene was obtained from the Gas Cracker Complex of Indian Petrochemicals Ltd., Nagothane. Methylaluminoxane was procured from Witco GmbH (Germany). The catalyst 2,6-bis[1-(2,6-diisopropylphenylimino) ethyl] pyridine iron(II) dichloride was synthesized as described in Chapter 5. Acenaphthequinone, 2, 6-diisopropylaniline and nickel dibromide were procured from Aldrich, USA and used as such. The clay used was Cloisite 20A procured from Southern Clay Products, USA. This clay is basically montmorillonite type modified by dimethyl-ditallow ammonium cations, containing approx. 65% C18, 30% C16 and 5% C14 chains. The modifier concentration was 95 millieq/100 g of clay. The average inter-gallery spacing is approximately 24 Å.

6.2.2. Synthesis of [(N, N'-diisopropylbenzene)-2,3-(1,8-naphthyl)-1,4-diazabutadiene)] dibromo nickel (II)

6.2.2.1. Dibromo(1,2-dimethoxyethane) nickel(II)

In a 100 mL round bottom flask, 2 g of nickel (II) bromide and 20 mL of anhydrous ethanol were placed. The homogenous green solution was stirred under reflux for 2

hours. The ethanol solution was evaporated to the stage of incipient crystallization at the boiling point and diluted with 15 mL of 1,2-dimethoxyethane (dried over lithium aluminium hydride). A pink colored precipitate formed, which was collected and washed successively with anhydrous 1,2-dimethoxyethane and dried under vacuum.

6.2.2.2. [(N, N'-diisopropylbenzene)-2,3-(1,8-naphthyl)-1,4-diazabutadiene]

4 mL (21 mmol) of 2,6-diisopropylaniline and 20 mL of methanol were taken in a 100 mL round bottom flask. 3 g (16.5 mol) of acenaphthenequinone was added slowly and stirred overnight. The reaction mixture was filtered, washed several times with methanol. The solid mass was recrystallized from chloroform-hexane mixture.

^{1}HNMR. 7.9 (d, 2, naphthyl), 7.4 (t, 2, naphthyl), 7.25 (s, 6, H aryl), 6.15 (d, 2, naphthyl), 3.05 (septet, 4, C**H**$(Me)_2$), 1.25 (d, 12, CH(C**H**$_3)_2$, 1.0 (d, 12, CH(C**H**$_3)_2$)

6.2.2.3. (N, N'-diisopropylbenzene)-2,3-(1,8-naphthyl)-1,4-diazabutadiene) dibromonickel (II)

0.750 g (1.5 mmol) of the ligand and 0.440 g (1.43 mmol) of $NiBr_2$(DME) were weighed into a flame-dried Schlenk flask inside a dry box. 20 mL of dichloromethane was added to this mixture. An orange colored solution was formed, which was stirred for 18 hours to obtain a reddish brown suspension. The reaction mixture was allowed to settle and some amount of dichloromethane was removed by means of a cannula. To the resulting mass, dichloromethane was added, stirred for sometime and filtered through a cannula. The product was washed with dichloromethane and the reddish brown complex was dried *in vacuo.* yield was 700 mg (65 %)

Elemental analysis calculated for $C_{36}H_{40}N_2NiBr_2$: C, 60.12; H, 5.61; N, 3.89. Found C, 59.73; H, 5.35; N, 3.66.

6.2.3. Synthesis of clay supported catalysts

6.2.3.1. 2,6-bis[1-(2,6-diisopropylphenylimino) ethyl] pyridine iron (II) dichloride catalyst supported on modified clay

A typical synthetic procedure is as follows:

The modified clay used in the synthesis was preheated at 100°C in vacuo for 4 h. 1 g of clay was taken in a 250 mL round bottom flask and to it 30-50 mL of dry toluene was added. To it 1 mL of MAO solution (4.2 mmol of Al/mL) was added. The mixture was stirred for 1 h. Theereafter, 80 mg of the iron catalyst suspended in 10 mL in dry toluene was added slowly to the mixture. The color of the catalyst changed immediately from deep blue to brick red. The mixture was further stirred for 2 h. Finally the solvent was removed under reduced pressure and the solid was dried.

6.2.3.2. (N, N'-diisopropylbenzene)-2,3-(1,8-naphthyl)-1,4-diazabutadiene) nickel (II) dibromide supported on modified clay

The modified clay used in the synthesis was preheated at 100°C under vacuum for 4 h. 1 g of clay was taken in a 250 mL round bottom flask and to it 30 ml of dry toluene added. To it 1 mL of MAO solution (4.2 mmol of Al/ml) was added. The mixture was stirred for 1 h. 100 mg of the nickel catalyst was suspended in 10 mL of dry toluene and was slowly added to the clay mixture. The clay suspension attained a light blue color. This was then stirred for 2 h. Finally the solvent was removed under reduced pressure and the solid was dried.

6.2.4. Ethylene polymerization using the clay supported catalysts

Ethylene polymerizations were performed using the clay-supported catalysts at 6 bar pressure for 1 h at 30°C using Buchi Miniclave glass reactor with a capacity of 50 and 200 mL, equipped with a magnetic needle. Details of the polymerization procedures are described in chapter **3**.

6.2.5. Ethylene polymerization using homogeneous iron catalyst in presence of modified clay C-20A

1 g of the clay, preheated at 100°C at 4 h, was taken in a 250 ml round bottom flask and to it 30 ml of dry toluene added. To it 1 ml of MAO solution of concentration of 4.2 mmol of Al/ml was added. The mixture was stirred for 1 h. The solvent was removed and the clay dried under vacuum. Approximately 100 mg of this clay was

added to a glass reactor, cooled under ethylene atmosphere. 50 mL of dry toluene was added to the clay and the mixture was stirred for 20 min under ethylene atmosphere. The catalyst was introduced into the reactor as a suspension in toluene, followed by addition of MAO using a hypodermic syringe. Ethylene polymerizations were performed at 5 bar pressure for 1 h at 30°C. The reaction was terminated by adding acidified methanol. The polymer was filtered, washed and dried under vacuum.

6.2.6. Characterization of the catalysts

Wide angle X-ray scattering of the catalysts were performed and compared with the modified clay samples. The X-ray diffraction experiments were performed using Rigaku Dmax 2500 diffractometer with a Cu-Kα radiation (λ=0.15418 nm). The system consists of a rotating anode generator with a copper target and a wide-angle powder goniometer fitted with a high temperature attachment. The generator was operated at 40 KV and 150 mA. All the experiments were performed in the reflection mode. The sample holder was a copper block and powder samples were attached to it for analysis. The scanning rate was 1°/min from 2θ =2° to 2θ = 10°.

6.2.7. Characterization of the polymers

6.2.7.1. Wide angle X-ray diffraction

Wide-angle X-ray scattering of the polymer samples were done using experimental procedures described in section **6.2.6**. Powdered polymer samples were attached to the sample holder and scanned at the rate of 1°/min from 2θ =2° to 2θ = 10°.

6.2.7.2. Transmission electron microscopy

Transmission electron microscopy of the composite samples was performed using a JEOL model 1200EX instrument, operated at an accelerated voltage of 80 kV. Samples for TEM were prepared by dispersing the polymer powder in toluene using a sonicator model Branson 3200, for 10 min. One drop of the dispersion was placed onto a carbon coated TEM copper grid. The drop was allowed to dry for 1 min. Data

capture was done using side-mount CCD camera procured from Gatan USA, and using the software 'Gatan Digital Micrograph'.

6.2.7.3. Molecular weight and molecular weight distribution

The molecular weight and molecular weight distribution of the polymers were measured using GPC (see chapter **3**) Before performing the GPC of the polymers the samples were extracted in trichlorobenzene (TCB) at 140°C. Approximately 250 mg of the PE-clay composite was taken in a packet made of two filter papers (Whatman-1 grade) and submerged in TCB at 140°C. The clay inside the packet was seen to be agglomerating. After 30 min the packet was removed and the hot TCB was poured into methanol and the precipitates were filtered and dried. This entire process was repeated twice to ensure complete separation of PE from clay. Typically the final weight of the polymer obtained was approximately 150-200 mg.

6.3. Results and discussions

6.3.1. Preparation and characterization of clay supported catalysts

The clay samples were pretreated with MAO prior to treating them with the catalysts. Since the clay swells in toluene and forms a dispersion, it was not possible to wash the solid after supporting the catalysts in the manner it was done in case of silica support. Thus, the entire quantity of MAO and the catalysts used remained in the solid catalyst. This was also confirmed by the metal estimation using ICP and Al estimation by titrimetric analysis. In case of the nickel catalyst (**Cat-Ni-1)** 1g of clay was taken and 100 mg of the nickel catalyst was added. In case of the iron catalyst supported-catalysts were made having different clay contents (Table 6**.1**). In all the cases the clays were pretreated with different quantities of methylaluminoxane based on the amount of clay used. In one of the clay supported iron catalyst the quantity of the catalyst was doubled in order to check the effect of catalyst concentration.

WAXD of the clay before and after treatment with MAO is shown in Fig 6**.3.** The WAXD shows that after treating the clay with MAO there is a reduction in the 2θ,

which corresponds to an increase in the d-spacing of the clay galleries from 24Å to approx. 30Å. This shows that the MAO occupies the intergallery space of the clay. Tudor et al. (27), did not observe any change in intergallery distance of hectorite upon treatment with MAO. However, their sample of hectorite had no hydrophobic modifier. No further change in the 2θ was observed when the MAO treated clay was reacted with the catalyst.

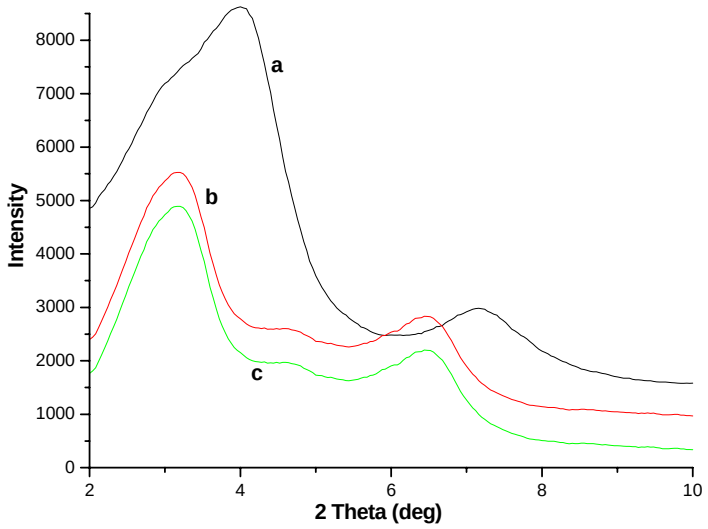

Fig 6.3: Comparison of the WAXD peaks of **(a)** C-20A**, (b)** C-20A treated with MAO, **(c)** C-20A/MAO treated with the Fe (II) catalyst

Table 6.1: Composition of C-20A (pretreated with MAO) supported catalysts

Catalyst	Mol catalyst $\times 10^3$	Amount of clay	Mol Al $\times 10^3$	Yield of clay support	% M[1]	%Al[2]	Al/Ni
Cat-Ni-1	0.14	1 g	4.2	1.4 g	0.59	8.1	30
Cat-Fe-1	0.13	1 g	4.2	1.4 g	0.53	8.2	32
Cat-Fe-2	0.13	3 g	12.6	4.1 g	0.18	8.2	97
Cat-Fe-3	0.13	5 g	21	6.5 g	0.11	8.7	160
Cat-Fe-4	0.26	3 g	12.6	4.4 g	0.33	7.7	49

[1] ICP analysis

[2] Titration

6.3.2. Ethylene polymerization using clay supported catalysts

6.3.2.1.Clay supported nickel catalysts (Ni-1)

Polymerization of ethylene was performed using catalysts Ni-**1** and the corresponding soluble catalyst with methylaluminoxane as the cocatalyst. The results are shown in Table **6.2**. As expected the polymerization gave branched amorphous polymers which show no melting endotherm in DSC.

All the polymers exhibit a Schultz-Flory distribution of molecular weight indicating that the nature of active centers are similar for the homogeneous and the supported catalysts (Fig **6.4**). The percentage of the clay in the polymers varied between 2.5-6.0%. No substantial difference in the catalytic activity was observed with changes in Al/Ni ratio. Catalytic activity, however, decreased with increasing nickel concentration.

Table 6.2: Ethylene polymerization using the clay supported (N, N'-diisopropylbenzene)-2,3-(1,8-naphthyl)-1,4-diazabutadiene) dibromonickel catalyst

Entry No.	Wt of Clay (mg)	[Ni] $\times 10^6$ mol	[Al] $\times 10^3$ mol[1]	Al/Ni Ratio[2]	Yield (g)	Activity (KgPE/ mol Ni/h)	Wt % Clay	$\overline{M_w}$ $\times 10^{-3}$	PDI
Homogeneous -**Ni**									
1.	--	14.2	22.7	1600	3.2	225	--	121	2.1
Ni-1									
2.	102	14.2	22.7	1630	2.6	187	3.8	131	1.85
3.	107	14.7	17.0	1230	2.6	189	3.8	125	2.38
4.	98	13.6	10.9	830	3.2	230	3.1	195	2.83
5.	100	13.9	2.8	230	2.5	180	4.0	164	1.85
6.	50	7.0	5.6	830	1.6	239	2.5	153	2.05
7.	202	28.1	22.6	830	2.5	90	6.3	216	2.10

[1] The MAO used is in addition to that used for catalyst preparation

[2] Total MAO, includes MAO used during catalyst preparation and during polymerization

6.3.2.2. Clay supported iron catalyst (Fe 1-4)

Polymerization of ethylene was performed using catalysts Fe-**1** to Fe-**4** as well as the corresponding soluble catalyst. The results are shown in Table **6.3**. As expected all the catalysts gave crystalline polymers with a sharp melting endotherm in DSC. The obtained polymers exhibited a distinctly bimodal distribution (Fig **6.5**) characteristic of the iron catalyst. There was no effect of Al/Fe ratio upon the activity of the catalyst.

In a separate study the iron catalyst and the clay (previously treated with MAO) were individually added to the reactor and ethylene was polymerized (entry **2**, Table **6.3**). The catalyst activity was found to be similar to that of the homogeneous catalyst.

6.3.3. Molecular weight and molecular weight distribution

In case of the clay supported iron catalysts, a comparison of the polymers obtained from the homogeneous catalysts and catalyst **Fe-1** shows an increase in the molecular weights of the polymers obtained from catalyst **Fe-1** under identical condition (Table **6.3**). This shows that there is an effect of the heterogenization of the catalyst upon the molecular weight. However there is no change in the MDW pattern in case of both the catalysts. It can also be seen that as the concentration of clay increases form **Fe-1** to **Fe-2** and **Fe-3** there is a steady fall in molecular weight of the polymers (Fig **6.5**). This was observed because of the fact that with the increase in the clay concentration there is an increase in the concentration of surface attached MAO, leading to a higher degree of chain transfer to aluminum. However, the trend is quite opposite in case of the nickel catalyst (Fig **6.4**). There is an increase in the polymer molecular weight of the polymers with the increase in the clay concentration (Table **6.2**, entry 4, 6 and 7). This can be readily understood by the fact that chain transfer to aluminum is insignificant for the nickel catalyst. In case of the iron catalyst it is also observed that the GPC peak due to the low molecular weight fraction of the polymer increases with the increase in clay concentration (Fig **6.5**).

Table 6.3: Ethylene polymerization using the clay supported 2,6-bis[1-(2,6-diisopropylphenylimino) ethyl] pyridine iron (II) dichloride catalyst

Ent No.	Wt of clay (mg)	[Fe]× 10^6 mol	[Al]× 10^3 mol[1]	Al/Fe Ratio[2]	Yield (g)	Activity, Kg PE/ mol Fe/h	% Clay	Tm (°C)	Mp_1	Mp_2× 10^{-3}
Homogeneous-**Fe**										
1.	--	10.0	10.0	1000	11.8	1186	--	136.0	1980	58.6
Homogeneous-**Fe** + Clay										
2.	102	10.0	16.0	1600	11.4	1142	1.1	133.0	1180	46.3
Fe-1										
3.	104	13.1	21.0	1630	10.7	823	0.94	133.0	1080	48.2
4.	101	13	13.0	1030	6.5	500	1.5	133.0	3450	68.8
5.	106	13.1	7.9	630	10.0	769	1.0	135.0	6520	126.2
6.	104	13.1	2.6	230	8.0	615	1.2	135.3	6800	142.6
Fe-2										
7.	305	13	21.0	1700	9.5	731	3.2	128.7	340	42.9
8.	302	13	13.0	1100	10.0	769	3.0	128.4	890	41.6
9.	300	13	7.8	700	11.0	846	2.7	129.5	1470	54.2
10.	301	13	2.6	300	11.8	908	2.5	135.3	1980	36.6
Fe-3										
11.	500	13	21.0	1760	9.0	692	5.9	129.5	650	54.2
12.	502	13	13.0	1160	8.5	654	5.9	128.7	1400	51.5
13.	510	13.1	7.9	760	9.0	692	5.6	133.3	1400	56.1
14.	500	13	2.6	360	9.5	731	5.3	135.4	2170	56.6
Fe-4										
15.	312	26.3	42.1	1650	11.8	454	2.5	127.5	740	28.2
16.	301	26	26.0	1050	11.0	423	2.7	128.9	1290	43.2
17.	304	26	15.6	650	12.0	462	2.5	131.8	3300	47.6
18.	305	26.1	5.2	250	12.0	461	2.5	133.5	3810	51.6

[1][Al] used in excess; [2]Total MAO, including MAO used during catalyst synthesis and during polymerization.

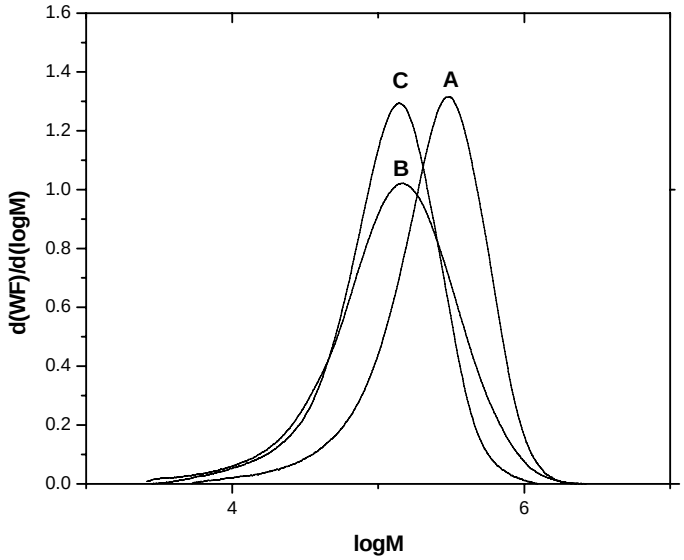

Fig **6.4**: GPC of poly(ethylene)s obtained with nickel catalyst (**A** entry 7, **B** entry 4, **C** entry 6, Table **6.2**)

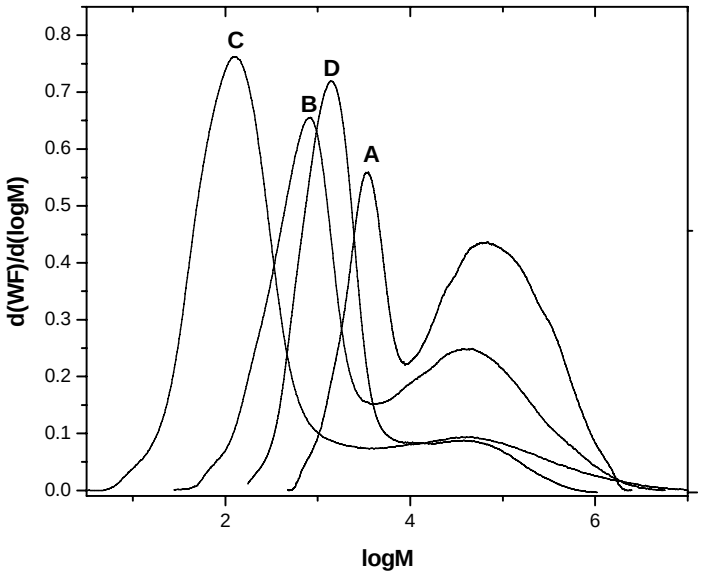

Fig 6.5: GPC of poly(ethylene)s obtained with iron catalysts (**A** entry 4, **B** entry 8, **C** entry 12, **D** entry 16, Table **6.3**)

6.3.4. Structure and properties of polyethylene-clay nanocomposites

Wide angle X-ray diffraction patterns of all the polymer-clay nanocomposites were recorded in the 2θ range of 2 to 10° and compared with the diffraction pattern of the clay before and after supporting the catalysts.

In case of the nickel catalyst **Ni-1** all six polymers synthesized showed high degree of exfoliation of the clay particles inside the polymer matrix as evidenced by the complete disappearance of the crystalline peaks of the clay (Fig **6.6**). However with the Iron catalyst the extent of exfoliation was found to be dependent upon several factors, i.e., concentration of the clay, concentration of the catalyst and Al/Fe ratio. Similar observation was reported by Heinemann et al (30). The presence of n-alkyl branches, resulting form α-olefin copolymerization or migratory insertion polymerization, appears to enhance the compatibility between the polymer and the silicate layers, in case of nickel catalyst.

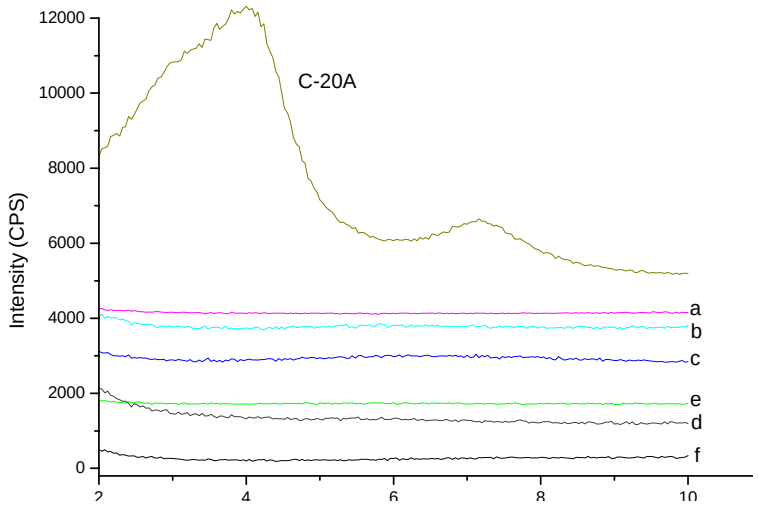

Fig 6.6: WAXD of polymers obtained using **Ni-1,** (a-f entry no. 2-7, Table **6.2**)

In case of the iron catalyst, the amount of clay used during polymerization was found to affect the extent of exfoliation. A similar observation was reported by Chen et al in the case of a polyurethane-clay nanocomposite (32).

A comparison of the intensity of the WAXD peaks of different samples show that the extent of exfoliation is in the order **Fe-1** > **Fe-2** > **Fe-3,** which is in the reverse order of content of clay in the polymer (Fig **6.7**-**6.9**). Also, a comparison of polymers obtained from catalysts **Fe-2** (Fig. **6.8**) and **Fe-4** (Fig. **6.10**) shows that higher concentration of catalyst in the clay leads to a greater degree of exfoliation.

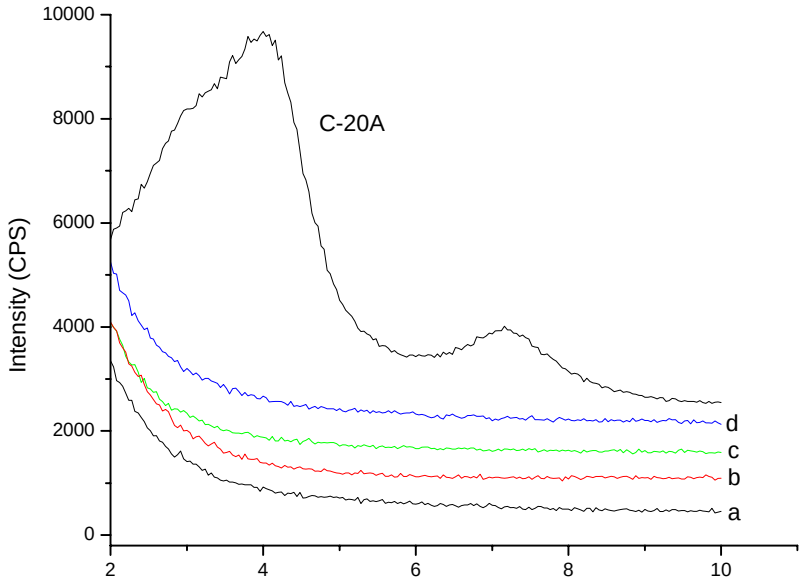

Fig 6.7: WAXD of polymers obtained using **Fe-1**, (a-d entry no. 3-6, Table **6.3**)

Al:Fe ratio does not influence the catalyst activity. However, it is found to affect the degree of exfoliation (Fig **6.9**).

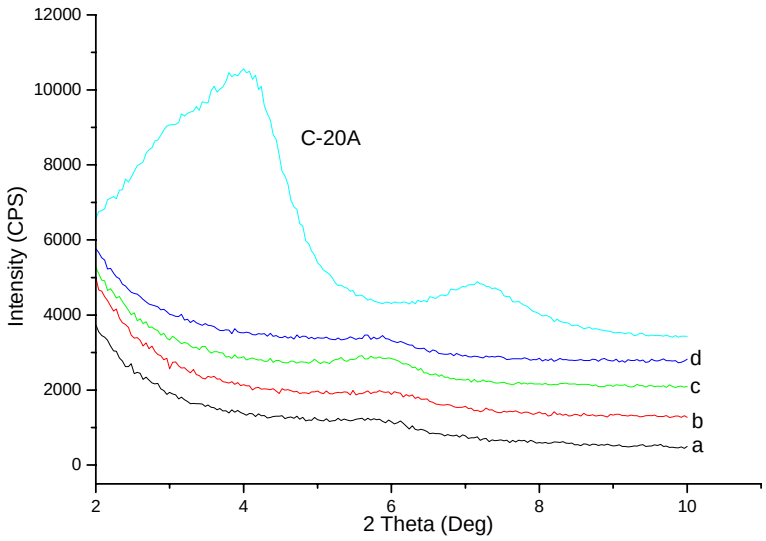

Fig 6.8: WAXD of polymers obtained using **Fe-2** (a-d entry no. 7-10, Table **6.3**)

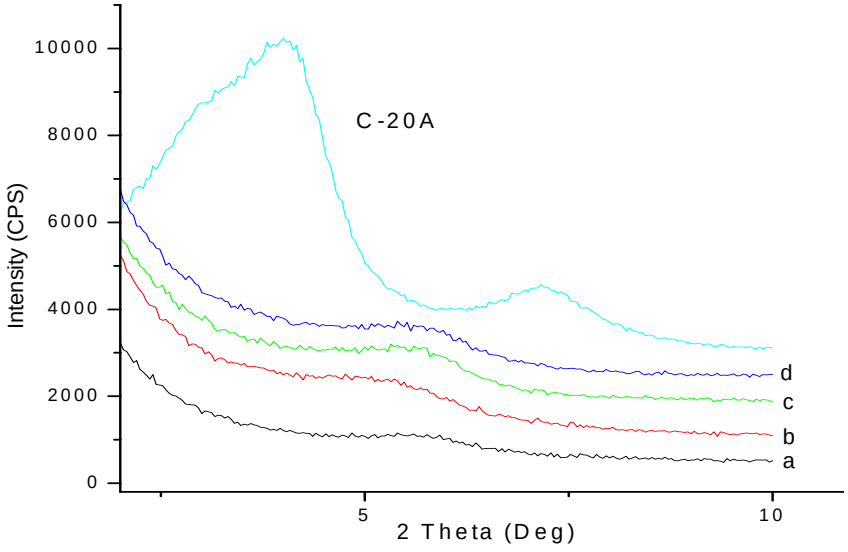

Fig 6.9: WAXD of polymers obtained using **Fe-3,** (a-d entry no. 11-14, Table **6.3**)

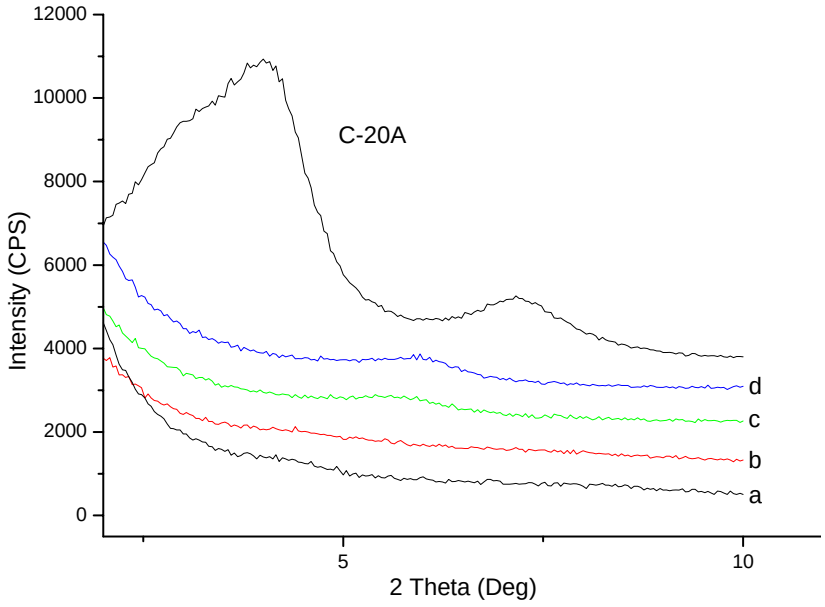

Fig 6.10: WAXD of polymers obtained using **Fe-4,** (a-d entry no. 15-18, Table **6.3**)

The T_m of the polyethylene-clay nanocomposites are lower compared to pristine poly(ethylene) prepared in absence of clay (entry no. 1, 4, 8 and 12, Table **6.3**)

The crystallite size and % crystallinity of poly(ethylene)s obtained from clay supported Fe (II) pyridylamine catalyst (Fe-**1-3**) are shown in Table **6.4**. The crystallite size was estimated from full width at half maxima for the PE peak at $2\theta = 21.3°$ using the Scherer's formula.

Table 6.4: Effect of clay concentration on crystalline properties of the poly(ethylene) clay nanocomposites

Sample	% clay	FWHM	Crystallite size (nm)	% crystallinity
Entry No.1, Table **6.3**	0	0.3265	24.34	>95
Entry No.4, Table **6.3**	1.5	0.4323	18.38	88.9
Entry No.8, Table **6.3**	3.0	0.3628	21.90	88.5
Entry No.12, Table **6.3**	5.9	0.3325	23.90	88.3

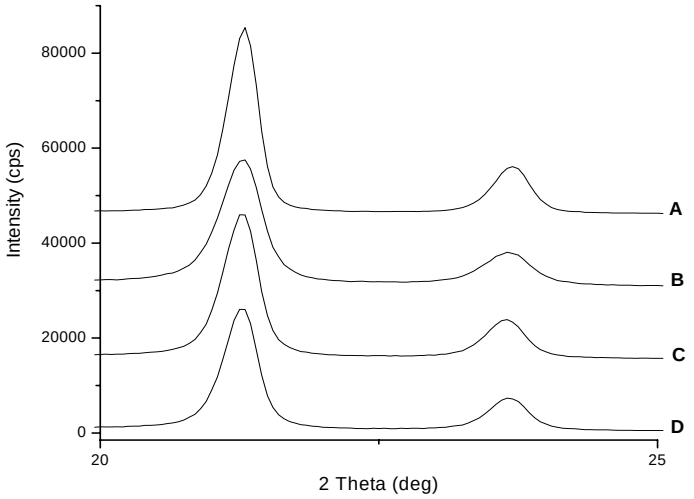

Fig 6.11: WAXD of the polymers obtained from the iron catalyst in the range of 2θ = 20- 25° (**A** entry 1, **B** entry 4, **C** entry 8, **D** entry 12, Table **6.3**)

Interestingly, sample at entry no. 4, Table **6.3** shows a significant increase in FWHM and decrease in crystallite size compared to pristine PE. This sample also shows clear exfoliation of clay (Fig **6.13**). Sample at entry no. 8, Table **6.3** shows higher crystallite size and lower FWHM that sample 4. Sample 8 is only partially exfoliated as shown by TEM micrograph (Fig **6.14**). Thus a relationship exists between crystallite size and degree of exfoliation. Similar observation have been made in the case of mica-poly(ε-caprolactum) nanocomposites (33) and mica-PET nanocomposites (34). The crystallite sizes of both poly(ε-caprolactone) and PET in completely exfoliated samples were significantly lower then pristine polymers. It can be concluded that well dispersed silicate layers represent physical barriers that can restrict crystal growth of the confined poly(ethylene)s. Thus, exfoliated clays in these nanocomposites exhibit the characteristic of a nucleating agent.

The exfoliation of the clay in the polymer matrix was further established by transmission electron microscopy. Fig **6.12** depicts the TEM micrographs of the polyethylene-clay nanocomposites obtained from the iron catalyst **Fe-1** (entry 4, Table **6.3**). The exfoliated clay particles, approximately 10 nm × 100 nm oriented randomly in all directions, can be seen in the micrograph.

Similar TEM images have been reported by Sun and Garces (35) where the clay particles were completely exfoliated to a single platelet or a few tactoids when

polypropylene clay nanocomposite were obtained by in situ polymerization using a metallocene catalyst. Heinemann et al (32) also have reported TEM evidence for improved dispersion of the clay in PE-clay nanocomposites prepared by in situ polymerization compared with composites prepared by melt compounding.

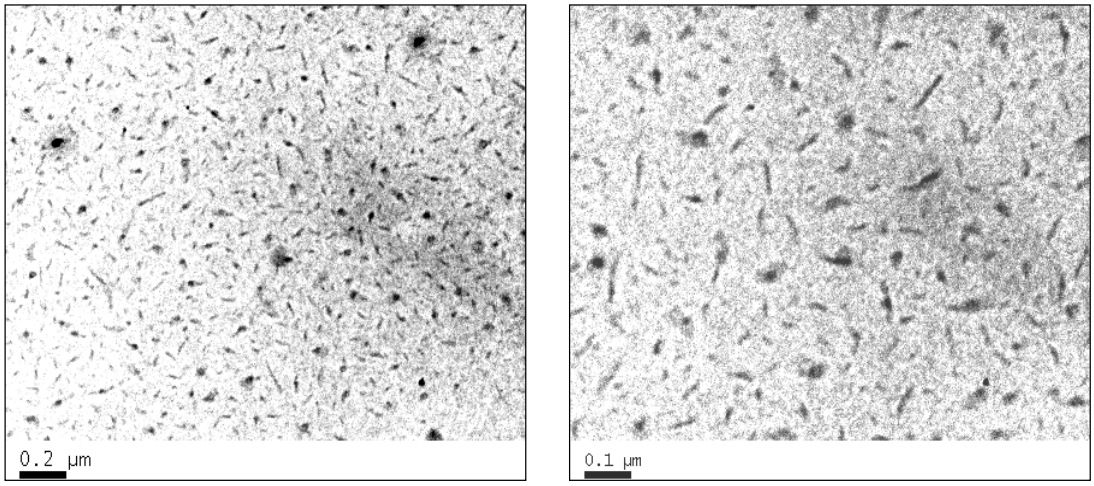

(a) **(b)**

Fig 6.12: TEM micrograph of fully exfoliated composite **Fe-1** (entry 4 Table **6.3),** at **a:** 200 nm **b:** at 100 nm scale

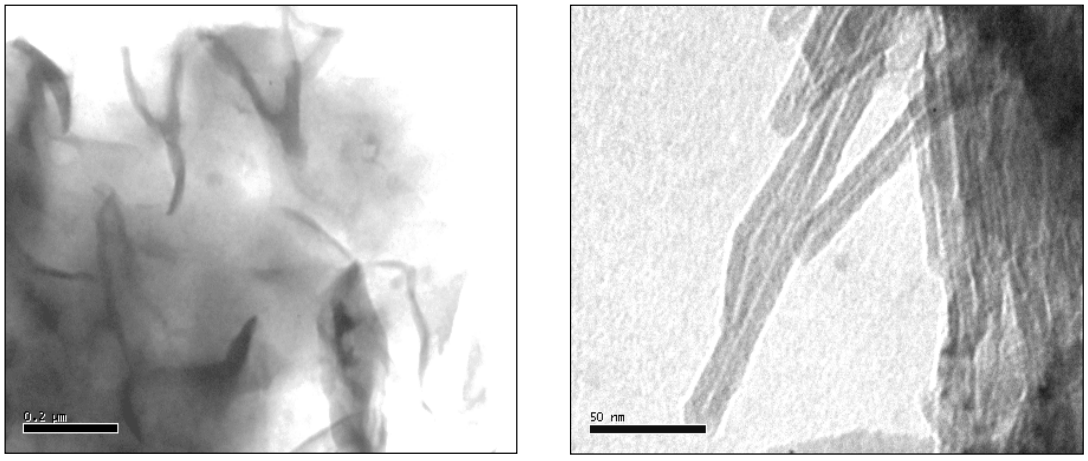

a **b.**

Fig 6.13: TEM micrograph of partially exfoliated composites (**a** entry 8 Table **6.3**, **b** entry 12, Table **6.3**)

Fig **6.13** depicts the TEM micrograph of a partially exfoliated sample **Fe-2** (entry 8, a) and **Fe-3** (entry 12, b). The micrographs show partially exfoliated clay with much larger platelets sizes. At higher magnification intercalation of the polymers inside the clay platelets is visible (Fig **6.13, b**).

TEM micrograph of the nanocomposites obtained using the nickel catalyst exhibit a different morphology (Fig **6.14**). This is rather unusual in that the dispersed phase has a dimension of only 20-50 nm. This dimension is much smaller then the typical platelet dimension of clay. The reason for this observation is not clear at the present.

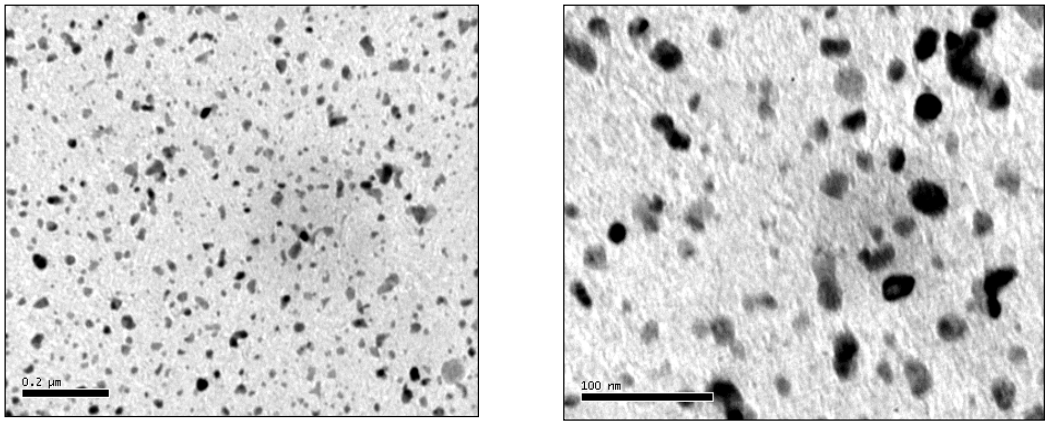

a. **b.**

Fig 6.14: TEM micrograph of the composite derived from **Ni-1** (entry 4, Table **6.2**)

6.3.5. Polymerization of ethylene using homogeneous Fe (II) pyridylimine catalyst in presence of clay

Heinemann et al (30) reported the preparation of polyethylene clay nanocomposites using a nickel catalyst, namely, N,N'-bis(2,6-diisopropylphenyl)-1,4-diaza-2,3-dimethyl-1,3-butadiene nickel (II) the structure of which is similar to the catalyst used in the present study. They used Na-bentonite modified with dimethylstearylbenzylammonium or dimethylstrearylammonium cations. The clay was added to the reactor and dispersed in dichloromethane. The polymerization was started by adding the catalyst to the reactor which was saturated with ethylene. Using the Fe (II) pyridylimine catalyst a similar experiment was performed (entry 2, Table **6.3)**. The modified clay, C-20A, was pretreated with MAO and dispersed in toluene.

The polymerization was started by addition of the catalyst followed by the cocatalyst to the reactor. The product thus obtained was compared with that obtained from a preformed clay supported iron catalyst under similar condition (**Fe-1**, entry 3, Table **6.3**). The polymerization activity as well as T_m and Mp_1 and Mp_2 are similar in both cases. However, there is a significant difference in the WAXD pattern of the two products (Fig **6.15**). It can be seen that the product obtained from the preformed clay supported catalyst is predominantly exfoliated. However, the product obtained from a mixture of Fe catalyst and clay shows only intercalation.

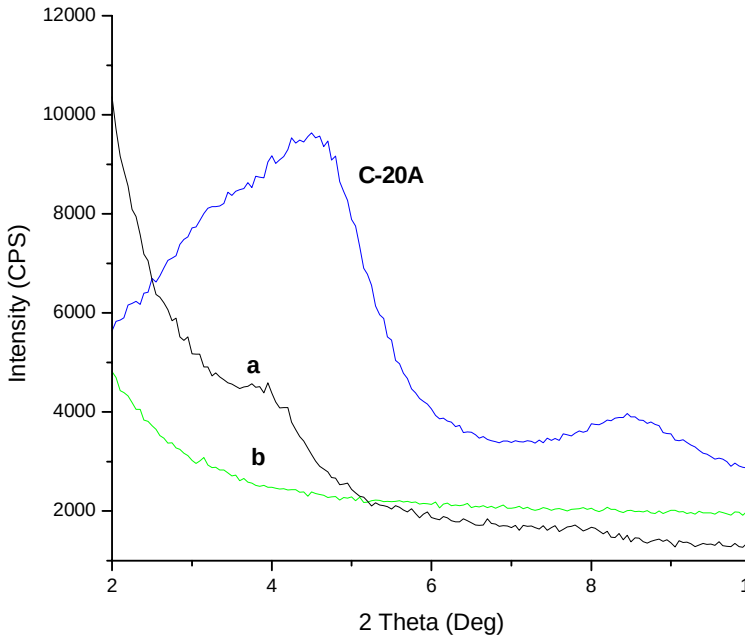

Fig 6.15: Comparison of the WAXD peaks of the C-20A and the composites obtained from a homogeneous catalyst in presence of clay (entry 2, Table **6.3**) and b catalyst **Fe-1** (entry 3, Table **6.3**)

6.3.6. Rheological behavior of the composites obtained from the clay supported iron (II) catalysts

The rheological behavior of the nanocomposites obtained from the clay supported iron (II) catalysts were studied (36). Two polymer samples were chosen for the study, namely, that obtained using **Fe-1** as catalyst containing approximately 1% clay (**Fe-1**,

Table **6.3**) and obtained using **Fe-3** as catalyst containing approximately 5% clay (**Fe-3**, Table **6.3**). The results were compared with a pristine polymer obtained using a homogeneous Fe catalyst.

The salient conclusions of the study are as follows:

1. The nanocomposites obtained using **Fe-1** catalyst is significantly more elastic than that of the pristine PE

2. The composites obtained using **Fe-1** catalyst showed a high elastic modulus G' and a lower crossover frequency, probably due to the high molecular weight of the polymers. The composites also did not show any plateau effect, indicating that the effect is essentially determined by the nature of the matrix.

3. The nanocomposites obtained using **Fe-3** catalyst showed an even higher G', which may be due to the confinement of the polymer chains within the clay layers and the resulting retardation of the molecular relaxation process. A plateau region is observed in the lower frequency.

4. The nanocomposite obtained from using a mixture of homogeneous catalyst and the clay showed a lower G' in comparison to the composite obtained using **Fe-1.**

Additional details of this study can be found in reference 34.

6.4. Conclusions

In this chapter we report a method for heterogenizing two late transition catalysts, namely, (N, N'-diisopropylbenzene)-2,3-(1,8-naphthyl)-1,4-diazabutadiene) nickel (II) dibromide and 2,6-bis[1-(2,6-diisopropylphenylimino) ethyl] pyridine iron (II) dichloride on modified clay (C-20A). The catalysts, thus, prepared can be used for preparing polyethylene nanocomposites. Salient conclusions resulting from the study are :

1. The amount of the clay is an important factor in determining the extent of exfoliation/intercalation of the polymer into clay. The larger the amount of clay used lesser is the degree of exfoliation.

2. The degree exfoliation is greater when the polymerization is performed at higher Al/Fe ratio.

3. Complete exfoliation leads to polyethylene with lower crystallite size and lower crystallinity.

4. When ethylene is polymerized using a mixture of homogeneous iron (II) catalyst, and clay, the degree of exfoliation is significantly lesser compared to when the polymerization is performed using a preformed clay supported catalyst. This observation suggests that in the supported catalyst, at least part of the active centers, reside within the galleries of the clay.

6.5. References

1. Giannelis, E. P.; Krishnamoorti, R.; Manias, E. *Adv.Polym.Sci.* **1999,** *138* (Polymers in Confined Environments), 107-147.

2. Alexandre, M.; Dubois, P. *Mater.Sci.Eng.* **2000,** *28*(1-2), 1-62.

3. Carrado, K. A. *Appl.Clay Sci.* **2000,** *17*(1-2), 1-23.

4. LeBaron, P. C.; Wang, Z.; Pinnavaia, T. J. *Appl.Clay Sci.* **1999,** *15*(1-2), 11-29.

5. Ray, S. S.; Okamoto, M.; *Prog. Polym. Sci.* **2003**, *28*(11), 1529-1641.

6. Giannelis, E. P. *Adv.Mater.* **1996,** *8*(1), 29-35.

7. LeBaron, P. C.; Wang, Z.; Pinnavaia, T. J. *Appl.Clay Sci.* **1999,** *15*(1-2), 11-29.

8. Wang, Z.; Pinnavaia, T. J. *Chem.Mater.* **1998,** *10*(12), 3769-3771.

9. Lemmon, J. P.; Lerner, M. M. *Chem.Mater.* **1994,** *6*(2), 207-210.

10. Wang, Z.; Lan, T.; Pinnavaia, T. J. *Chem.Mater.* **1996,** *8*(9), 2200-2204.

11. Lan, T.; Kaviratna, P. D.; Pinnavaia, T. J. *Chem.Mater.* **1994,** *6*(5), 573-575.

12. Nicoud, J. F. *Science* **1994,** *263*(5147), 636-637.

13. Burnside, S. D.; Giannelis, E. P. *Chem.Mater.* **1995,** *7*(9), 1597-1560.

14. Usuki, A.; Kojima, Y.; Kawasumi, M.; Okada, A.; Fukushima, Y.; Kurauchi, T.; Kamigaito, O. *J.Mater.Res.* **1993,** *8*(5), 1179-1184.

15. Wang, Z.; Pinnavaia, T. J. *Chem.Mater.* **1998,** *10*(12), 3769-3771.

16. Munzy, C. D.; Butler, B. D.; Hanley, H. J. M.; Tsvetkov, F.; Peiffer, D. G. *Mater.Lett.* **1996,** *28*(4-6), 379-384.

17. Doh, J. G.; Cho, I. *Polym.Bull.(Berlin)* **1998,** *41*(5), 511-518.

18. Akelah, A.; Moet, A. *J.Mater.Sci.* **1996,** *31*(13), 3589-3596.

19. Vaia, R. A.; Giannelis, E. P. *Macromolecules* **1997,** *30*(25), 8000-8009.

20. Kato, M.; Usuki, A.; Okada, A. *J.Appl.Polym.Sci.* **1997,** *66*(9), 1781-1785.

21. Kawasumi, M.; Hasegawa, N.; Kato, M.; Usuki, A.; Okada, A. *Macromolecules* **1997,** *30*(20), 6333-6338.

22. Laus, M.; Francescangeli, O.; Sandrolini, F. *J.Mater.Res.* **1997,** *12*(11), 3134-3139.

23. Liu, L.; Qi, Z.; Zhu, X. *J.Appl.Polym.Sci.* **1999,** *71*(7), 1133-1138.

24. Ogata, N.; Kawakage, S.; Ogihara, T. *J.Appl.Polym.Sci.* **1997,** *66*(3), 573-581.

25. Ruiz-Hitzky, E.; Aranda, P.; Casal, B.; Galvan, J. C. *Adv.Mater.* **1995,** *7*(2), 180-184.

26. Gopakumar, T. G.; Lee, J. A.; Konto poulou, M.; Parent, J. S. *Polymer* **2002,** 43, 5483-5491.

27. Tudor, J.; Willington, L.; O'Hare, D.; Royan, B. *Chem.Commun.* **1996,** (17), 2031-2032.

28. Jin, Y. H.; park, H. J.; Im, S. S.; Kwak, S. Y.; Kwak, S. *Macromol. Rapid. Commun.* **2002**, 23(2), 135-140.

29. Alexandre, M.; Dubois, P.; Sun, T.; Garces, J. M.; Jerome, R. *Polymer* **2002,** 43, 2123-2132.

30. Heinemann, J.; Reichert, P.; Thomann, R.; Mulhaupt, R. *Macromol.Rapid Commun.* **1999,** *20*(8), 423-430.

31. Bergman, J. S.; Coates, G. W.; Chen, H.; Giannelis, E. P.; Thomas, M. G. *Chem.Commun.(Cambridge)* **1999,** (*21*), 2179-2180.

32. Chen, T-K; Tien; Y-I; Wei, K-H. *Polymer* **2000,** *41*, 1345-1353.

33. Messersmith, P. B.; Giannelis, E. P. *J. Polym Sci. A Polym. Chem.* **1995,** *33*, 1047-1057.

34. Saujanya, C.; Imai, Y.; Tateyama, H. *Polym. Bull.* **2002,** *49*, 69-76.

35. Sun, T.; Garces, J. M. *Adv. Mater.* **2002**, *14*(2), 128-130.

36. Girish Galgali Ph. D. thesis submitted to University of Pune (Chemistry Department), 2003.

7. Summary and conclusion

The research embodied in this thesis involves heterogeneous catalysis for olefin polymerization using transition metal catalysts. The thesis can be broadly divided into two parts. In the first part silica is studied as a support for the olefin polymerization catalysts and in the second part modified clay is used as a heterogenizing solid.

In case of silica-supported catalysts two systems were chosen for the study, namely, a metallocene, Cp_2ZrMe_2, and 2,6-diacetylpyridine-bis-(2,6 diisopropylphenyl amine) iron (II) dichloride. The two catalysts are chosen because of differences in their ability to react with the surface of silica. The silica surface contains free hydroxyl groups with which Cp_2ZrMe_2 can react forming a covalent bonding, whereas, the iron catalyst is expected to be inert towards the free hydroxyls of silica. The objective is to study and compare the behavior of these two different kinds of catalysts for polymerization of ethylene.

In most of the published and patented literature metallocenes are generally supported on silica after pretreatment with MAO and, sometimes, with other aluminum alkyls like TMA. Such surfaces have no sites to anchor the catalysts. Supported catalysts, thus, prepared exhibit a polymerization behavior very similar to homogeneous catalyst. Metallocenes can also be directly reacted with silica surface. Upon reacting Cp_2ZrMe_2 with silica, containing different relative concentrations of isolated and paired hydroxyl groups, several organometallic sites can be generated, wherein, the metallocene is chemically anchored to the surface. Some of these surface-anchored sites may be polymerization active, whereas, some others may be inactive. It was observed previously that when metallocenes react with the paired hydroxyls the resulting catalysts become inactive to polymerization.

Using silica supported Cp_2ZrMe_2 as a model an attempt has been made to explain the nature of active site generated on the surface of silica. The stoichiometry of the reaction was examined by estimating the depletion of free hydroxyls on silica surface after supporting the catalyst. It was established that the free hydroxyls of silica react with both the Zr-Me bond (resulting in methane as a byproduct) and Zr-Cp bond (resulting in cyclopentadiene as a byproduct). The catalytic sites generated on the silica surface were probed by X-ray photoelectron spectroscopy. The results show that broadly two different

kind of catalytic centers are generated, namely, ZrO (of lower binding energy Zr) and ZrO_2 (of higher binding energy Zr) upon reaction of isolated and paired hydroxyls of silica respectively. It is known that the relative concentration of isolated and paired hydroxyls of silica can be controlled by calcining silica at different temperatures. Consequently it is also possible to control the relative concentration of ZrO and ZrO_2 species. For example calcining silica at 600° leads to predominantly isolated hydroxyls on the surface. It was observed that the supporting Cp_2ZrMe_2 to silica, calcined at 600°C only ZrO species is formed, whereas supporting Cp_2ZrMe_2 at silica calcined at 400 and 200°C a mixture of ZrO and ZrO_2 are formed, the relative concentration of ZrO_2 being higher in the latter. It was also observed that the catalytic activity for ethylene polymerization is inversely proportional to the relative concentration of ZrO_2 in the supported catalyst. Based on the above observations a probable structure of active site has been suggested.

In one experiment the metallocene was supported on silica pretreated with MAO and the results were compared with that supported onto untreated silica. It was observed that the MAO pretreated catalyst exhibit lower catalyst activity as well as initial rates of polymerization. This shows that the catalyst where the metallocene is directly anchored to the silica surface has a higher stability in comparison with MAO pretreated catalyst where the active site is anchored to the surface of silica via weak electrostatic interactions.

In case of the silica supported bis-(imino)pyridyl iron (II) catalyst no change of free hydroxyls on the silica was observed before and after supporting. Also no significant change in the XPS binding energy of iron center was observed by supporting the catalyst on the silica containing different concentration of free hydroxyls. On repeated washing of the solid catalyst a portion of the catalyst was found to be extracted from the solid support. All these observation confirm that the iron catalyst is not chemically bound to the surface of silica.

Nevertheless, silica support seems to confer a stabilizing effect on the catalysts. This is inferred from the nature of polymerization kinetics of the supported and homogeneous

catalyst. This behavior is attributed to the existence of a weak hydrogen bonding between the free hydroxyls of silica and the chloride ligand.

Catalysts were also prepared by first pretreating silica with MAO followed by addition of Fe (II) catalyst and connecting a complex of Fe (III) catalyst-MAO with silica calcined at 400°C for 8 h. It was observed that the catalyst activity decreases when the silica is pretreated with MAO. Under these conditions, there are no hydroxyl groups on silica. Therefore the catalyst is most probably held on the surface of silica through weak physical adsorption. It is also observed that peak molecular weight is substantially higher with the above two catalysts. This is presumably due to lower concentration of active sites formed when a MAO pretreated silica is used as the support or due to loss of active sites generated when a complex of Fe (II)-MAO is brought in contact with silica.

Two late transition metal catalysts [(N, N'-diisopropylbenzene)-2,3-(1,8-naphthyl)-1,4-diazabutadiene) nickel (II) dibromide and 2,6-bis[1-(2,6-diiso propylphenylimino) ethyl] pyridine iron (II) dichloride were supported onto the surface of the modified clay C-20, which had been previously pretreated with MAO. The intercalation of MAO and catalysts within the galleries of the clay were examined by WAXD. Polymerization of ethylene was performed using the clay-supported Fe (II) and Ni (II) catalysts. The influences of experimental parameters such as quantity of clay, catalyst concentration and Al/M ratio on catalyst activity and polymer properties were studied. The structure of the composites were examined by WAXD.

Treatment of clay with MAO results in an increase in the inter-gallery spacing which implies intercalation of the MAO within the clay galleries. However, no further change in the inter-gallery spacing was observed upon treating the MAO treated clay with either Fe (II) of Ni (II) catalysts.

The clay supported nickel catalysts polymerized ethylene to amorphous polymers of high $\overline{M_w}$ and narrow molecular weight distribution. WAXD showed that the Ni (II) catalyst produces completely exfoliated nanocomposites when the clay content in the matrix is between 2-6wt%. The results were authenticated transmission electron micrograph.

The iron catalyst polymerized ethylene to crystalline polymer and hence bimodal molecular weight distribution. WAXD studies indicated that the catalyst is capable of

completely or partially exfoliating the clay depending upon the content of clay. The exfoliation of the clay in the polymer matrix was further established by transmission electron microscopy. The crystallite size of the nanocomposites obtained from the full width at half maxima for the PE peak shows that there is a relationship between the extent of exfoliation and the size of PE crystallite in the nanocomposites. In a separate study ethylene was polymerized using a homogeneous Fe (II) pyridylimino catalyst in presence of clay in a physical mixture. Under these conditions only intercalated nanocomposites are obtained. This shows that the intercalation of the catalyst inside the galleries of clay is an important prerequisite for the formation of completely exfoliated nanocomposites.